A Selection of published/presented papers

Volume I(2)
(1979-1983)

Papers 23-45

S Lee

A SELECTION OF PUBLISHED PAPERS

by S. LEE

UNIVERSITI MALAYA

23. 1979 "The Vacuum Spark as a device for the generation of fusion neutrons" Proceedings of the Colloquium on Laser Developments and Applications Pg. 23-33, S. Lee.

24. 1980 "Plasma Conditions Required for Energy Application" International Conference on Physics and Technolgy - Procs. of Conference in Bull. Mal. Inst. Phys. 1, 4, 152 - 160, S. Lee.

25. 1980 "Modules for Applied Physics Experiments - An Integrated Approach" Bulletin of the Malaysian Institute of Physics,Vol. 1, No.1, Pg. 17-23, S. Lee.

26. 1980 "A Low-Cost Tokamak" - Bull. Mal. Inst. Phys. 1 2, 14-22, S. Lee.

27. 1980 "Measurement on the blue (425 - 475 nm) Content of solar radiation to determine the equivalence of solar radiation and radiation of lamps used in the treatment of neonatal hyperbilirubinemia" Bull.Mal.Inst.Phys. Vol.1, 3, 63-67, S. Lee.

28. 1980 "Experimental Physics Research in the University of Malaya" - Bull.Mal. Inst.Phys. 1 , 3, 34-36, B.C. Tan, S. Lee.

29. 1980 "8th International Conference on Plasma Physics and Controlled Nuclear Fusion Research, Brussels, 1980" - Bull.Mal.Inst.Phys. 1, 32-33, S. Lee.

30. 1981 "Conventional Energy Supplies and Non-Conventional Energy Research in Malaysia" - Invited paper presented at the COSTED Seminar on Energy Options for Developing Countries Madras 23-27th Feb. 1981, S. Lee, B.C. Tan. - Bull. Mal. Inst. Phys. 2, 3, 173-187.

31. 1981 "Report on Seminar on Energy Options for Developing Countries Madras 23-27 Feb 1981" Bull.Mal.Inst.Phys. 2, 1, 1-4, S. Lee.

32. 1981 "Performance and Optimization of a Laser Initiated Vacuum Spark" Bull. Mal. Inst. Phys. 2, 1, 50-58, C.S. Wong, S. Lee.

33. 1981 " Laser Shadowgraphic Technique Applied to the Plasma Focus" Bull.Mal.Inst.Phys. 2, 2, 105-113, S. Lee, Y.H. Chin.

34. 1981 "Review of Plasma Physics Research in Malaysia" Symposium on Plasma Research, Theory and Experiment, International Centre for Theoretical Physics, Trieste, Italy, June 1981, S. Lee.
- Fusion Energy - 1981 (IAEA - SMR - 82), 288 - 295.

35. 1981 " Geometrical Optimization of the Dense Plasma Focus" Symposium on Plasma Research, Theory and Experiment, International Centre for Theoretical Physics, Trieste, Italy, June 1981, S. Lee, Y.H. Chen.
- Fusion Energy - 1981 (IAEA - SMR - 82),296-303.

36. 1981 "The Vacuum Spark as a Fusion Device" Symposium on Plasma Research, Theory and Experiment, International Centre for Theoretical Physics, Trieste, Italy, June 1981, C.S. Wong, S. Lee.
- Fusion Energy - 1981 (IAEA - SMR - 82) 336 - 341.

37. 1981 "Neutron Measuremnts of a 12 KJ Plasma Focus" Mal. J.Sci. 6B, 167 - 174, C.S. Wong, S. Lee and S.P. Moo.

38. 1981 "The Pinch Phase of a Plasma Focus" Bull.Mal.Inst.Phys.2, 4, 240-250, S. Lee.

39. 1981 Ciri-ciri sebuah Laser delima denyutan dan kegunaannya untuk penyelidikan dalam bidang Fizik Plasma - C.S. Wong & S. Lee.
Bull. Mal. Inst. Phys.,24, 206-214.

40. 1982 "High Density High Temperature Plasma Production in Fast Z-Pinches" 9th.Ann. Plasma Phys. Conf. Oxford July 1982, S.Lee with others.

41. 1982 "Microcomputer Implementation of Magnetohydrodynamic Computation including Real Gas Effects" Bull. Mal. Inst. Phys. 3, 4, 197-203, S.Lee.

42. "Energy Balance and the Radius of Electromagnetically Pinched Plasma Columns" - Plasma Physics (in press), S.Lee.

43. "Observation of Radial Equilibrium and Transition to a Helix of a Gas-embedded Z-Pinch" - submitted to Phys.Rev. A - A.E.Dangor, M.B.Favre Dominguez, S.Lee.

44. "Application of energy balance to compute plasma pinch ratios"-J. Applied Physics (in press) - S.Lee

45 "Radius ratios of argon pinches" in preparation for the Australian J.of Physics - S.Lee

The Vacuum Spark as a device for the generation of fusion neutrons

S. Lee

Introduction

In the areas of research on fusion physics there is an interest in laboratory-generated hot plasmas compressed to a high density and therefore, of necessity, having a very short confinement time.

One class of devices generate what are essentially point plasmas which are enabled to attain high densities and temperatures by a concentration of energy both space-wise and time-wise. Among this class of point plasmas (see Fig. 1) are the pinch, the exploding wire, the plasma focus, the vacuum spark and the laser focus.

The pinch is now regarded as a classical dense plasma device, relying on a large pulsed current to heat a test gas at low pressure and subsequently to compress it by a self-pinching J x B effect. The plasma focus, essentially a pinch but incorporating a phase of shock heating prior to pinching produces a plasma of more extreme conditions. In the exploding wire, a solid wire is vapourised and the vapour then pinched.

The pinch has been used for many years to study fusion processes in plasmas and the plasma focus has extended the range of investigation both to higher plasma densities (10^{19} cm^{-3}) as well as to higher neutron yields (up to 10^{12} neutrons per shot using a mixture of deuterium and tritium as the test gas)[1]. Recently the exploding wire has also generated neutrons with the use of a 'deuterided' wire.

The vacuum spark may in this context be described as a pinch in a vapour created in a vacuum. The main differences between the vacuum spark and the pinch are:

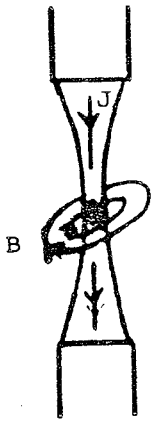

Pinch

exploding wire

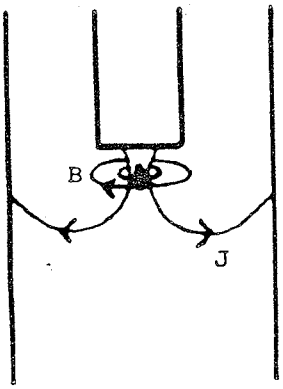

plasma focus

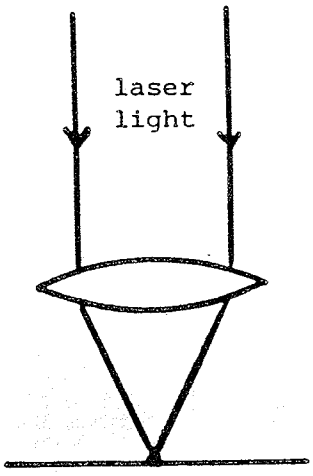

laser focus on
solid target

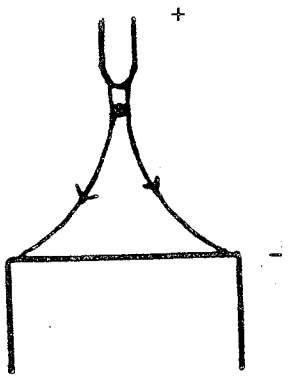

spark in
vacuum

Fig. 1 Point plasma devices

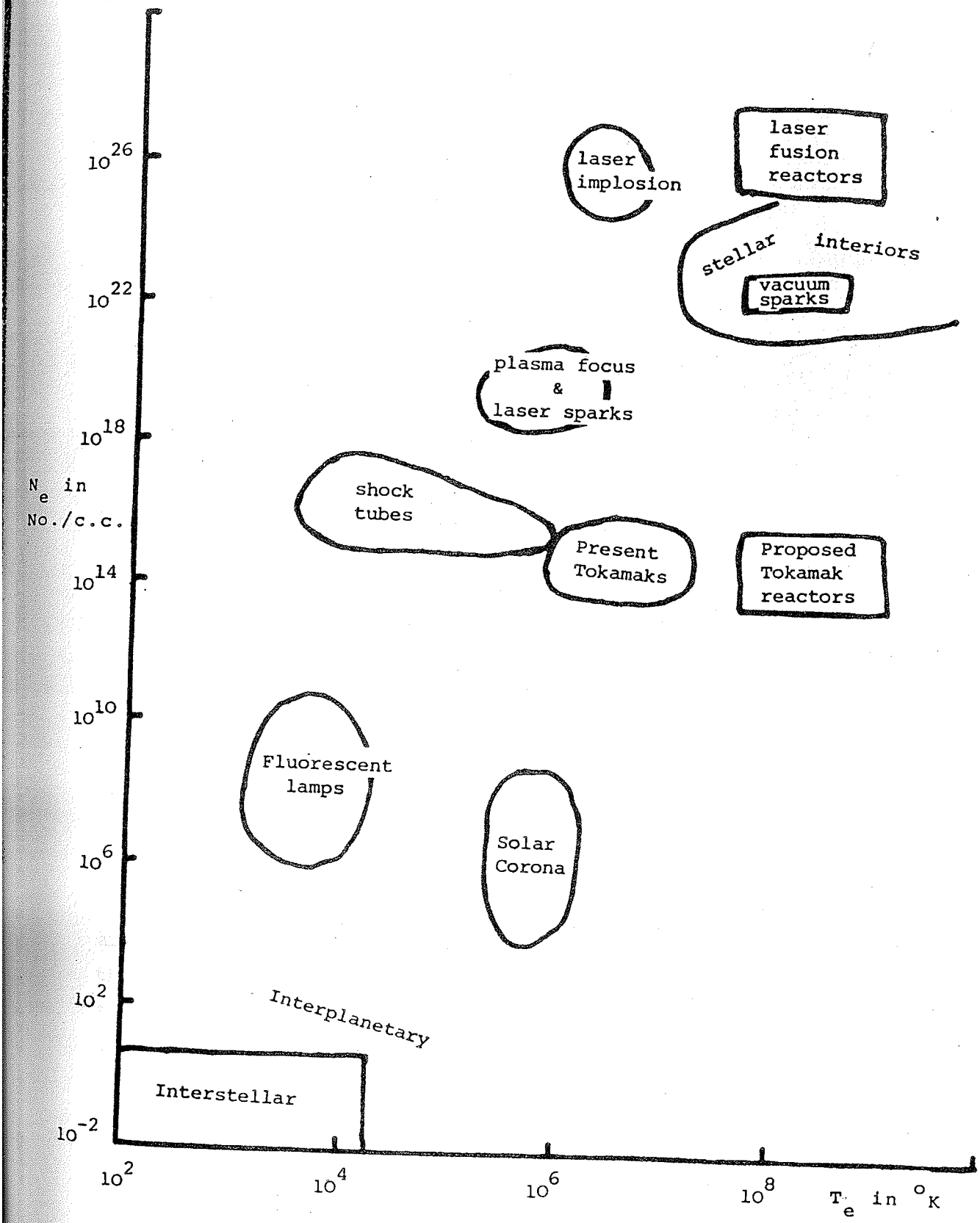

Fig.2 N_e - T_e domain comparison for various types fo plasmas

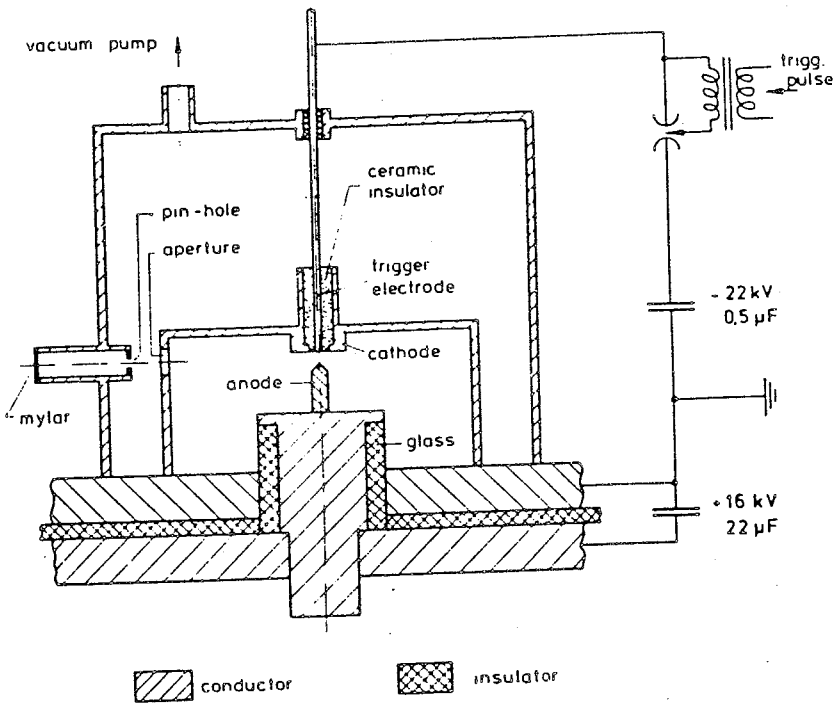

Fig. 3. Schematic of experimental set up.

(i) the electrical current flows in a medium containing a relatively small number of particles whose distribution is also determined by whichever particular method the vapour is produced (usually by a beam striking the cathode).

(ii) the pinching occurs with this vapour in a vacuum and not, as in the case of the pinch, in an originally uniformly distributed ambient gas.

(iii) in the classical vacuum spark experiments the vapour in which the final compression appears is that of a high-Z metal such as Fe or Ti whereas the pinch experiments are usually conducted with hydrogen or deuterium.

Be that as it may, experiments have shown that vacuum sparks in heavy metal vapours produce point plasmas microns in diameter existing for about 50 ns with an electron density exceeding 10^{21} per c.c. and an ion temperature of about 10 keV. Such extreme conditions have for long ensured for the vacuum spark a place in the laboratory as the only device capable of generating the conditions within the interior of stars. (see Fig. 2).

The vacuum spark[2,3], with its high ion density and ion temperature, also attracts interest from the point of view of laboratory fusion. For this purpose, the classical device has to be converted to operate in a deuterium vapour. These crucial questions then arise : (i) would a deuterium vacuum spark maintain the same high electron density as the high-Z vacuum spark? If so, the deuterium vacuum spark would have a greater than 10-fold increase in ion-density. (ii) would a deuterium vacuum spark maintain the same high ion temperature as the high-Z vacuum spark?

Vacuum Spark Experiments at Juelich

Fig. 3 is a schematic of the experimental set-up in Juelich (1976). The test chamber was pumped down to 10^{-4} torr at which point it was observed that the electrodes could hold off consistently a voltage of 16 kV which was

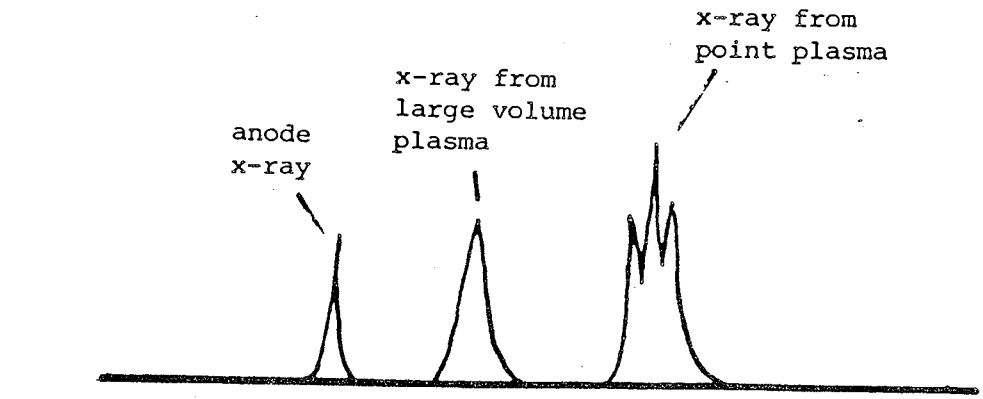

Fig. 4 (a)

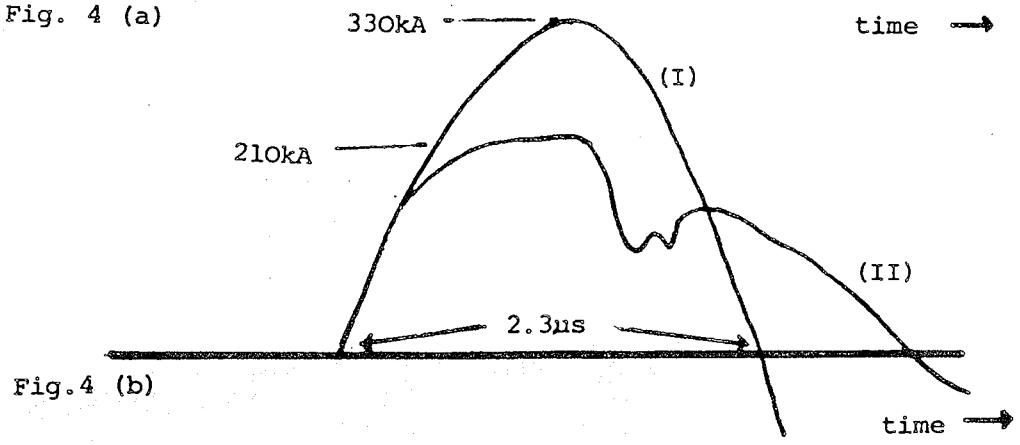

Fig.4 (b)

Fig. 4 (a) X-ray from the vacuum spark at 16 kV

(b) Current waveform (I): 17kV, (II): 16kV

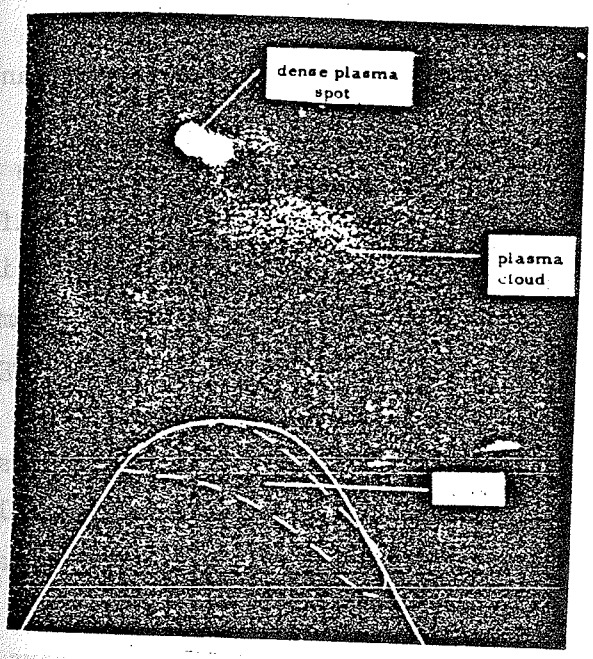

Fig.5a. Soft X-ray pinhole photographic sensitivity of 1-2.5A. The circular distinct bright spot has a diameter corresponding to the pinhole size of 0.4 mm.

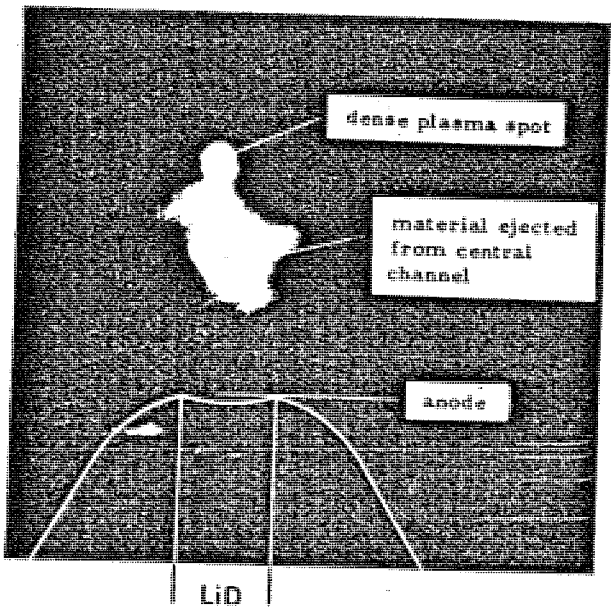

Fig.5b. Soft X-ray pinhole photographic sensitivity of 1-2.5A. The anode, in this case, has a central channel filled with LiD. The circular spot at the top of the intense image has a diameter corresponding to the pinhole size of 0.4mm.

also across the 22 μF capacitor bank. To trigger the vacuum spark, a sliding spark (22 kV, 0.5 μF) was initiated across the surface of the ceramic insulator between the cathode and the trigger electrode. This released electrons which then accelerated towards the anode in a beam. The electrons struck the anode throwing out a cloud of vapour of the anode material which then spread across the inter-electrode space producing a plasma which then carried the main current from the 22 μF capacitor bank.

In this device operated at 16 kV, the current waveform for the first half cycle was much extended in time, compared with the second half cycle. Strong dips in the current waveform were observed corresponding in time to the production of hard x-rays which occasionally penetrated 10 mm of lead. Less penetrating x-rays were also observed earlier in the discharge (Fig. 4). Whenever the current dips appear in the current waveform, the x-ray detector show the characteristic vacuum spark x-ray waveforms and soft x-ray pin-hole photographs show a dense plasma phase in the form of small regions in the interelectrode space emitting strongly in the 1 - 2.5 Å band.

At 17 kV, the current waveform became sinusoidal and no x-rays were detected as indicated in Fig. 4. The comparison of traces (I) and (II) of Fig. 4 (b) shows very clearly that a very intense electro-plasma-mechanical coupling occurred at 16 kV and that this coupling was completely absent at 17 kV[4].

These main characteristics were recorded for the vacuum spark for both types of electrodes used i.e. a solid tantalum anode and a stainless steel anode with a central channel filled with fused LiD. However when LiD was used in the anode, the soft x-ray photographs show images of greater optical density than comparative shots using the solid tantalum anode (Fig. 3). Bursts of neutrons typically 10^7 in number having energies in the range 2-3 MeV were also detected, correlated to the formation of the dense plasma spots.

With the Juelich set-up, the dense plasma phase of the vacuum spark

was observed for a narrow range of voltages around 16 kV. This limited the input energy to 3 kJ, which would limit the neutron yield since for current-pinched devices of this type, in general, neutron production can be expected to scale as E^n where n is in the region of 2.

There appeared to be 2 factors in the Juelich set-up which, if improved upon, could be expected to enhance the neutron yield of the vacuum spark.

1. Voltage-holding

There is evidence from the current trace that above 17 kV the discharge has gone over to a surface discharge mode, or as suggested alternatively by Prof. Morgan[5] to a long-path discharge mode; in either case, the discharge would thus divert away from the desired inter-electrode space in which the vacuum spark could form with all its characteristic electromechanical intensity.

This problem has been solved, it is believed, since, with a redesign of the back-wall insulator, and by cleaning the interior of the test chamber, the system at the Universiti Malaya now holds 35 kV consistently.

2. high Z-vapour

LiD was chosen for the anode channel partly because the low-Z Li ions are expected to have a minimum effect on the plasma as far as cooling through Bremsstrahlung is concerned. However in the Juelich device, the method of triggering most certainly ensured that this advantage was annulled since the electrons released by the sliding spark would have preferred to move towards and impact with the stainless steel material surrounding the channel containing the LiD.

To overcome this, in the present set-up here in the University of Malaya, the trigger electrode is removed and the triggering will be done by

focussing the light from a pulsed 80 MW ruby laser onto the LiD in its channel. This will ensure that the initial 'action' occurs without high-Z contaminants.

Conclusion

This device is now a laser focus initiating a Li-D plasma to be further compressed as a vacuum spark. In connection with the plasma focus work which is already established in the Department[6] this new work appears to offer many possibilities. First of all we could try to use our established snow-plow model[7] to describe the spark. But we shall not get very far with this model because, with the enhanced electromechanical effects (as apparent from the current trace) the spark is even more anomalously resistive than the plasma focus. The electron Hall parameter is at least 10^4 compared to 10^3 for the plasma focus and the ion Hall parameter also 10^4 to 30 for the focus. Under these circumstances, it is estimated that if as little as 10 kA of the total current flowed through the dense plasma spot, the drift velocity would be such as to lead to energy coupling to the plasma via the two-stream instability.

One way to study this would be to revert to current-voltage measurements and try to define experimentally at which point in time the plasma is in a predominantly inductive phase and when it is in a resistive phase. This data could then be correlated to neutron measurements and also to measurement of instability signals appearing on the current waveform.

Ruby laser facility available at the Universiti Malaya

The ruby laser is of a twin flash-lamp pumped type with a 4" x 5/8" ruby rod as its lasing element. Several accessory features have been designed for it, including an intra-cavity etalon for mode-selection to inprove its coherence length to over 1 metre. There is also a spark-gap light-pulse chopper, operated by the laser itself, which chops the light pulse to 2 ns. With these accessories the following modes of operation are available:

1.	Multimode	- 1.5 J	20 ns half width	70 MW
2.	Multimode chopped	- 0.5 J	2 ns half width	250 MW
3.	S T M	- 35 mJ	20 ns half width 1 metre coherence length	15 MW
4.	S T M chopped	- 10 mJ	2 ns half width 1 metre coherence length	50 MW

Mode 1 is most suitable for heating or vapourising samples and for large volume diagnostics or low-return scattering experiments. Mode 2 is suitable for better time resolution e.g. for diagnostics of transient events. Mode 3 & 4 are specially designed for holographic work.

Acknowledgement

The ruby-laser facility is a gift of the Alexander von Humboldt (AVH) Foundation of the Federal Republic of Germany to the Physics Department, Universiti Malaya. This laser system is a part of a major equipment grant given to the Department by the AVH Foundation and the Kernforschungsanlage Juelich (Nuclear Research Establishment at Juelich), West Germany, in the framework of a post-fellowship cooperation programme resulting from the award of an AVH Fellowship to S. Lee and taken up as a sabbatical leave programme in 1975/76.

References

1. Mather J.W., Dense Plasma Focus in 'Methods of Experimental Physics' Vol. 9 Part B, Academic Press (1970).
2. Cohen L, Feldman U, Swartz M, Underwood J.H., J. Opt. Soc. Am. Vol. 58 No. 6 843-845 (1968).
3. Lie T.N., Phys. Rev. A. 3, 865-871 (1971).
4. Lee S., Conrads H., Phys. Lett. 57A, 233-236 (1976).
5. C. Grey Morgan, Private communication.
6. Lee S., Editor, Procs. Seminar on Plasma Focus Work in K.L. (1976).
7. Lee S., Chen Y.H., Procs. 12th. Int. Conf. Phenomena in Ionized Gases Eindhoven, Netherland, paper 353 (1975).

PLASMA CONDITIONS REQUIRED FOR ENERGY APPLICATION

S. Lee, FIPM
Jabatan Fizik
Universiti Malaya
Kuala Lumpur

INTRODUCTION

In recent years there have been several reports in popular literature about break-throughs by American and European Groups in the race to harness fusion energy. Temperatures of 100 million degrees Celsius have been claimed and confinement times of 0.1 second with a particle density of 10^{14} per cc are reported to have been achieved, indicating an $n\tau$ of 10^{13} cm^{-3} sec. It is widely quoted that the two conditions for a break-even deuterium-tritium plasma are an Ideal Ignition Temperature of 4 keV (about 45 million degree Celcius) and an $n\tau$ of 10^{14}; so that it would appear that break-even is just around the corner, especially when we note that $n\tau$ in toroidal machines have been stagnant for a decade or so at about 10^{10} before leaping dramatically to 10^{12} around the mid-seventies and then to a reported 10^{13} in 1977. A great deal of optimism is generated and although the enthusiam is of a very healthy nature it is necessary, in order to maintain a balanced perspective, to occasionally examine the basis on which minimum plasma conditions are derived.

TYPICAL EXPERIMENTS

Figure 1 shows a typical 'medium-sized' toroidal device for producing and confining a hot plasma[1]. The cut-away section shows the toroidal plasma, ohmic heated by currents induced in the plasma by currents in the external primary windings. The vacuum vessel surrounding the plasma is shown, as is the toroidal field coils producing the confining axial magnetic field. A device of such a size is capable of a temperature of several tens of million degrees and an $n\tau$ of 10^{12}.

SCALING-UP TO THE FUSION REACTOR REGIME

Figure 2 shows a conceptual tokamak reactor design illustrating the considered viability of the basic toroidal principle. 'Scaling-up' from present generation of experimental devices to a reactor involves increasing the axial bias field B_ϕ (to 10f) the axial plasma current (to 10 MA) and the minor radius 'a' of the toroidal plasma (to 2 m).

The scaling-up of the plasma current increases the plasma temperature which is further augmented by additional means of heating such as beam injection. This increase in plasma temperature and the scaling up of B_ϕ and 'a' serves to increase $n\tau$ which scales according to classical diffusion theory as:

$$n\tau \propto B_\phi^2 T_e^{\frac{1}{2}} a \qquad (1)$$

where T_e is the electron temperature[2,3]

FUSION REACTIONS

The purpose of producing and confining a hot plasma is to produce energy from

nuclear fusion reactions such as the following:

$$ {}_1D^2 + {}_1D^2 \rightarrow {}_2He^3 + {}_0n^1 + 3.27 \text{ MeV} \qquad (2) $$

$$ {}_1D^2 + {}_1T^3 \rightarrow {}_2He^4 + {}_0n^1 + 17.6 \text{ MeV} \qquad (3) $$

Deuterium is present in water to the extent of 1 atom of deuterium to 6500 atoms of hydrogen and the deuterium available in 1 litre of water is equivalent in nuclear fusion energy content to 300 litre of petrol. Thus one millionth of the deuterium present in the waters of the world has the energy potential (through the D-D reaction) for 10,000 years of world consumption calculated at 1970 US per capita rate.

In order to utilize the nuclear fusion reactions for energy production, 3 minimum conditions have often been stated as:

a) Thermalization
b) Ideal Ignition Temperature
c) The $n\tau$ criterion

The basis for these minimum conditions will now be reviewed.

THERMALIZATION

Experimental data indicate that in the range of temperatures up to 100 keV (1 keV = 1.16×10^7 ^oK) the fusion cross-section increases rapidly with temperature. For example for the D-D cross-section between 10 - 100 keV the following best fit equation has been quoted[4]:

$$ \sigma_{DD} = \frac{288}{W_D} \exp\left(-\frac{45.8}{W_D^{\frac{1}{2}}}\right) \text{ barns} \qquad (4) $$

where W_D = relative kinetic energy of the interacting nuclei in keV. This rapid rise with W is indicated in relative scale in Figure 3.

Curve 1 in Figure 3 represents a number of particles, say N, having an essentially mono-energetic distribution. The total number of fusion reactions for these N particle is proportional to

$$ \int \sigma(W) \frac{dn}{dw} $$

which is represented pictorically by the shaded area marked 1' in Figure 3.

If the same number of particles, N, is allowed to thermalize as indicated in trace 2, the total number of fusion reactions for the N particles is increased as shown by the shaded area marked 2'. The contribution to the fusion reactions comes mainly from the higher energy particles in the distribution. Thus thermalization enhances the total number of fusion reactions and is to be considered as an implied minimum condition in the discussion of the other two minimum conditions.

IDEAL IGNITION TEMPERATURE

From classical electromagnetic theory it can be shown that the Bremsstrahlung radiated from a plasma increases with $T_e^{\frac{1}{2}}$ where T_e is the electron temperature.

A treatment which includes quantum mechanical effects gives the following expression[5]:

$$P_{br} = 5.35 \times 10^{-25}\, n_e \Sigma(n_i Z^2)\, T_e^{\frac{1}{2}} \quad W/cm^3 \qquad (5)$$

with T_e in eV; and n_e, n_i are respectively the electron and ion number densities and Z the charge number of the ions.

The power density produced from the fusion reaction may be written as

$$P_{th} = \tfrac{1}{4} n_i^2\, \overline{\sigma V}\, Q \qquad (6)$$

where Q is the energy produced per fusion reaction and $\overline{\sigma V}$ is averaged over the Maxwellian distribution. The very rapid increase in $\overline{\sigma V}$ over the temperature range 1 to 20 keV for the D-D and D-T reactions is shown in the following table[4].

Values of $\overline{\sigma V}$ at specified temperatures

Temperature (keV)	D-D ($cm^3 s^{-1}$)	D-T ($cm^3 s^{-1}$)
1.0	2×10^{-22}	7×10^{-21}
2.0	5×10^{-21}	3×10^{-19}
5.0	1.5×10^{-19}	1.4×10^{-17}
10.0	8.6×10^{-19}	1.1×10^{-16}
20.0	3.6×10^{-18}	4.3×10^{-16}
60.0	1.6×10^{-17}	8.7×10^{-16}
100.0	3.0×10^{-17}	8.1×10^{-16}

From this table P_{th} for the D-D and D-T fusion reaction may be plotted as a function of kinetic temperature, as shown in Fig. 4 for the case of $n_i = 10^{15}$ cm^{-3}. The Bremsstrahlung power from the plasma is also plotted. The temperature at which the P_{th} curve cuts the P_{br} curve for a particular fusion reaction is called the Ideal Ignition Temperature (IIT). At this temperature the thermonuclear power equals the Bremsstrahlung power and this marks the lowest temperature at which the plasma, once heated to that temperature, can sustain itself at that temperature without any further external input power. For the D-T reaction the IIT is just a shade above 4 keV. At this temperature and at a density of 10^{15} cm^{-3} $P_{th} = P_{br} =$ 1 Megawatt m^{-3} and the plasma pressure is 13 atmospheres. For the D-D reaction the IIT is 36 keV.

MINIMUM nτ

In a 'break-even' plasma, the energy available at the end of a pulsed cycle must be sufficient to heat the gas to operational temperature for the next cycle. This condition is not necessarily fulfilled even through the plasma temperature may momentarily exceed the IIT. This is because whereas to heat up n fuel particles to temperature T requires an amount of energy $\frac{3}{2}nkT$ independent of heating time, the fusion energy produced (and the Bremsstrahlung energy radiated) is a function

of the containment time τ. Thus 'break-even' may be defined by equating the energy available at the end of a cycle to the energy required to heat the fuel for the next cycle. In this equation it is found that the product nτ assumes a controlling role.

To derive the break-even condition[4], consider fuel gas density of n atoms/cm^3, requiring 3 nkT per cm^3 of input energy for heating this plasma to thermonuclear temperature T. If P_{th} and P_{br} are respectively the thermonuclear power produced and the Bremsstrahlung radiated per cm^3 in the plasma contained for τ sec., then the corresponding energies are τP_{th} and τP_{br}. At this point one may note that although the Bremsstrahlung is regarded as lost for the purpose of sustaining the thermonuclear plasma, in a reactor the Bremsstrahlung will certainly be reabsorbed since even with an operating temperature of 50 keV, the radiation is predominantly in the soft x-ray region. Likewise the thermal energy 3 nkT of the hot plasma.

At the end of the cycle the total energy available is $\tau P_{th} + \tau P_{br} + 3\ nkT$ per cm^3. The application of this energy is however subjected to an efficiency factor less than one. Assume this factor is $\frac{1}{3}$ and we may write:

$$\frac{1}{3}(\tau P_{th} + \tau P_{br} + 3\ nkT) \geq \tau P_{br} + 3\ nkT \qquad (7)$$

where the equality sign indicates the break-even condition and the greater than sign indicates a better than break-even situation. The right hand side is recognised as the amount of energy required to implement heating to temperature T for the next cycle.

This break-even condition may be algebraically rearranged as:

$$R = \frac{P_{th}/3n^2kT}{P_{br}/3n^2kT + 1/n\tau} > 2 \qquad (8)$$

In this form it may be observed that since $P_{th} \sim n^2$ and $P_{br} \sim n^2$ as indicated by equation (5) and (6) the break-even condition (8) may be regarded as a condition on the value of the product nτ rather than n.

It is instructive to plot R, at given T, against nτ and repeat for various T. This is done as an example for $n = 10^{15}/cm^3$ for a D-T plasma, the values of P_{th} and P_{br} being taken from Fig.4. The result is shown in Fig. 5.

It may be seen that for T = 4 keV corresponding to the IIT of D-T the value of R does not reach the break-even value of 2 for all values of nτ. This means that although a D-T plasma may be operated at its IIT of 4 keV, there is no possibility of a break-even assuming the model presently discussed. At 6 keV an nτ of 6×10^{15} is required for break-even and at 20 keV an nτ of 3.1×10^{14} is required. Above 20 keV larger values of nτ than 3.1×10^{14} are required. Thus with this model the minimum nτ for break-even occurs at 3.1×10^{14}.

CONDITIONS FOR ENERGY APPLICATION

The above discussion based on a simple model should suffice to indicate that the often quoted break-even conditions of T = 4 keV and $n\tau = 10^{14}$ cm^{-3}-sec are only very rough indications of what will actually be needed for break-even. The

discussion may also contain sufficient data to allow an estimate to be made of the conditions within a practical D-T reactor plasma. These may be:

$$n\tau = 10^{15}\ cm^{-3}\text{-sec at}\quad T = 20\ keV$$

To achieve an $n\tau$ of 10^{15}, devices using various combinations of n and τ are proposed, of which two, one employing the tokamak concept and the other employing the laser compression techniques, appear to hold forth the best promise. These two research areas and their proposed reactor operational regime are shown in the n_e vs T plasma domain map of fig, 6 which gives a comparative picture of these two devices relative to several other plasmas both natural and produced in the laboratory.

The tokamak reactor will be a quasi-steady magnetically confined device and hence the choice of n is dictated by the technology of producing a confining field over the large volume of the torus. For example at $n = 10^{14}\ cm^{-3}$, (hence $\tau = 10$ seconds), the plasma kinetic pressure would be 6 atmospheres at the required temperature of 20 keV. A confining field of 4T is thus indicated assuming a plasma β of 10% where β is the ratio of the plasma kinetic pressure to the confining magnetic pressure.

FUSION ENERGY RESEARCH

In the international effort to prove the feasibility of a break-even machine an immense area of physics and technology has still to be covered. The technological frontier may be considered to be in the aspects of machine scaling. In the case of the tokamak, the scaling-up to break-even conditions involves increase in plasma volume (radius and aspect ratio), increase in heating, increase in stabilizing field and plasma β whilst maintaining approximate classical scaling-up of τ with temperature. In the case of laser fusion, the technological frontier involves pellet structures, increase in laser power, and 'tailoring' of the laser pulse.

Whilst research at these technological frontiers appear necessarily the preserve of the larger laboratories in developed countries, large amounts of research data and technological development are required to enable a better understanding of the physics and technology necessary to continuously push upwards the frontier towards break-even. Herein lies a role for the smaller laboratories and the developing countries. Realsing that the early successful implementation of a break-even programme may eventually be dependent on a more concerted international effort than presently available the IAEA[5,6] has in 1978 recommended research areas and devices which are suitable for development and study in developing countries; such studies to have a two-fold purpose: 1) to advance the technological level of scientists in developing countries and 2) to contribute to the international effort in fusion research.

FUSION RESEARCH IN MALAYSIA

The plasma focus and small tokamak are the two devices recommended in the IAEA report[6] as suitable for the attention of laboratories in developing countries. At the University of Malaya, the plasma physics group has operated a home-made plasma focus UMDPF1 machine since 1971[7]. Neutrons from the D-D fusion reaction

was first detected from the UMDPF1 in October 1972. In 1977 a second capacitor bank became available as the result of a generous gift from the Kernforschunganlage (Nuclear Research Centre) Juelich and the Alexander von Humboldt Foundation of the Federal Republic of Germany which also donated a 60 megawatt pulsed ruby laser. A laser-initiated fusion spark experiment was started. The two devices enable plasma studies to be made in Kuala Lumpur within the range of T: 10^6 - 10^9 ^oK; $n\tau$: up to $10^{12} cm^{-3}$-sec with fusion neutrons of greater than 10^9 per pulse and an emission rate exceeding 10^{16} per second during the pulse.

These studies and others going on in Brazil, Argentina, India, Pakistan and other developing countries herald an increasing participation and interest in the international fusion research programme aimed towards the attainment of plasma conditions required for energy application.

REFERENCES

1. "Tokamak Reactors for Breakeven - A critical study of the Near-Term Fusion Reactor Program" - International School of Fusion Reactor Technology, Erice 1976; Pergamon Press (1978)
2. S. Lee, "A Low-Cost Tokamak", Bull. Inst. Phys. Malaysia 1-2, 14-22 (1980)
3. Y.H. Chen, "Autumn College on Plasma Physics", Bull. Inst. Phys. Malaysia, 1-2, 30-34 (1980)
4. S. Glasstone, R.H. Lovberg, "Controlled Thermonuclear Reactions", D. Van Nostrand Co. Inc. (1960)
5. International Fusion Research Council "Status Report on Controlled Thermonuclear Fusion", Nuclear Fusion, 18-1, 137-149 (1978)
6. Report of the IAEA Consultants' Meeting on Fusion Programme for Developing Countries (1978)
7. S. Lee, "Plasma Fusion Research at the University of Malaya", Procs. of Symp. of Physics 67-74 (1977)

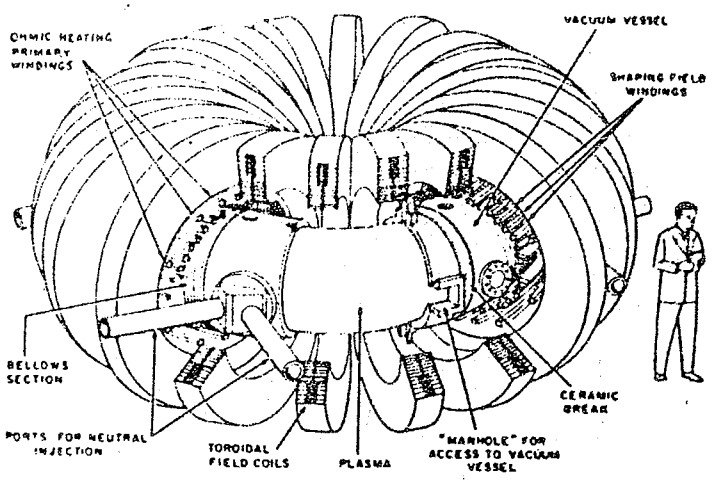

Fig.1. A typical experimental Tokamak.

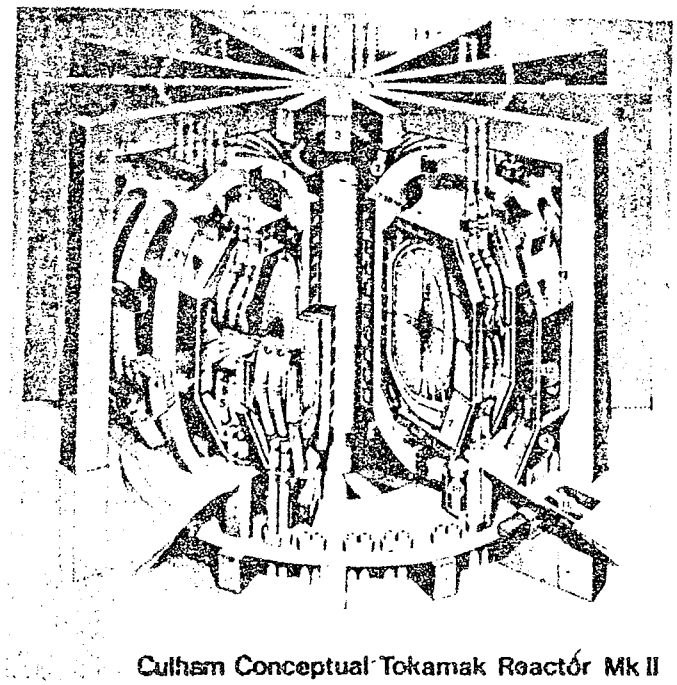

Key to regions

(1) Toroidal field coils
(2) Poloidal field coils
(3) Core
(4) Blanket module
(5) Cooling ducts
(6) Duct joints
(7) Shield structure and vacuum wall
(8) Shield door
(9) Shield cooling
(10) Shield support
(11) Servicing floor
(12) Injector, refuel and control access.

Fig. 2. Artist's impression of a Tokamak Reactor.

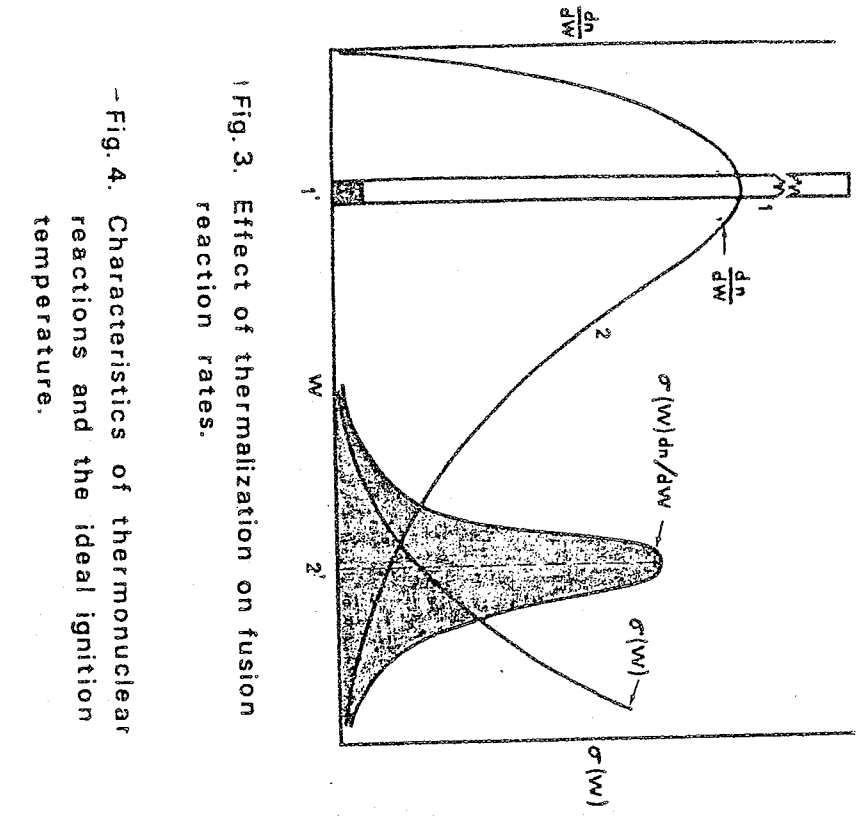

Fig. 3. Effect of thermalization on fusion reaction rates.

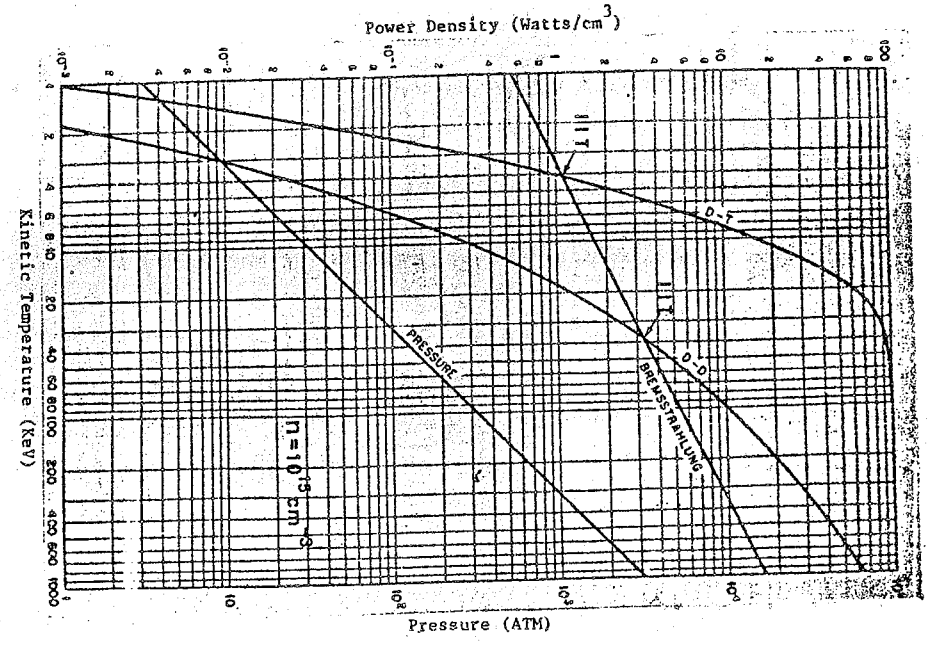

Fig. 4. Characteristics of thermonuclear reactions and the ideal ignition temperature.

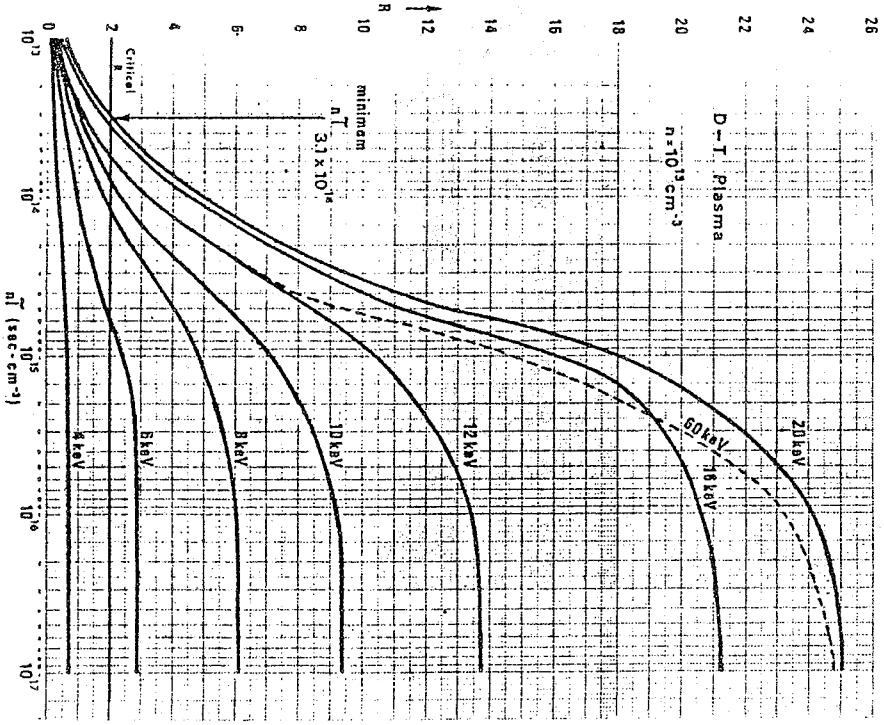

Fig. 5. Minimum $n\tilde{T}$ for pulsed cycle with conversion efficiency of ⅓.

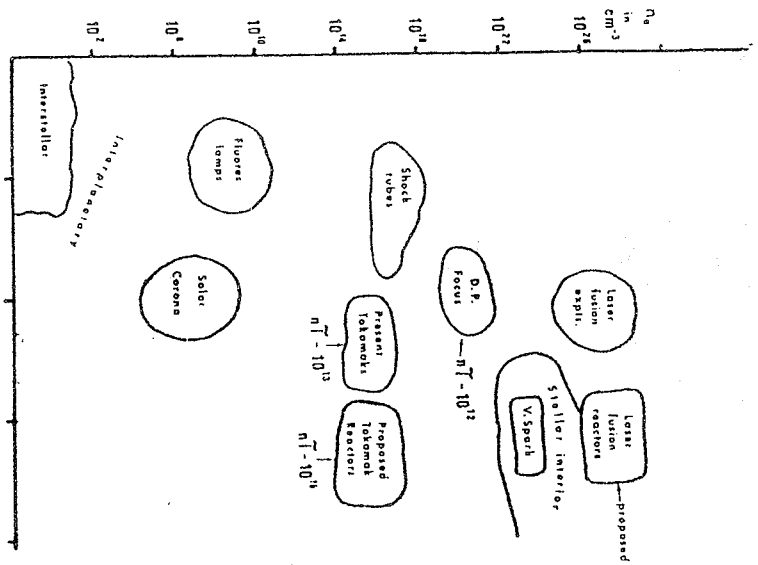

Fig. 6. Plasma Domain Map

Buletin Fizik Vol. 1 No. 1 1980

Modules for Applied Physics Experiments - An Integrated Approach

S. Lee
Jabatan Fizik
Universiti Malaya

Introduction

The transition from teaching packages of Theoretical and Experimental Physics to those of Pure and Applied Physics in the Department of Physics, University of Malaya has been described by C.Y. Tay[1]. Three laboratories have been serving the Applied Physics courses and these are the Radiation Laboratory, the Electronics Laboratory and the Applied Physics Laboratory. The Applied Physics Laboratory has developed in three major areas. Firstly in material testing experiments have been developed in tensile testing, viscosity measurements, phase measurements, x-ray powder method and ultrasonic flaw detection techniques. These experiments are complemented by vacuum techniques; pneumatic feedback experiments and field plotting techniques.

The second area is laser optics. Here a series of experiments have been introduced around an unifying or integrating concept; the concept of stimulated emission as exhibited in three useful properties of the simple helium-neon laser namely, directionality, coherence and monochromaticity. Many experiments, all emphasizing simple rather than sophisticated techniques and some with practical application, are included in the series. Experiments involving interference and diffraction effects, in particular, enable the students to experience how these three properties of the He-Ne laser enable useful observations to be made in the simplest possible manner, with the fringe measurements thrown on and measured direct from the walls of the laboratory! In a very simple air-cell interference experiment, a measurement of a change of length to a sensitivity of one ten-thousandth of a mm is made.

In the third area of development, an opportunity presented itself to try a completely fresh approach since in this area of development i.e. pulse techniques, it was intended to design completely original experiments. It was decided to design as an example, a series of experiments based on the L-C-R circuit with its 3 modes of electrical discharge, namely, the underdamped oscillation and the critically-damped and overdamped discharge. This basic concept is linked to a simplified technology of pulse generation and the technology is in turn linked to applications such as ultrasonics and stroboscopy. With this integrated approach it is hoped that the students can in one series of experiments experience the integration of a basic concept through simplified technology to industrial applications. The series of experiments is arranged in module form as illustrated schematically in fig. 1.

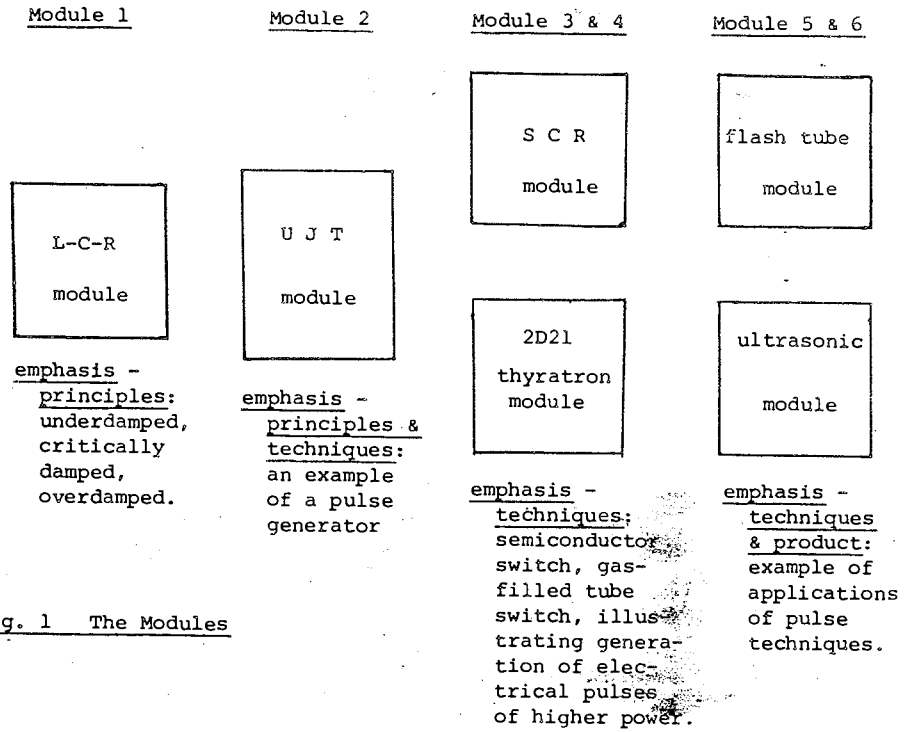

Fig. 1 The Modules

Module 1

Module 1 starts from the very basic principle of simple harmonic oscillation, progressing to calculations and measurements of current and voltage amplitudes and frequencies for nearly simple harmonic oscillation ($R < 2\sqrt{\frac{L}{C}}$) to observations of critical damping ($R = 2\sqrt{\frac{L}{C}}$) and over damping ($R > 2\sqrt{\frac{L}{C}}$). The observations are made on an oscilloscope and students are expected to have a feel for the errors involved in the measurements.

The circuit is shown in Fig. 2.

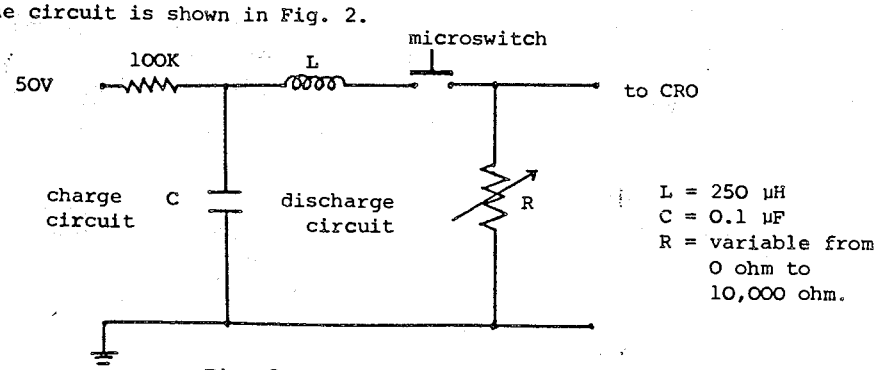

Fig. 2 Basic L-C-R circuit of module 1

Module 2

Module 2 illustrates one simple way of generating sharp pulses of variable frequency using an Unijunction transistor (UJT). The emphasis here is on the functional aspects with only one technique highlighted to the students, i.e. the use of the time constant RC to determine the rate of switching of the UJT, as shown in Fig. 3.

The students measure pulse shape and pulse frequencies for different settings of RC.

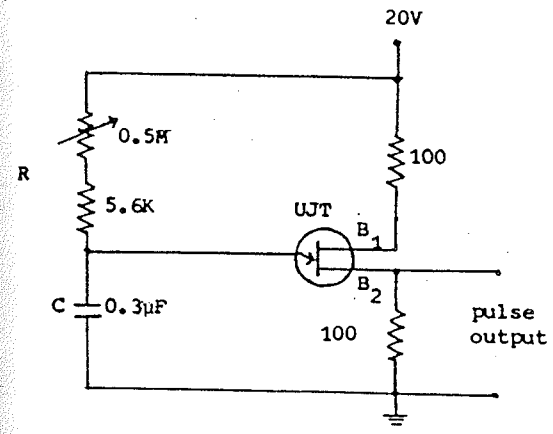

Fig. 3 Pulse generator circuit using an Unijunction transistor.

UJT = unijunction transistor
e.g. 2N2646.

Module 3

This module illustrates the use of a silicon-controlled rectifier (SCR) to switch a capacitor in an overdamped L-C-R circuit. The emphasis is on the general technique and the appreciation of the increased level of power i.e. a low power pulse (UJT module) switches a pulse of higher power (SCR module). The circuit is shown in Fig. 4.

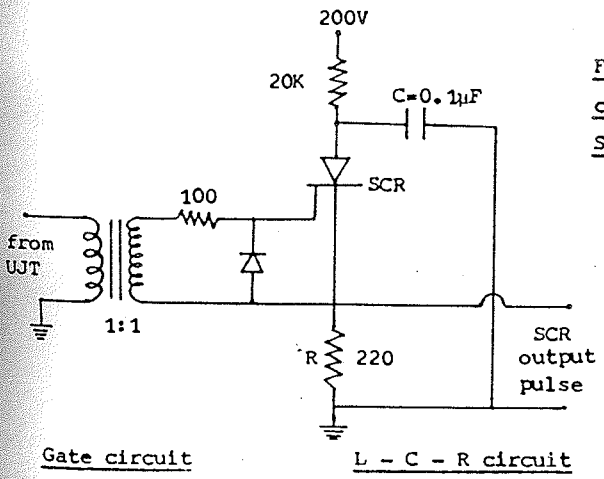

Fig. 4 Overdamped L-C-R circuit employing an SCR switch.

The inductance L of the circuit is not specifically fixed but consists of the stray inductance of connecting wires and circuit element totalling about 1 μH.

SCR= silicon-controlled rectifier,
e.g. MCR107-6.

The students measure pulse shape, power and pulse frequencies for different settings of the RC of the UJT circuit. In addition they may measure the delay-time (in the region of 0.2 μsec) between the UJT and the SCR pulses.

Module 4

This module illustrates the use of a gas-filled tube as a power-switch for an overdamped L-C-R circuit. The emphasis is on the general technique and on the comparison between the 2D21 thyratron and the SCR.

The students note the requirement for heater current and for negative grid biasing, perform the same measurement as for the SCR module and in addition note the effect of a variation of the grid bias voltages.

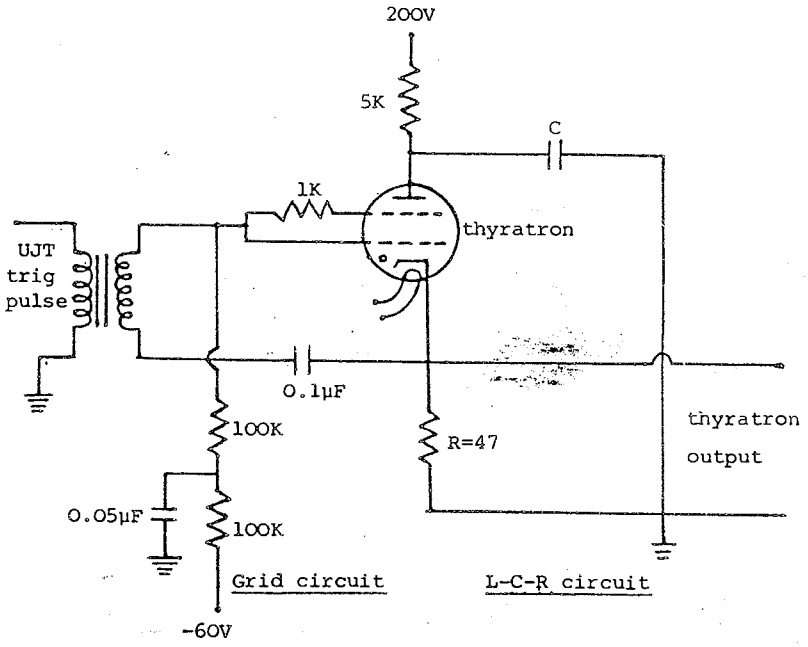

Fig. 5 Overdamped L-C-R circuit employing a thyratron switch

C = 0.01μF chosen as a suitable value for the subsequent application of this module for powering the ultrasonic module. L = stray inductance. thyratron = e.g. 2D21 xenon-filled.

Module 5 - application module - high speed flash and stroboscope

This module consists of a xenon-filled flash-lamp across which a capacitor C is connected, the circuit being a critically damped L-C-R circuit with stray inductance totalling about 1 μH forming L and the resistance of the xenon plasma forming R. The flash lamp (FX-6A) holds the voltage of 600V to which C is charged until the trigger pins receive a high voltage pulse (1.5 - 3 kV). This high voltage pulse

is supplied from SCR module with a 10 turns: 200 turns ferrite pulse transformer acting as a step-up stage.

The circuit is as shown:

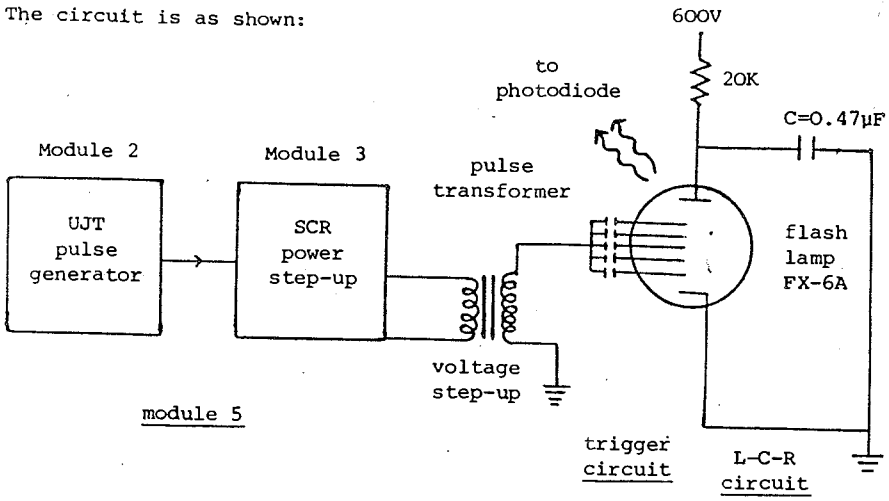

Fig. 6 Application of a critically damped L-C-R circuit for generation of high speed light pulses of high power

The students connect the modules and examine the shape of the light pulse on an oscilloscope via a high speed photodiode. They measure the energy of the light emitted per pulse and estimate the efficiency of the flash in lumens/watt. They next use the modules as a stroboscope to determine the frequency of rotation of a motor shaft or a fan.

Module 6 - application module - ultrasonic echo techniques

This module consists of an air-core inductor of a few turns placed across the thyratron output and connected in parallel to a 2 MHz piezo-electric probe acting as an ultrasonic transmitter. The simplicity of the arrangement is itself of educational value as shown in Fig. 7.

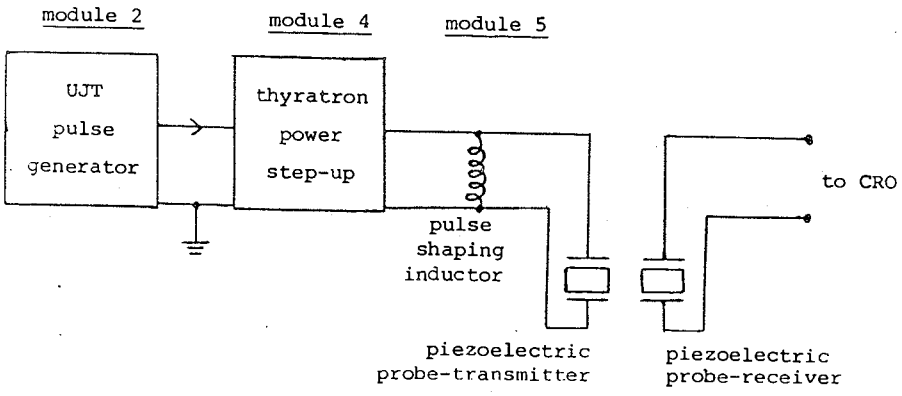

Fig. 7 Application of underdamped L-C-R circuit for generation of ultrasonic waves

The probe used is a 2 MHz Baugh and Weedon double-probe.

The students examine the waveform of the pulse across the input of the transmitter noting that although the circuit is at best only approximately tuned, forced oscillation of the probe is evident.

Next, the probe is placed in contact with the water surface in a beaker of water and the receiver probe is connected to the CRO. Echo series are noted and the speed of sound in water calculated by 'time-of-flight' method. Similarly echo pulses in various metal specimens are examined and speed of sound in these specimens computed.

Programme

The students perform the experiments working in pairs, each pair completing the 6 modules in 6 periods of 2½ hours each. Developments are continuously incorporated into the experiments e.g. at the moment submodules are being contemplated in the ultrasonic module to illustrate techniques of improving echo detection such as pulse clipping, demodulation, amplification and other aspects of pulse shaping. Other application modules are also being considered.

Beyond these modules

Beyond these modules the students have the opportunity to carry out experiments using an ultrasonic facility with A-Scan (point-by-point echo-computation method using CRO display) and C-Scan (radiographic - style) capabilities. This facility consists of a Matec ultrasonic generator - receiver, a philips double-beam CRO, an Emefco scanning tank and spark recorder interfaced with the Matec receiver by means of a six-channel spark intensity quantizer and is placed just next to the pulse-technique module experiments to give the students a sense of continuity and application for the pulse-technique experiments. In an adjacent room, high speed photography experiments are conducted as a fourth year project using a General Radio stroboscope which does not do very much more than our very elementary set-up of modules 2, 3 and 5.

Beyond the laboratory the students have the opportunity to see the application and extension of pulse techniques to various experiments in the research laboratories e.g. a variety of pulsed lasers, nitrogen, flash-lamp pumped dye laser in the laser laboratory and a 100 Megawatt ruby laser in the plasma laboratory, high current L-C-R discharge in the 4th year shock tube experiment and the fusion experiments in the Plasma Laboratory. They are already aware of the growing number of applications for pulsed techniques (e.g. stroboscopy, ultrasonics and radar) in industrial, commercial and research institutions in Malaysia.

Conclusion

These modules represent an effort to develop a series of experiments connecting on the one hand with an important basic physical principle and on the other hand with applications at a fairly high level of technology. Each module is kept basic with little refinement or trimming. It is hoped that in a series such as this, students will lose a little of the sense of isolation of individual experiments and gain a little of a sense of integration between theory and technique and between technique and application.

Acknowledgement

Acknowledgement is made for the effort that Chiang Soo Har has contributed in the assembly of these modules and the help he has rendered in the preparation of this article.

References

1. C.Y. Tay "Applied Physics in the Department of Physics, University of Malaya" in Procs. Symposium on Physics, Jabatan Fizik, Universiti Malaya 37-41, 1977.

****

Laser Research Programme at the University of Malaya

B.C. Tan, S.A. Hussain, S. Lee, K.O. Lee, K.S. Low,
A.C. Chew, Y.H. Chen and Raja Mustapha
Department of Physics
University of Malaya.

I. Introduction

Towards the end of 1976 the concept of forming a group within the Department of Physics, University of Malaya, to initiate research in lasers and their applications was mooted. The group was subsequently formed and a research grant was awarded by the F Grant Committee of the University of Malaya in 1978 from which basic equipment, listed in Table 1, were purchased.

The activities of the group comprise developing lasers of all types and using them as well as those purchased for research in various fields. These are discussed later.

II. Facilities

The Argon Ion Laser has a BeO discharge tube with a high efficiency cooling system. It has a CW power of 9 watts all-lines from 454.5 to 528.7 nm with 3 watts each at 488.0 and 514.5 nm. Significant UV radiation is obtainable at 351 and 364 nm. By changing the discharge tube and the optics, the laser can be converted into a Krypton Ion Laser which has strong lines in the infrared.

The Dye Laser uses rhodamine 6G which comes out in a jet and is pumped with the Argon Ion Laser lines of 488.0 and 514.5 nm. The output is tunable from 570 to 640 nm. With an input of 9 watts, as much as 1.4 watts output has been measured. With wedge tuning, linewidths of 40 GHz are obtainable. If upgraded to piezoelectric tuning, linewidths of 5 GHz can be expected.

The other important back-up equipment include a 1 M Czerney-Turner spectrometer, a 100 MHz photon-counter, a fast 400 MHz scope and a chart recorder.

Table 1: Laser equipment at the University of Malaya

	Equipment	Manufacturer	Specifications
1.	CW Argon Ion Laser	Spectra Physics Model 171	9W all-lines (454.5 - 528.7 nm) 3W each at 488.0 & 514.5 nm
2.	Dye Laser R6G	Spectra Physics Model 375	572 - 640 nm tunable 1.4W with 9W input 40 GHz linewidth 8 GHZ tuning resolution
3.	Scanning interferometer	Spectra Physics Model 410	Scanning range 550 - 650 nm FSR 1200 GHz Bandpass 24 GHz
4.	1 M Czerney-Turner spectrometer	Spex Model 1704	175 nm - 1.5 μm resolution 40 GHz
5.	Dual trace storage scope	Tetronix 7834	400 MHz
6.	Photon counter	Ortec - Brookdeal 5 C1	100 MHz, 10 ns pulse pair resolution dual channel disc amplifier digital lock-in with chopper
7.	Photomultiplier	EMI 9558 QB	200 - 850 nm
8.	XY/t recorder	Watanabe WX-4401	100 cm/s speed 0.5 s/cm to 50 s/cm sweep.

III. Development of Lasers

The group has undertaken to construct six lasers, both pulsed and continuous, radiating from the UV to the far IR. Table 2 summarises these lasers, some have been completed while some are under construction at the time of writing.

Nitrogen Lasers

A pulsed N_2 laser which lases at 337.1 nm has been constructed. It has a short pulse duration of ∿10 ns and peak power of ∿100 kW and is useful in spectroscopic studies of transient plasmas.

A different design of this TEA-design laser with a peak power of 700 kW is under construction. It will be a useful pump source for dye cells from which high power tunable pulses of radiation can be obtained.

Flashlamp-pumped Dye Lasers

A confocal flashlamp-pumped dye laser is under construction . The active medium is rhodamine 6 G which is tunable from 570 to 620 nm. The expected energy is about 1 J. This laser will be used to pump a cresyl violet dye cell to produce a broadband (650 - 690 nm) 100 mJ pulse. This laser will be tuned to study H_α absorption and the energy of the pulsed 656.3 nm line is estimated to be about 25 mJ.

CO_2 Lasers

The only CW laser under study by the group is a CO_2 laser. This laser is expected to produce more than 20 W power at 10.6 μm. It is also planned to boost the power to 100 W for cutting, drilling and other material processing purposes.

TEA - CO_2 Lasers

A TEA - CO_2 laser which will operate in the pulse mode at 1 J is under construction. It will be used to study some transient plasmas.

Table 2: Laser construction programme at the University of Malaya

	Type	Wavelength	Energy, power	Status
1.	Pulsed N_2	337.1 nm	(a) 100 kW, 1 mJ	Lasing
			(b) 700 kW, 7 mJ	Construction
2.	Flashlamp-pumped dye laser, R6G, pulsed	570 - 620 nm tunable	∿1 MW, ∿1 J	Construction
3.	Intermediate-laser dye laser system (cresyl violet) pulsed dye-cell	650 - 690 nm tunable	∿30 kW, ∿30 mJ	Construction
4.	CO_2 laser continuous	10.6 μm	20 W	Testing
5.	TEA - CO_2 pulsed	10.6 μm	10 MW, 1 J	Construction

IV. Some proposed studies

(a) Pollution monitoring

Using the high power Argon Ion Laser, fluorescence detection of atmospheric pollutants, for example NO_2 and NO, could be performed.

This is based on the absorption of the laser signal by the pollutants and the subsequent detection of the fluorescent radiation from the pollutants.

Light Detection and Ranging (LIDAR) techniques based on non-resonant Raman backscattering can be utilised with the N_2 or flashlamp-pumped dye lasers. This technique can provide information on the range, concentration and identity of pollutant gases.

(b) Multi-photon Spectroscopy

High resolution spectroscopy can be obtained using high power tunable laser sources, together with techniques like Doppler-free spectroscopy. Fine and hyperfine structures of molecules, isotope shifts, Zeeman and Stark levels can all be studied.

V. Conclusion

The laser group in the University of Malaya comprises eight staff members. Recently, two tutors who are reading for M.Sc. degrees have joined the group. The group has been advised by Professor C. Grey Morgan from the University College of Swansea. A symposium was held to identify useful research areas and the proceedings have been compiled. Detailed information on the available facilities and activities of the group, current or planned, are available from the proceedings.

****

PHYSICAL MODEL STUDIES IMPLICATING HEMODYNAMIC FACTORS IN THE PATHOGENESIS OF ATHEROSCLEROSIS

by

K. O. Lim
School of Physics
Universiti Sains Malaysia
Penang

INTRODUCTION

Atherosclerosis or intimal arteriosclerosis is a blood vessel disease whose existence has been well documented in China as early as some 2500 years ago[1]. It is characterized by the formation of fatty deposits, or atheromas, in the lining of blood vessels. The initial development of fatty streaks may be followed by the formation of fibrous plaques and later by calcification. However the relation between fatty streak development and fibrous plaque formation is still uncertain, though it is well known that atheromas consist mainly of cholesterol and other complex lipids.

Atherosclerosis is the major cause of death in developed countries like the United States[2] and Western Europe and its occurrence is fast increasing even in developing countries[1]. It is the principal cause

A Low-Cost Tokamak

S. Lee, FIPM
Jabatan Fizik
Universiti Malaya
Kuala Lumpur, Malaysia

Introduction

At a meeting held in 1977 at the International Centre for Theoretical Physics, Trieste, the International fusion programmes, advances and potentials were assessed. Arising from this and at the request of the I.A.E.A. a Status Report on Controlled Thermonuclear Fusion was put up in 1978.

The Report envisages that in the next century, three long-term source of energy could be available to replace dwindling fossil fuels: fusion, fission and solar energy, each one claiming its place when, depending on local conditions of supply and demand, its characteristics give it a competitive lead. Since the scientific basis for building controlled thermonuclear fusion devices with a net energy output was, even in 1978, no longer seriously in doubt, the Report recommended "a large and aggressive effort towards the practical demonstration of fusion power at the earliest possible date". In order to maximize efficient world-wide co-operation and planning in this field the Report recommended, among other steps, that a step should be taken to "identify problems where no large apparatuses are needed and which can be tackled by developing countries wishing to work in this area".

In December 1978, the I.A.E.A. Consultants met in Swierk, Poland[2] to consider this question of problem identification and the result of the Meeting was a "Report of the I.A.E.A. Consultants' Meeting on Fusion Programmes for Developing Countries". The recommendations centre on four categories of activities for developing countries, vis. (i) basic theoretical studies in plasma physics and collaboration with a major

fusion centre on analysis and interpretation of experimental data; (ii) studies of techniques with possible application outside as well as within the fusion field; such as research into properties of low temperature plasma devices and development of plasma guns and torches which already have industrial application; (iii) studies primarily dependent on established techniques and methods of atomic and nuclear physics for which no high temperature plasma device is needed. Such studies may include material studies and the measurement of atomic and nuclear cross sections using beam and beam foil technique; (iv) studies of intrinsic properties of high temperature (100eV or greater) plasma requiring either the purchase or construction of an appropriate plasma device. Two devices were mentioned, the first being the dense plasma focus (US$10,000 to US$15,000) and the second a low-powered tokamak (US$150,000 to US$400,000).

The Plasma Focus Group in Kuala Lumpur has since 1972 operated a dense plasma focus facility designed, constructed and tested entirely on native resources[3]. This dense plasma focus facility was the first machine, as far as the author is aware, constructed in a developing country, to produce fusion neutron in sufficient quantities to be detected and to produce data on neutron energy and distributions. The Universiti Malaya Group has since 1976 toyed with the idea of building a low-cost tokamak as this device produces a long-lasting plasma (1 millisec) as opposed to the very transient plasma of the plasma focus, lasting only 100 nanosecond. Whereas the plasma focus is eminently suitable for studying small-volume, short-lived, dense (10^{19}/c.c.) plasmas with very intense electromagnetic-mechanical interactions between megagauss magnetic fields and 10^{7}K plasmas, the tokamak would be suitable for studying large-volume, relatively long-lived plasmas of a more sedate and therefore more stable character. As the Tokamak is a serious contender to be the basic configuration of a future fusion reactor, the building of a tokamak would extend the experience of the plasma physics group further into the area of fusion technology and physics. There is, as far as the author is aware, no operational Tokamak in any developing country at present.

Break-even conditions

What would be the expected plasma parameters in a low-cost tokamak and how would these expected parameters relate to the parameters of a 'break-even' machine? To demonstrate a break-even machine it is necessary to produce in the laboratory a thermalised plasma, so hot and dense that its energy liberation via the nuclear fusion reaction equals to the sum total of the energy expended in heating the plasma. From cross-section considerations, the fuel would be a 1:1 mixture of deuterium and tritium.

Thermalization

In the range of reactor temperatures being considered, the cross-section for fusion increases rapidly with particle energy, and one feature is that in a thermal plasma of average energy E, most of the particles contributing to the fusion reaction have an energy of several E. Thus, thermalization multiplies the fusion cross-section; and is an essential feature for a practical reactor.

Ideal Ignition - Temperature

From consideration of Bremsstrahlung loss and fusion energy production it is known that, fortunately, whereas Bremsstrahlung power loss increases as T^2. The fusion power production increases as T^x where in the range of temperatures of interest, $x = 1.5$. Thus, there exists a temperature called the Ideal Ignition Temperature (IIT) which represents the lowest temperature for which a self-sustaining reactor can hope to be operated. For the D-T plasma the IIT is 4 keV (44 million ^{o}K).

$n\tau$ Criterion

In consideration of plasma density n, it is found that the relevant criterion is one involving the product n and τ where τ is the plasma containment time. The product $n\tau$ is involved because whereas to heat up n fuel particles to temperature T requires an amount of energy independent of the heating time, the Bremsstrahlung energy radiated and the fusion energy produced is a function of the time τ, so that in considering a pulsed cycle even at a temperature above the IIT, Lawson found that a

minimum value of τ was required to enable a sufficient fraction of the nuclei to undergo fusion to provide the break-even condition. For a D-T plasma, the minimum value of $n\tau = 10^{14}$ particle-sec cm^{-3}.

In summary, for a break-even experiment with a D-T plasma we require a thermal plasma in which

$$T = 4keV$$
$$n\tau = 10^{14} \text{ particles-sec } cm^{-3}$$

The Tokamak Concept

Linear pinch

From the historical point of view, it is convenient to discuss the tokamak concept starting from the idea of the linear pinch discharge.

It was realised early by Bennett that when a large electric current flows through an ionized gas, the $\underset{\sim}{J} \times \underset{\sim}{B}$ force resulting from the interaction of the current with its self-magnetic field can cause a "pinching" effect on the gas resulting in compression and heating, with the plasma temperature apparently being proportional to the square of the current. However, pinch experiments soon show that the plasma column is not stable in this magnetic configuration and within a few microseconds of its formation breaks up due to instabilities of various types.

Stabilized linear pinch

To stabilize the discharge, it was found effective to include an axial magnetic field. The stabilized linear pinch discharge, however, still had its limitations because, although the plasma column is stably confined along its length by the azimuthal magnetic field, there is no insulation between the plasma and the electrodes. Contamination of the plasma by the high-Z electrode material takes place, increasing the Bremsstrahlung and lowering the plasma temperature.

Stabilized toroidal pinch - no end losses

One of the approaches to overcome this problem was to have the discharge in a torus with the heating current induced in the gas by transformer action along the length of the torus. In this 'end-less' system there is no end loss and the plasma is again confined from the wall of the torus by the pinching force provided by the self-magnetic field of the plasma current. An axial field embedded in the plasma around the length of the torus provides stabilization.

Non-uniform magnetic field in torus - plasma drift losses

It was soon apparent that the toroidal system has its own drawback because, since the stabilizing field is curved and non-uniform across the torus, charge separation and plasma drift occured across the torus so that the plasma is destroyed very much more quickly than one would expect from consideration of classical diffusion time. This charge separation and plasma drift can, however, be compensated if the magnetic field lines in the system are non-degenerate, i.e., if each line does not close upon itself. This non-degeneracy is achieved by a rotational transform of the magnetic field.

Drift loss compensation - rotational transform

Happily, the tokamak with its stabilization field B_z and its poloidal field B_ϕ. It is found possible to ensure that the non-degeneracy of the field lines is maintained through the duration of a discharge if in one circuit of the torus, the resultant magnetic field does not spiral by more than 2π. This results, for a given B_z, in a limit for the poloidal field, i.e., a limit on the plasma current I_p. This limit is expressed as the Kruskall-Shapranov limit which states:

$$I_p \leqslant \frac{2\pi}{\mu} \left[a\left(\frac{a}{R}\right) B_z \right]$$

where a = minor radius of the torus

R = major radius of the torus

$\frac{a}{R}$ = aspect ratio

μ = permeability

Scaling up the plasma current

Empirically, it has been found necessary to restrict the operational value of I_p by a further fraction, $\frac{1}{q}$, where q = 2 to 3 is known as the safety factor.

Thus, in order to increase the plasma heating current and hence the plasma heating it is necessary to increase B_z, a and $\frac{a}{R}$.

Effect on τ

How would an increase in B_z, a and $\frac{a}{R}$ affect the containment time τ?

Although in a non-degenerate with stabilization the toroidal plasma is said to be confined, by no means can we expect an infinite life-time. This is because, although charge particles are confined by the field lines, collisions do occur which will knock the charge particles across the field lines resulting in what is termed 'classical diffusion'. Thus, ultimately, the life-time of the best-confined plasma is still limited to the time an arbitrarily defined proportion of the plasma diffuses out of the confines of the magnetic field. Taking this most optimistic condition, we have

$$n\tau \sim (B_z^2 T_e^{\frac{1}{2}}) a^2$$

where T_e is the electron temperature. Thus, as B_z, and a are scaled up to increase I_p and hence T_e, the effect on n is also an increase.

Although experimentally the $n\tau$ scaling is not observed to be as optimistic as that predicted by classical diffusion it is observed to be not as pessimistic as that prediced by diffusion through the collective process or by Bohm diffusion which predicts $n\tau \simeq B_z T^{-1} a$. The experimental data tend to indicate that new generation tokamaks have an $n\tau$ performance about half-way between classical and Bohm diffusion. For the purpose of planning, it appears that for scaling up from current experiments, the classical diffusion may be overly-optimistic where as for scaling down, classical diffusion may be overly pessimistic. Thus, in planning a machine scaled down from operational models, the expected value of $n\tau$

based on classical diffusion may well turn out to be pessimistic.

Scaling of plasma temperature

The scaling of plasma temperature is generally considered to be of less importance than the scaling of $n\tau$ for two reasons, the first being that as the temperature is increased, the plasma resistance diminishes and at high temperatures the plasma current becomes increasingly inefficient as a means of further heating. Thus, at the higher ranges of temperatures, conventional tokamaks require additional heating such as neutral beam injection, etc. For a low-cost tokamak this would not be necessary and one of the often quoted scaling equations may be used; such as the following based on neo-classical heat conduction:

$$T_i \sim (I_p B_z R^2 n)^{1/3}$$

where T_i is the ion temperature.

A low-cost tokamak

Although the IAEA consultants have estimated a cost of U$150,000 to US$400,000 for a low-cost tokamak, our plasma laboratory might attempt to build one with existing equipment and low resources. What kind of dimensions and magnitudes might we aim for?

If we design for a toroidal plasma of R = 0.1 m and $\frac{a}{R} = \frac{1}{5}$ with a stabilization magnetic field of B_z = 1T which could be supplied by an existing electrolytic capacity bank of 450V 0.1 F, then a maximum plasma current of 50kA could be planned for. This current could be supplied by existing capacitors rated at 10kV, 200 uF switched and crow-barred by ignitrons to provide a long-pulse current with a gently decaying tail. An experiment is being planned to find out if the crow-barred pulse is of sufficient duration (i.e. about 1 millisecond).

Scaling

Tables of existing results and expected results based on experimental

data and detailed computation are available in the literature and the following table I collects together some experimental/projected results of these machines.[4] The first column (IFR) gives operational data of the French machine which is widely quoted because of its good performance. The second column (JET) gives expected data for the Joint-European Torus (JET), which is being built in Culham, England. The third column contains a typical projection of the dimensions a fusion reactor might be expected to have and its operational conditions. The data for both JET and the reactor may be considered as scaled-up data. The last column contains a scaled-down Tokamak such as might be built at the Universiti Malaya using mainly available components. The one item that might present some difficulty is the vacuum chamber that is dough-nut shaped, 1 m in major diameter and with a minor diameter of 20 cm. The design for the chamber would have to include ports for pumping and diagnostic ports. To facilitate maintenance, the chamber may be assembled in segments rather than be manufactured as a complete 'dough-nut'.

For the planned operational values of magnetic field and plasma current which maintain their values only for the relatively short time of 1ms, the magnetic field coils will be of the simplest type. The plasma current may easily be coupled into the torus by means of an air-cored transformer.

The result will be a large-volume (100-litre) plasma at a temperature of 2 million ^{o}K lasting 1 ms. This will serve as a very useful source of studying near-thermonuclear deuterium plasmas and for the development and extension of diagnostic techniques.

Table I - Operational Torus, scaled-up torus and a low-cost scaled-down torus

	TFR(France) (Operational)	JET(EEC) (scaled up)	Reactor (scaled up)	Low-cost tokamak (scaled-down)
R_o (cm)	100	300	500	50
a(cm)	20	130	200	10
$\frac{R_o}{a}$	5	2.3	2.5	5
B_ϕ (T)	4	4	9	1
I_p (MA)	0.4	4	11	0.05
N_e (per cc)	6×10^{13}	4×10^{13}	6×10^{14}	3×10^{13}
τ ms	30	1000	1000	1
T_e (keV)	1	9	20	0.2
T_i (keV)	1	9	20	0.2
$n\tau$	2×10^{12}	4×10^{13}	5×10^{14}	3×10^{10}

References

1. International Fusion Research Council Nuclear Fusion 18 1(1978).

2. Report of the IAEA Consultants' Meeting on IAEA Report (1978) Fusion Programme for Developing Countries.

3. Procs. of Seminar on Plasma Focus Work in K.L. - Ed. S. Lee (1976). Plasma Fusion Research at the University of Malaya in Procs. of Symposium on Physics pg. 67-74 - Ed. S. Lee (1977).

4. See also 'Autumn College on Plasma Physics' by Y.H. Chen in this issue of the Buletin Fizik.

A MEASUREMENT ON THE BLUE (425-475nm) CONTENT OF SOLAR RADIATION TO DETERMINE THE EQUIVALENCE OF SOLAR RADIATION AND THE RADIATION OF LAMPS USED IN THE TREATMENT OF NEONATAL HYPERBILIRUBINEMIA

S. Lee, FIPM
Jabatan Fizik, Universiti Malaya,
Kuala Lumpur

Introduction

Phototherapy is now a standard measure in the management of neonatal hyperbilirubinemia[1]. Using daylight and blue lamp Tan[2] has determined that the minimal radiance at which phototherapy begins to be effective was 15 $\mu w/cm^2$ in the 425 to 475 nm range and that the saturation point of phototherapy appeared to be about 600 $\mu w/cm^2$ in the 425 to 475 nm range. The criterion for judging both minimal effectiveness and saturation was the measurement of the decline of the bilirubin level over an operational 24-hour period. A typical value adopted for phototherapy is 250 $\mu w/cm^2$.

Sunlight as a source for phototherapy has also been tried. But with sunglight, because of its high intensity and wide spectral range, overheating with phyrexia[1] and sunburn very easily occurs. Usually a 20-minute exposure to morning sun is the maximum permissible for an infant due to the danger of these side-effects.

The question then arises, what is the equivalence of a 20-minute exposure to morning sun in terms of the more controllable use of lamps? There are two factors in the establishment of this equivalence. Firstly, the equivalence can be considered in terms of incident energy in the 425 to 475 nm range. Thus, if the sun has a radiance in the 425 to 475 nm range of 100 times that of the lamps used then as far as energy equivalence is concerned an exposure to the sun for a period of time which is 1/100 the exposure to the lamps would ensure an equal amount of energy incident on the subject. Secondly, equivalence of incident energy may not really mean equivalence in effect, i.e. a 100 fold increase in radiance operational for a reduced period of 1/100 may not

produce an equivalent effect since from the literature[2] it is not clear whether the saturation effect reported is solely saturation to energy or solely saturation to radiance.

This issue, however, cannot resolved by the following measurement. Nevertheless, it has to be considered before any attempt to establish an effect equivalence may be made.

Measurement

A Metrix Luxmeter is used for this measurement with two ranges 0 - 500 lux and 0 - 2000 lux respectively. This meter uses a photcell which has been corrected by means of a filter to have a response almost identical to that of the human eye.

The range of response is between 4500 to 6500 Å with negligible response beyond this range. From the response curve supplied by the manufacturer, an integration over this curve yields an average sensitivity of 0.50 relative to peak sensitivity over the range 4500 to 6500 Å.

A relationship between the wattage of sunlight falling on the luxmeter and the luxmeter reading can be written down by considering the following two factors. (1) The spectral distribution of sunlight over the range of 4500 to 6500 Å is almost flat, deviating from a flat horizontal line by an average value of less than 5%. (2) At peak sensitivity, the luxmeter sensitivity is given as:

$$1 \text{ lux} = 0.161 \ \mu w/cm^2$$

Thus the wattage of the sunlight (in the range 4500 to 6500 Å) falling on the luxmeter

$$\frac{L}{0.5} \times 0.161 \ \mu w/cm^2 = 0.32L \ \mu w/cm^2.$$

where L is the luxmeter reading when placed in the sunlight.

The wattage of sunlight in the range 425 to 475 nm can now be estimated using the table of solar spectral irradiance given in table 6k - 17 on page 6-216 of the Handbook for Physics & Chemistry or by an integration of the solar spectral distribution such as is given in

Fig. 16 of Ref. 1. These procedures yield a figure of 0.27 as the ratio between the powers in the range 425 to 475 nm and the range 450 to 650 nm.

Thus the conversion expression for the luxmeter when placed in sunlight is:

radiance in the range 425 to 475 nm
= 0.32L $\mu w/cm^2$ x 0.27 = 0.09L $\mu w/cm^2$

Four readings were taken and recorded in Table I.

Table I

Reading no.	Luxmeter reading (with X400 attenuator)	radiance (435 - 475 nm)
1. 3.30 p.m. 31.7.78 dull day, sun hidden by thick clouds	10,000 lux	900 $\mu w/cm^2$
2. 8.30 a.m. 1.8.78 bright sunshine	17,000 lux	1500 $\mu w/cm^2$
3. 10.15 a.m. 1.8.78 bright sunshine	30,000 lux	2700 $\mu w/cm^2$
4. 12 noon 1.8.78 bright sunshine	50,000 lux	4500 $\mu w/cm^2$

These figures are compared to calculations based on data taken from Tan[4] and the Handbook of Physics and Chemistry[3]. Fig. 8 on page 40 of Ref. 4 gives the total radiation for the month of July as:

8.30 a.m.	20 $\mu w/cm^2$
10.00 a.m.	40 $\mu w/cm^2$
12 noon	58 $\mu w/cm^2$

Ref. 3 gives a value of 7.1% for the fraction of total solar energy in the range 425 to 475 nm. Combining the data of Ref. 4 and Ref. 3 above gives the radiance in the range 425 to 475 nm in July as:

8.30 a.m.	1400 $\mu w/cm^2$
10.00 a.m.	2800 $\mu w/cm^2$
12 noon	4100 $\mu w/cm^2$

Thus the present measurements are in close agreement with the estimates based on Ref. 3 and Ref. 4; although the data of Ref. 4 were

taken for Singapore.

Discussion

It appears that at 8.30 a.m. on a bright sunny morning, a representative figure for the purpose of discussion can be taken as 1500 $\mu w/cm^2$ for the radiance in the range of 425 to 475 nm. If we consider in terms of energy equivalence, 20 minutes exposure to this 'blue radiation' would be equivalent to an exposure of 20 $\mu w/cm^2$ for a period of 24 hours. On this basis of equivalence, this 20 minutes exposure would produce a minimal decline in bilirubin level of 1-2% using data of Fig.4 of table II of Ref. 2. The actual effect could be even more minimal if we note that the solar radiance of 1500 $\mu w/cm^2$ in the range of 425 to 475 nm is in the saturation region as discussed in Ref. 2. As was discussed earlier in the Introduction, if the saturation effect detected by Tan[2] were a radiance saturation effect then this would mean that the effect of sunlight (20 minutes exposure early morning sunlight) might be too small to be measured. If however the saturation effect were an energy saturation effect then a minimal decline of 1-2% might be measurable as extrapolated from the data of Tan[2].

Conclusion

20 minutes of exposure to 8.30 a.m. sunlight gives an energy equivalence of 20 $\mu w/cm^2$ in the range 425-475 nm incident over a 24 hour period. From published data, this exposure is expected to produce a minimal (hardy detectable) 1-2% decline in bilirubin level, if we assume that equivalence in incident energy gives an equivalent effect. This is in agreement with preliminary observations made by Lin[5].

On the other hand, an exposure of 80 minutes would give an energy equivalent of 80 $\mu w/cm^2$ over a 24-hour period which according to Ref. 2 would give a considerable decline in bilirubin level of 19%.

Without some form of filtering of the unwanted portions of the solar spectrum such a long exposure is evidently not desirable because of the attendant side-effects of overheating and sunburn.

References

1. K. L. Tan — The Seventh Haridas Memorial Lecture (1977) "Some Aspects on the Management of Neonatal Jaundice in Singapore"

2. K. L. Tan — "The Nature of the Dose-response Relationship of Phototherapy for Neonatal Hyperbilirubinemia" J. of Pediatrics, pg. 448-452 (1977)

3. Handbook of Physics and Chemistry

4. B. C. Tan — M. Sc. Thesis (1962) Singapore "An Investigation of the Solar Radiation at Singapore"

5. H. P. Lin — Private Communication (1978)

Buletin Fizik Vol.1 No.3 1980

EXPERIMENTAL PHYSICS RESEARCH IN THE UNIVERSITY OF MALAYA

B.C. Tan, FIPM and S. Lee, FIPM
Jabatan Fizik, Universiti Malaya,
Kuala Lumpur

The following are the main areas of experimental research currently being pursued at the Physics Department of the University of Malaya. Unless otherwise stated, the research is funded by the F-grant allocation from the University of Malaya.

1. Plasma Physics

The activities of the Plasma Physics Group centres around the Plasma Research Laboratory in which are housed two major machines, namely the UMDPFI (University of Malaya Dense Plasma Focus I) and the UMDPFII (University of Malaya Dense Plasma Focus II). The UMDPFI was designed and built locally, parts of it were donated by the U.K. government under the Colombo Plan. It consists of four module having 25 pieces of 0.6 μF Wego condensers rated at 40 kV. The modular condenser banks can be operated indenpendently or simultaneously. Research with this facility has been concentrated on the dense plasma focus.

The UMDPFII machine and its 60 megawatt pulse ruby laser were donated by the Alexander von Humboldt Foundation and the Nuclear Research Establishment of the Federal Republic of Germany. This machine consists of 12 pieces of 1.85 μF Maxwell condensers rated at 60 kV. Metal strips connect the condensers to the vacuum spark gap thereby reducing the inductance and hence making the machine a very fast one. The machine will operated as a vacuum spark incorporating an anode with an insert of solid lithium deuteride. Switching and initial plasma formation is achieved by the ruby laser pulse.

Among the ancillary equipment are an Imacon camera, a Kerr cell camera, a transient digitiser, a screen cubicle and several good oscilloscopes.

2. Thin Films

The study of thin films of organic materials has been actively pursued. Preparation of these thin films is done in a vacuum evaporator. Measurements on the evaporated films include dc conductivity from liquid air temperature to 150°C and optical absorptivity at room temperature. Change over from amorphous to structured forms of the organic materials are studied by the X-ray diffraction method.

3. EM Scattering

Research is being done into EM scattering at microwave frequencies. The apparatus include a sweep-source generator and detecting devices. Presently, the scatterer is a cylindrically arranged cage. The experiment is performed in a specially constructed anechoic room.

4. Liquid Crystals

A study of phase transitions in liquid crystals from room temperature to 100°C is being initiated using platinum resistance thermometers and special adiabatic calorimeters.

5. Radioisotopes

Using a Phillips neutron generator the studies on activation analysis are performed on several isotopes. In this connection, the thermalisation of 14 MeV neutrons in paraffin wax was studies and a number of short-lived radioisotopes are produced. The very short-lived isotopes (∿ a few seconds) pose a serious difficulty in dead-time corrections for long counting intervals. A simple method is proposed for such cases. Ancillary equipment include a multichannel analyser and sodium iodide detectors along with liquid GM counters.

6. Laser Physics

A new Laser Physics Section has been formed to investigate pollution, namely, the identification, the concentration and the range of pollutants in chosen industrial areas. For this project, a 9 Watt CW Argon Ion Laser with associated detecting and measuring equipment have been purchased.

To develop technical skills with lasers, a proposal is made to construct simple lasers. An ultraviolet N_2 laser, a CO_2 infrared and a dye-laser have been constructed. The dye-laser is being used for absorption spectroscopy studies.

The CW CO_2 laser will be pushed to higher powers (100 W) for electrothermal cutting purposes. A TEA-CO_2 laser is being planned for plasma heating as well as multiphoton experiments.

bertugas, bertanggungjawab, mudahsuai, bersikap, kritik dan kreatif. Universiti mempunyai tanggungjawab untuk menyediakan kemudahan-kemudahan perlu bagi melaksanakan tugas pengajaran dan pembelajaran dengan baik dan sempurna agar ia boleh menghasilkan siswazah yang berpengetahuan, berkemahiran dan bersikap baik dan sempurna sejajar dengan kehendak negara.

8th INTERNATIONAL CONFERENCE ON PLASMA PHYSICS AND CONTROLLED NUCLEAR FUSION RESEARCH

S. Lee, FIPM
Jabatan Fizik, Universiti Malaya,
Kuala Lumpur

This Conference was organised by the International Atomic Energy Agency with the cooperation of the Plasma Physics Laboratory - Association "Euratom - Belgian State" Brussels. The Conference took place from 1st to 10th July 1980 in Brussels, and was preceded by a Special Session on INTOR (International Tokamak) on 31st June, 1980 and followed by an International workshop on the Plasma Focus on 11th July, 1980.

The Conference placed emphasis on Tokamak and inertial confinement systems. On these topics comprehensive papers were given by the various laboratories on experimental results, theortical calculations, plans for further experiments and design of reactors and reactor technology based on the Tokamak and the laser fusion concepts. For laser fusion the technological frontier appears to be involved in the increasing of laser energy and the tailoring of both laser pulse and the target pellets. For Tokamaks, medium sized machines are being constructed including the TEXTOR in West Germany, the JET in England (EEC project) and the JT60 by the JAERI, Japan Atomic Energy Research Institute. It is anticipated that when these and other medium-sized Tokamaks start to produce 'break-even' or near 'break-even' plasmas before the end of this decade, the technological frontier will be involved with tritium-handling, superconducting magnets, reactor wall materials

and auxiliary power injection. Foreseeing these problems, papers were discussed at this Conference on many aspects pertaining to them.

Several alternative fusion concepts were also discussed. These ranged from steady state toroids through long-pulse toroids to short-pulse linear systems that seem to go right back to the early-day classic linear pinch; which in this updated version has a large current flowing in a narrow (sub-mm) laser-initiated current-channel within a high pressure D-T gas.

Registered participants number 550 from 40 countries. Of these 17 participants were from developing countries including Argentina, Brazil, India, Kenya, Malaysia, Mexico, Pakistan, Turkey, and Zaire. This participation from developing countries mirrors the growing interest and ability of their scientists in the exciting and promising area of fusion energy. Brazil has started a Tokamak program to be followed soon by India which already has active plasma and laser activities as have Pakistan and Argentina. Malaysia was able to join in critical discussion in the plasma focus session and the International Plasma Focus Workshop.

It was very clear from the discussions, formal and informal, that many of the devices and techniques are well within the capabilities of some of the laboratories in developing countries, so that the classical concept that developing countries could only and therefore should only handle low-technology research appears to be not universally valid today. Scientists from developing countries gathered at the Conference were all of the opinion that the IAEA has taken a positive step in its present stand to encourage plasma research in developing countries, emphasizing on areas and projects that have proven to be fruitful.

CONVENTIONAL ENERGY SUPPLIES AND NON-CONVENTIONAL ENERGY RESEARCH IN MALAYSIA*

S. Lee, FIPM and B.C. Tan, FIPM
Physics Department, University of Malaya
Kuala Lumpur 22-11, Malaysia

Conventional Energy Supplies in Malaysia

Oil supplies 94% of current energy consumption in Malaysia. The other 6% is contributed almost entirely by hydro-power, wood and charcoal[1]. Total energy consumption in 1980 was 4.4 boe (barrel oil equivalent) per head of population per annum. This compares with the Japanese consumption of 25 boe and with the American consumption of 63 boe per head per annum.

Oil

Official estimates of the recoverable oil reserves in Malaysia is in the neighbourhood of 1 billion barrels. This estimate is generally agreed to be conservative. A more realistic estimate has been suggested to be in the neighbourhood of 3 billion barrels[2]. The extraction rate in Malaysia has risen from 346,000 barrels in 1966 to 100 million barrels in 1979. This compares with a domestic consumption of about 60 million barrels in 1980 (population 13.4 million). Malaysia is therefore a net exporter of oil.

A logistic curve has been suggested to help the understanding of production and as an aid to phase production. The logistic curve suggests an annual rate of production $\frac{dQ}{dt}$ which is proportional to the cumulative production Q and to the remnant reserve $Q_u - Q$ where Q_u is the original total reserve. A view of the crude oil production in Malaysia is shown in Figure 1 which compares the actual production with the logistic curve[2]. This figure indicates that current production greatly exceeds the logistic curve and suggests the need for careful control of our production rate.

K. K. Wong[2] has compared the Malaysian petroleum production logistic curve with the projected Malaysiam energy consumption rate assuming an

---

*Based on an invited paper presented at the COSTED Seminar on Energy Options for Developing Countries held in Madras 23rd - 27th February 1981.

annual increase of 7.3%. The projected consumption curve rises above the production curve in the mid 1990's at which point Malaysia will become a net importer of oil. Based on actual production trends, a cross-over point can be expected before 1990, unless the reserves of petroleum prove to be considerably greater than presently revealed.

Other resources

Malaysia has other energy resources which could be developed. These are listed as follows[2,4]:

Material	Quantity (million tons)	Total energy value (10^3 TJ)
Non-renewables		
lignite	600	5,300
natural gas	22×10^{12} ft^3	25,000
Renewables (per annum)		
rubber wood	7.0	88
timber waste	0.5	6
palm oil waste	8.8	55
domestic and animal waste		7
rice waste	1.2	15
sugar cane waste	0.9	11
solid municipal waste	1.8	11
hydro		61
		254

Among the non-renewables resources, lignite has one-third and natural gas almost twice the energy potential of our oil reserves. The renewables have the energy potential of 40 million boe per annum. The other resources are not exploited except for hydro-electric power and the limited use of some agricultural waste.

The Bintulu LNG plant is scheduled to produce 6 million tonnes of LNG per year (70 million boe) for export to Japan. The lignite deposits are of low grade quality and mining and burning this low grade lignite may cause

environmental problems. The agricultural waste at present represents not only an used resource, but its disposal as waste has resulted in environmental pollution. Attempts are already being made to solve the twin problem of wastage and pollution. There is little doubt that this source will contribute significantly to the energy needs of the nation before the end of the century.

'Soft' energy path

With our resources in oil, gas, lignite, agricultural waste and plentiful sunshine, there are proponents for Malaysia to follow an exclusively 'soft' energy path, For example in the paper by K.K. Wong[2] an energy plan was proposed for Malaysia as illustrated in Figure 2. This plan envisages increasing use of lignite, natural gas, bio-waste, biomas, starting around 1995 with contributions from solar cell and solar air-conditioning around the turn of the century. By 2030 the plan has lignite, natural gas, biowaste and hydro-power supplying about half of the nation's energy needs, with the other half being supplied by biomass, solar cell and solar air-conditioning. Noting that by 2030 the total demand curve shows Malaysia's energy consumption to be 30 times the 1980 consumption, the envisaged contribution by solar cells amounts to almost 200 million boe per annum or 3 times the total 1980 energy consumption.

The role of 'hard' energy

There is another school of thought which argues that, 1) oil and gas should be reserved as much as possible for industrial and transport sectors and as feedstock for petro-chemical industries, and 2) biomas, solar cells and solar air-conditioning etc will not contribute to the extent proposed by the 'soft' energy proponents.

Ahmad Tajuddin[3], for example, has projected a required increase for electricity from 2000 MW (1980) to 11,000 MW by the year 2000. His studies recommend a nuclear capacity of 6300 MW to 11,100 MW by the year 2005. A review by the Malaysian National Electricity Board in the mid-1970's suggested that there is an economic feasibility for power reactors sometime in the 1990's.

100% 'soft' package vs a 'soft-hard' mixed package

The case for planning for a 100% soft-energy programme appears to hinge on whether biomas, solar-cells, solar air-conditioning and possibly other solar-based technology could supply the nation with up to 50% of its energy requirement by 2020-2040; an amount of energy equal to 3000×10^3 TJ or 1300 million boe per annum. To examine the feasibility of such a scheme, it should be noted that the land area needed for energy plantations to supply 10^6 TJ (15% of energy needs in 2030) is 6000 square miles or 10% of the total land area of Peninsular Malaysia. For the amount of electricity envisaged to be supplied by solar cells, up to 1000 square miles have to be covered with solar cells and support structures; similarly several hundred square miles will have to be covered with collectors for the solar air-conditioning systems. The size of the required areas compares with an estimated figure of less than 100 square miles for the total surface area of roof structures currently in Malaysia.

The question of availability of land, availability of construction resources and the environmental impact of the novel usage of such large tracts of land have to be examined besides the question of cost of solar cells which is unlikely to go below US$1.00 per peak watt unassembled cost.

It appears unavoidable that an examination of the above questions will show large gaps in the energy supply picture as envisaged by Figure 2. The gaps will apear by the year 2000 and will widen towards the year 2040. Nuclear proponents recommend filling this gap with nuclear fission reactors.

Status of nuclear fission as an energy source

The material progress of Man is directly related to his usage of energy. The use of wind energy and the energy of flowing water enabled some amount of work to be done; but it was the large scale burning of fuels during the industrial revolution which led to the rapid growth of modern civilization as we know it today. The key to that particular phase of rapid growth of civilization appears to be the switch from the use of diffuse forms of energy to the massive use of concentrated fuels.

The atomic age has brought an even more concentrated fuel, nuclear fuel,

for nuclear burning. One nation is already moving rowards a major dependency on nuclear fission - France. From 1980 to 2000, the production of electricity in France by nuclear reactors will rise from 20% to 80%. However in the long term, nuclear fission can only be a transitional solution. Leaving aside the politically volatile nature of fissile materials and the serious problems of radioactive pollution and waste disposals that can arise through a world-wide dependence on uranium, mankind is still faced with the fact that there is a limited supply of economically recoverable fissile fuel, estimated at 10 million tons of U_3O_8. Even assuming that breeder reactors are perfected, this amount of uranium ore is sufficient to supply the energy needs of the world for only 1 to 2 centuries.

Nuclear burning will come into its own only with the development of the nuclear fusion reactor.

Nuclear fusion as an energy source

Nuclear fission is the splitting up of a heavy nucleus such as uranium 235. In this reaction energy is release. The atomic bomb is an example of the harnessing of this energy for violent purposes. The nuclear fission reactor is an example of the controlled use of this energy source.

Nuclear fusion is the process wherein two light nuclei fuse together forming a heavier nucleus. In this reaction energy also is released. The hydrogen bomb is an example of the violent release of energy from this process. The sun is a natural fusion reactor.

The biggest advantage of a fusion energy source is that, once developed, it will provide energy practically for infinity. The fuel is deuterium, an isotope of hydrogen which exists in all water to the extent of one deuterium atom to 6500 atoms of ordinary hydrogen. The fusion energy potential of 1 litre of water equals the combustion of 300 litres of gasoline. The fusion energy potential of only 1 part per million of the deuterium contained in the waters of the world is sufficient to provide 100,00 times the present world energy consumption. Moreover, the end product of the reaction is helium and the radioactive waste problem is minimal when compared with the fission reaction. A fusion reactor using the magnetic fusion principle will operate

with a low particle density and a relatively low energy density so that an explosion would not be more violent than an explosion involing an oil-fired power plant of equal capacity.

Development of fusion research

W.H. Bennett had developed in 1934 the theory of the constricted discharge current in a gas; but it was not until 1946 that the use of electric currents to generate high temperatures was demonstrated by Thonemann in Oxford and Ware at Imperial College. By the early 1960's several early ideas has been tested, notably the much publicized stellarator and it was realised that the application of brute force alone could not succeed. Whilst a large heating current was applied the plasma had to be contained, and subtly, by magnetic fields. Enough was learned for it to be realised that scientific feasibility of fusion energy would have to be proven as a first goal.

Scientific feasibility would be proven when break-even conditions are attained. Break-even would be achieved when in a heating cycle the gross energy input to heat the plasma equals to the net energy output from the plasma from thermonuclear fusion reactions. It is known that two critical parameters are involved in the establishment of break-even. These are the ignition temperature and the thermal insulation factor which is the product of fuel particle density n and the containment time τ at the ignition temperature.

For a deuterium-tritium plasma break-even will be achieved when the following plasma parameters are simultaneously attained:

temperature of 45^{o} million ^{o}C

$n\tau$ product of 10^{14} cm^{-3} sec.

Scaling for $n\tau$

The scaling law for $n\tau$ for a Tokamak configuration is now known. To achieve an $n\tau$ of near 10^{15} for a reactor regime the following Tokamak machine parameters are required:

1. large minor diameter of at least 4 m
2. large major diameter of at least 12 m
3. large heating current of at least 10 million amperes sustained for seconds
4. large stabilising magnetic field over the entire plasma colume of 5 T sustained for seconds.

The construction of a Tokamak with these machine parameters require several technological developments including production of the required large volume magnetic field, tritium handling and reactor wall technology. A recent development in the United States has given the fusion research fraternity a glimpse of the serious commitment that at least one major power has undertaken towards the development of this energy source. This is the Magnetic Fusion Engineering Act 1980 adopted by the U.S. Congress establishing the following national goals: to prove engineering feasibility by early the 1990's and to operate a magnetic fusion demonstration plant by 2005.

The confidence and commitment that the U.S. has expressed in fusion as an energy source must at least in part be due to the world-wide progress in plasma containment in Tokamak experiments. This is illustrated in Figure 3 In this figure it is seen that the promise shown in early 1950's experiments soon led to a decade of frustration when in the 1960's the value of $n\tau$ could not be pushed past 10^{11} cm^{-3} sec. The breakthrough came in 1973 when the French TFR group reported results with $n\tau$ in excess of 10^{12} cm^{-3} sec. These results were quickly confirmed by similar Tokamaks and the PLT group in Princeton raised the $n\tau$ parameter to 10^{13} cm^{-3} sec in 1976. The next generation of Tokamaks planned for operation around the mid 1980's includes the JET (Joint European Torus of the EEC), the JT-60 (Japan), T-20 (USSR) and the TFTR (USA). These machines, with plasma diameters of the order of 1-2 metre are expected to be marginally touching the scientific feasibility regime. Doubtless plans are being made now, at least in the U.S., for machines which will operate clearly in the scientific feasibility regime and the demonstration reactor regime. On the international scale the INTOR (International Tokamak) project currently being discussed by a study group initiated by the IAEA might develop into the international project to clearly demonstrate scientific feasibility.

The scope of the current international effort to harness fusion energy is depicted schematically in figure 4.

Research on non-conventional energy sources in Malaysia

In the above, a survey has been made which shows that Malaysia, like other countries of the world, has to plan her energy development carefully. The reserves of oil give the country a breathing space to implement the use of natural gas and lignite by the 1990's. At the same time the country has to continually increase the hydroelectric output and undertake research into the conversion of bio-waste into energy, the cultivation of biomass for fuel and the collection of solar energy for air-conditioning and electricity production. Projecting a rate of increase in energy consumption of 7% per annum, it is expected that despite all these developments, serious gaps will appear in the energy supply early in the 21st century, so that the introduction of nuclear fission reactors has to be seriously considered. In the long term, for Malaysia as well as for the world, even nuclear fission will only be a transitional source of energy, In anticipation of long term needs, development of fusion energy becomes essential.

Research into renewable sources of energy

Bio-waste is already used in Malaysia in a limited extent for energy generation; e.g. many palm oil mills use palm oil waste to generate much of their own requirement of energy. Other types of waste are being looked into. Recently the University of Malaya has developed a furnace for pollution-free sawdust disposal. Such a furnace could also serve a second purpose as a heat generator. SIRIM (Standard and Industrial Research Institute of Malaysia) has developed a simple device to convert rubber wood into charcoal. Some research on the production of alcohol from bio-waste and bio-mass is being carried at various institutions[5-10]. A group at the USM (University of Science Malaysia) has made careful measurements of the energy content of local plant material and plant waste[11].

Research into solar collectors is being carried out in several institutions. At the University of Malaya studies are being made on designs of flat-plate solar heat collectors and the application to solar water

heaters[12]. At the UPM (University of Agriculture Malaysia) and SIRIM, solar drying is being developed[13] and at the USM solar cell fabrication and the use of solar cells for powering water pumps has been studied[14].

Fusion research

In the early 1960's low temperature plasmas were studied at the University of Malaya. An electric capacitor bank was acquired as a gift of the U.K. government through the Colombo Plan. In 1970 this capacitor bank was redesigned as a powerful electric current generator producing 2 million amperes of pulsed current which when applied to a plasma focus device produced plasma temperatures of 8 million ^{o}C, sufficient for fusion neutrons to be detected from the deuterium plasma in 1973.

A period of technical development followed in plasma measurement, diagnostics and modelling specifically concerning neutron yield, energy and distribution, soft X-ray yield and spectroscopy, plasma temperature, density, dynamics and electromagnetic characteristics and in optimising the performance of the plasma focus[15].

In 1976, a second capacitor bank was acquired from the Kernforschungsanlage Juelich together with a pulsed ruby laser from the Alexander von Humboldt Foundation. This enable laser diagnostics of the plasma focus to be developed. A new experiment 'laser-initiated fusion spark' was developed attaining a temperature of 90 million ^{o}C in 1980.

Currently a small Tokamak is being planned.

Fusion research and developing countries

In 1978 the IAEA reviewed world-wide work on fusion[16,17]. The status report concluded that the time was ripe for a large effort towards the practical demonstration of fusion power. In order to optimize world-wide cooperation in this effort the Report recommended, among other steps, that action should be taken to identify problems where no large apparatuses are needed and which can be tackled by developing countries.

One of the concrete steps taken by the IAEA as regards the encouragement of fusion activities in developing countries is the holding of a 'Spring

College on Fusion Energy' at the ICTP in Trieste this May at which fusion work in developing countries was highlighted

Conclusion

In this paper, the energy situation in Malaysia, as an example of a developing country, has been reviewed. It is seem that an effort is being made to develop 'soft'-energy sources to supplement the depleting fossil fuel. It is also seen that there are scientists in Malaysia who are aware of the essential nature of a permanent solution to the energy problem - a solution which appears to depend on the development of fusion energy.

In order to emphasise the long-term implications of the energy problem to the developing countries and the world, this paper concludes with figure 5 which looks at the projected consumption curve of the world against the projected supply curves of fossil fuels, fissile fuels and renewables. The general shape of these supply curves will not be disputed although with varying estimates of 'economically-recoverable' reserves the peaks of the fossil and fissile fuel curves may be varied from the positions they are assigned in this figure. The curve for the renewables is certainly not unduly depressed because optimistic goals set by the U.S., Japan and India regarding the percentage of energy consumption to be supplied by renewable sources by the turn of the century do not exceed 20%, 10% and 15% respectively.

The demand curve at first glance appears to rise to impossible heights. But Prof. Menon in his Inaugural address to the COSTED Seminar on Energy Options for Developing Countries in Madras (23-27 February 1980) mentioned an inevitable growth of world power consumption from the present 8 TW to a figure of 18 to 80 TW over the next 50 years. Prof. Chowdari in his address expressed disappointment that India would be barely able to double her energy consumption by the end of this century. These were all conservative estimates and are consistent with the 3% growth rate in energy consumption assumed in the demand curve of figure 5.

There is a fundamental reason why the energy consumption curve must rise inexorably by a factor of at least 20 times the present consumption. At present only a few precent of the people of the world have a standard

of living commensurate with the average human capacity to reason and to want. Because these few percent have, by endeavour, and in some case by luck, attained a good standard of living, the rest of humanity see the good things that come with a good standard of living and will continually strive towards achieving this higher standard. Considering a minimum projected increase in world population and assuming somewhat optimistically that the continual increase in energy consumption also leads to an eventual fairly uniform distribution of energy consumption over the world a 20 times increase in energy consumption by the third quarter of the 21st century will still be hardly enough to provide a universal reasonable standard of living.

Unfortunately, before this 20 times point is attained a critical point would have been reached, about the middle of the 21st century, at which the total energy output of fossil, fission with breeding, and renewable sources will become insufficient to sustain the increase in energy consumption. Such a situation will intolerably conflict with the inexorable social and political pressures for increase in energy consumption.

In fact the energy shortage would become increasingly intolerable long before the critical point is reached.

That critical point in human history will however be averted because whilst attending to our short term energy gaps by developing energy technology utilizing bio-waste, biomass, solar heating, solar electricity and wind and wave energy, the world, including the developing countries, is also looking toward the long term and will develop in time a permanent and limitless source of energy such as nuclear fusion.

References

1. Ministry of Energy, Telecommunications and Post 'Status of Energy Conservation in Malaysia', Tenaga 80, Kuala Lumpur (1980)
2. K.K. Wong, 'A Soft Energy Path for Malaysia', Tenaga 80, Kuala Lumpur (1980)
3. Ahmad Tajuddin, 'The Role of Nuclear Power in Electricity Generation in Peninsular Malaysia from the Mid 1990's Onwards', Tenaga 80, Kuala Lumpur (1980)

4. Abdul Rahim b. Haji Din, 'Malaysian Petroleum Policies and Plans', Tenaga 80, Kuala Lumpur (1980)

5. Hussein bin Rahmat, 'Methanol: The Liquid Energy Substitute for the Transportation Sector of Malaysia', Tenaga 80, Kuala Lumpur (1980)

6. W.C. Lim, 'The Prospects of Utilization of Bio-energy in Malaysia', Tenaga 80, Kuala Lumpur (1980)

7. Rahim Abidin, C.N. Chong, and T.S. Pang, 'The Scope for the Production of Alcohol for Energy Uses in Malaysia', Tenaga 80, Kuala Lumpur (1980)

8. J. Kader, M.S. Jangi and E.E.T. Teik, 'Tapioca Waste as a Source of Energy - Preliminary Work on Biogas Production', Tenaga 80, Kuala Lumpur (1980)

9. Rahim Abidin, C.N. Chong and K.H. Chia, 'Rice Husk as a Source of Energy', Tenaga 80, Kuala Lumpur (1980)

10. Mohamad Salleh Ismail, 'Gasohol - Its Potential in Malaysia', Tenaga 80, Kuala Lumpur (1980)

11. K.O. Lim, and R. Ratnalingam, 'Energy from Agricultural Wastes - Is it a Worthwhile Consideration in Malaysia?', Tenaga 80, Kuala Lumpur (1980)

12. K.S. Ong, 'Thermal Aspects of Solar Energy Utilisation', Procs. Int. Conf. on Physics - Bull. Inst. Phys. Malaysia, 1-4, 185 (1980)

13. Van Vi Tran, Selehuddin bin Mahmud and Zainal Abidin bin Ali, 'Experimental Results of a Continuous Solar Dryer for Paddy', Tenaga 80, Kuala Lumpur (1980)

14. D.G.S. Chuah, S.L. Lee and C.K. Koh, 'Water Pumping by Photovoltaic Solar Energy', Tenaga 80, Kuala Lumpur (1980)

15. S. Lee, 'Review of Plasma Physics Research in Malaysia', Symposium on Plasma Research, Theory and Experiment, International Centre for Theoretical Physics, Trieste, Italy, (June 1981),(to be published in the Procs.)

16. International Fusion Research Counil 'Status Report on Controlled Thermonuclear Fusion', Nuclear Fusion, 18, 1 (1978)

17. Report of the IAEA Consultants' Meeting on Fusion Programme for Developing Countries, Swierk, Poland (1978)

Fig. 1: Crude Oil Production Picture - Malaysia

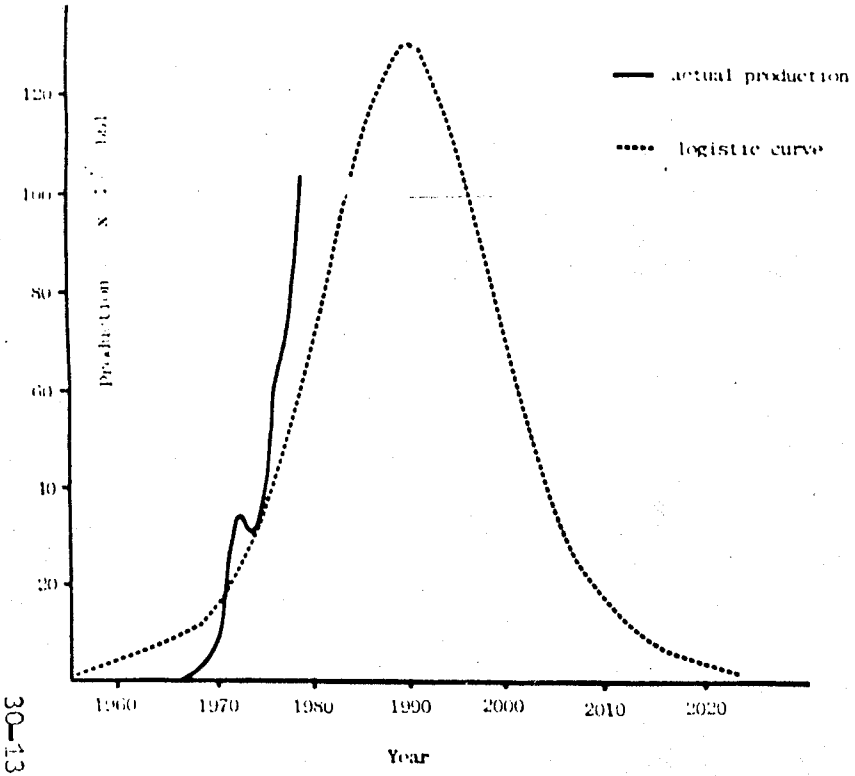

$Q_t = 2.8 \times 10^9$ bbl

1966 production 346,000 bbl

1978 production 100 million bbl

Figure 2: Energy Supply Sources for Malaysia till 2040.
(after Wong Kien Keong)

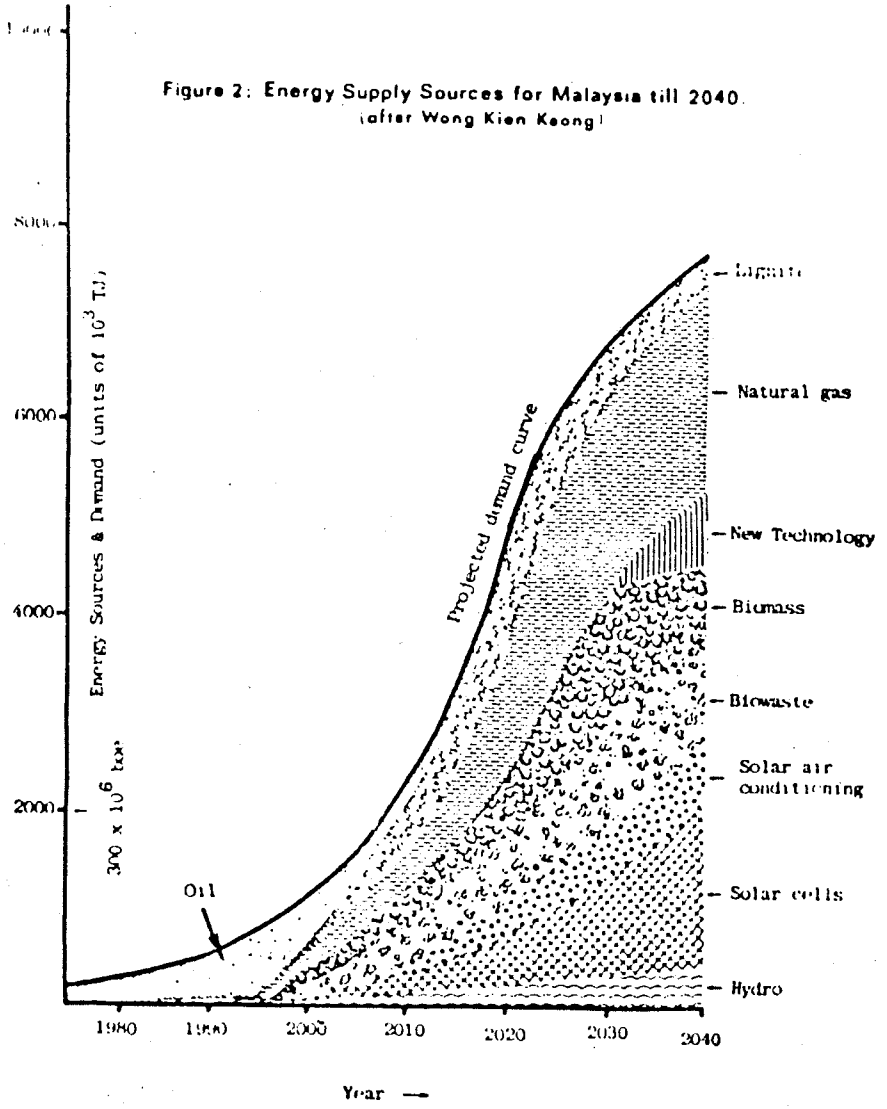

Fig. 3 Progress in Containment Time Experiments in Tokamaks

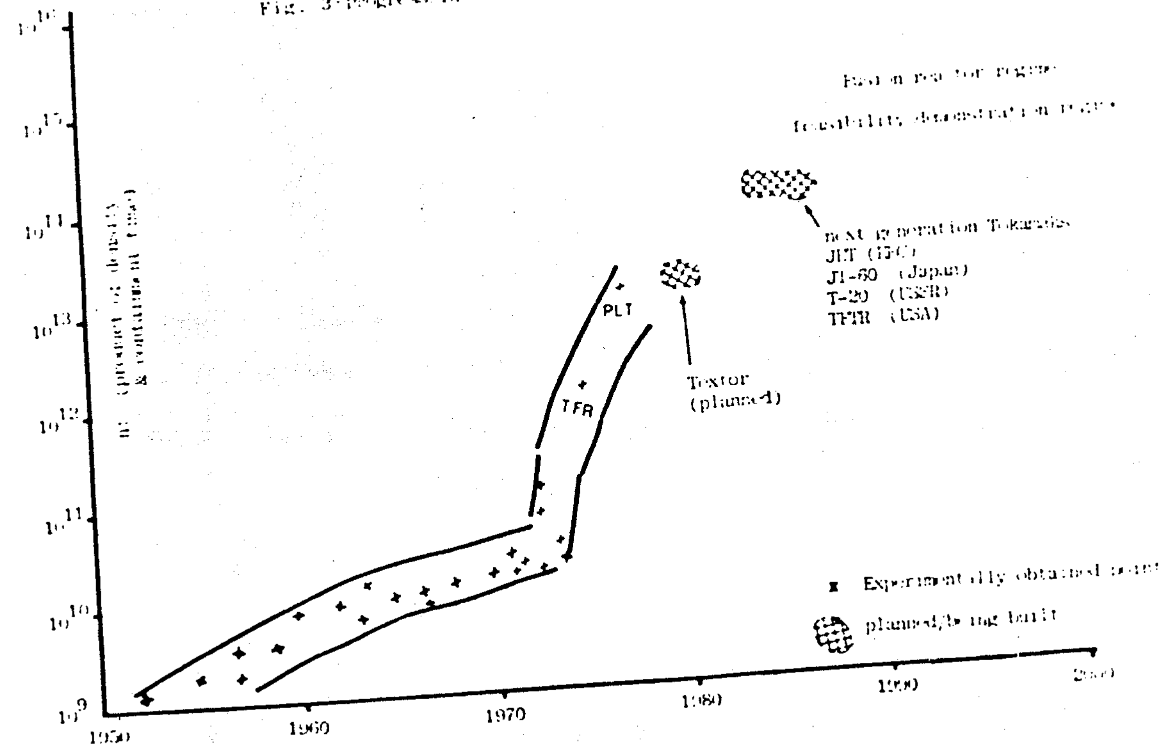

Fig. 4 International Program to build a Nuclear Fusion Reactor

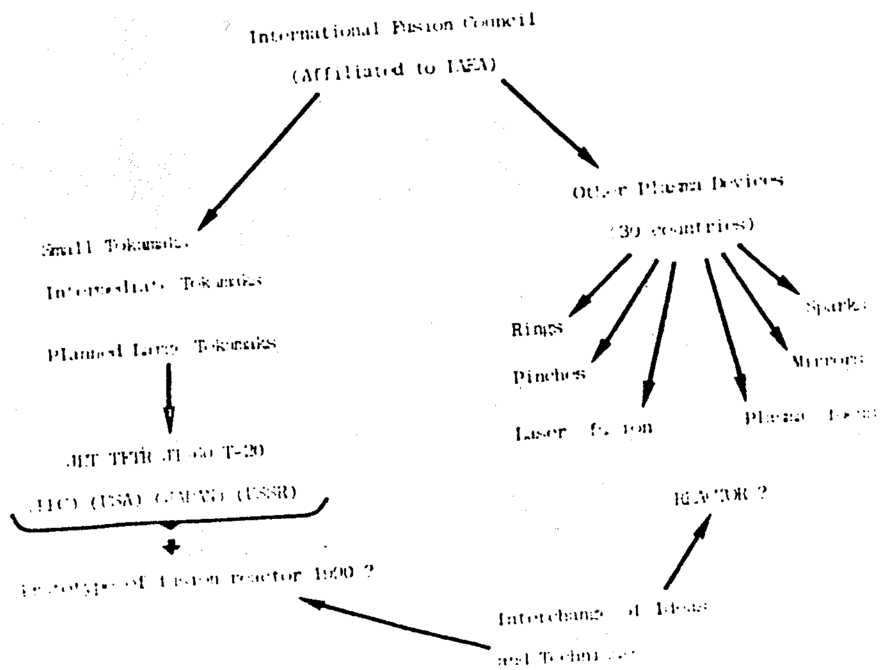

Figure 5: Impact of Fusion Energy on Future of Civilisation.

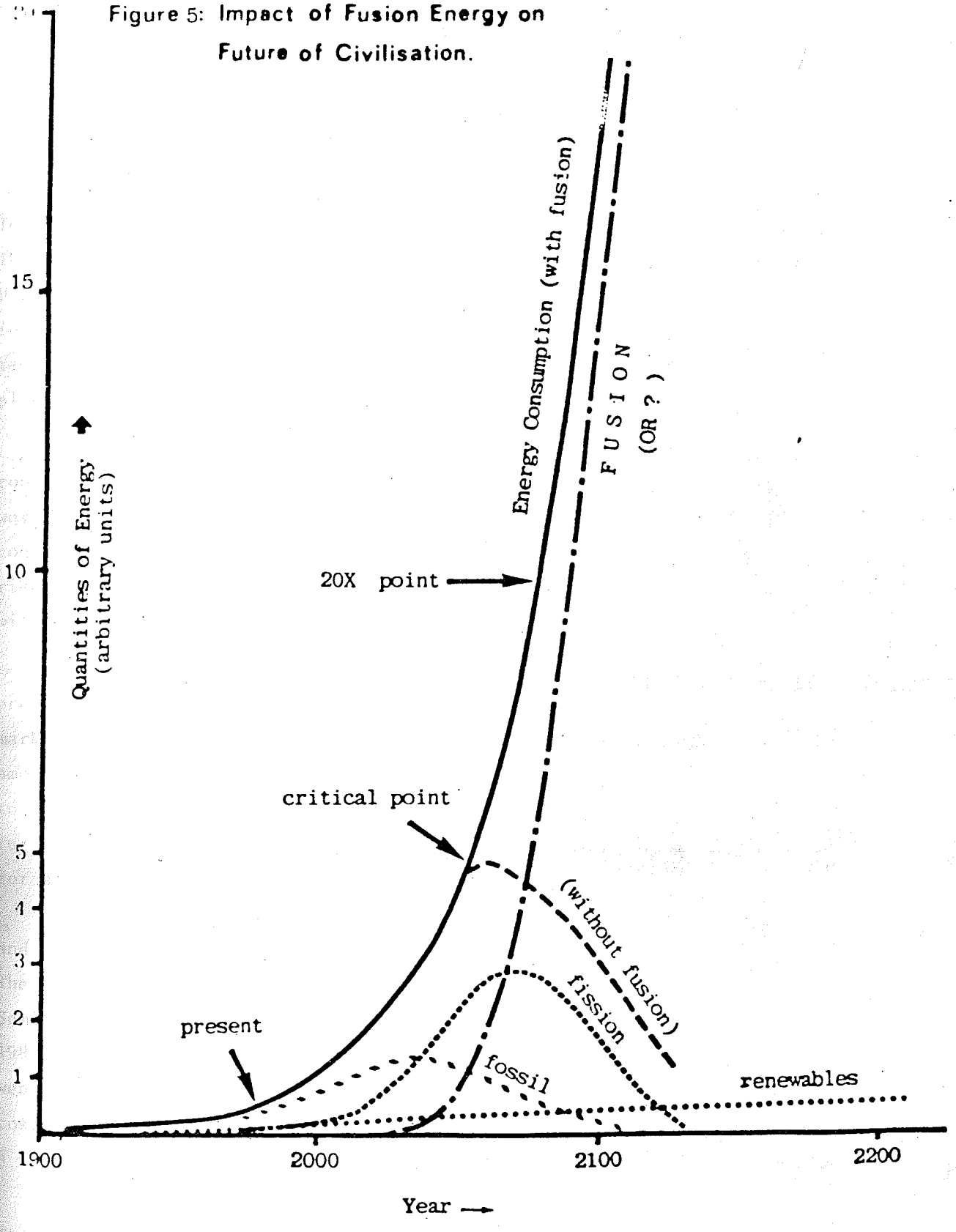

REPORT ON SEMINAR ON ENERGY OPTIONS FOR DEVELOPING COUNTRIES MADRAS 23rd - 27th FEBRUARY 1981

S. Lee, FIPM
Jabatan Fizik, Universiti Malaya
Kuala Lumpur

The Seminar was arranged by COSTED (Committee on Science and Technology in Developing Countries). Participants from India, Malaysia, Indonesia, Tanzania, Sri Lanka, Bengladesh, Australia, England, France and U.S.A. gathered to discuss energy options in various stages of development including solar heating, solar cells and solar electricity, solar refrigeration, wave and ocean thermal energy, wind energy, bio-gas, bio-plantations, fusion energy and hydrogen technology.

Professor Menon of the Indian Science Research Council set the tone of the Seminar by noting that the non-developed countries of the world has 70% of the world's population but only 20% of the world's energy consumption. He also noted that the world-wide consumption of power will rise from the present 8 TW to between 18 TW to 80 TW in 50 years. How will this increase in energy consumption be met?

Several delegates from India, Australia, Italy and the U.S.A. presented papers on solar cell technology, solar cell fabrication and marketing strategy. Research work on dendritic web silicon ribbon and amorphous silicon cells was discussed. There is a joint US-Italian plan to accumulate 10,000 tons of solar-grade silicon feedstock in preparation for mass production and intensive marketing. Two critical cost factors for solar cells to become competitive appear to be

i. US$ 10,00 per kg for solar grade silicon (10% efficiency)
and ii. US$ 2.00 per peak watt assembled cost.

The 1980 cost is $10.00 to $15.00 per peak watt and it was claimed at the Seminar that a cost of $3.00 per peak watt assembled could be attained by 1986. In particular Westinghouse aims to produce 18% efficient dendritic web cells by 1982 and to achieve US 68 cents per peak watt unassembled cost by 1986. Sales figures of 2 MWp was estimated for 1980 and by 1986 a world sales figure of 400 MWp was projected.

In Japan, several types of collector plates using ion-plated selective coating and evacuated-tubes are commercially produced and widely used for hot water production. A nickel-nickel oxide thin film has been developed with an absorption coefficient of 0.91 and emittance coefficient of 0.06 giving 54% collection efficiency which compares favourably with the 33% efficiency of black painted surfaces. There is legislation to encourage more widespread use of solar collectors as an oil-replacement measure. A first target of 1 million square metre of collectors is set for commercial buildings in Japan.

Another option on which emphasis was placed by delegates was bio-gas. Using animal waste and plants like water-hyacinth bio-gas plants can be assembled at a cost of 8,000 Rupees per kW compared to an average of 14,000 Rupees per kW of gride electricity. New and more efficient bio-gas designs are being researched and the UNESCO delegate also emphasised on related bio-technology. Noting that India has installed only 80,000 bio-gas plants compared to several millions in China, the Seminar agreed that there is great potential for this energy option in developing countries.

Two delegates from U.S.A. presented papers on Ocean Thermal Energy Conversion and discussed the 1 kW test plant that has been operated in Japan and the 40 MW OTEC pilot plant designed by John Hopkins University. Another aspect of energy from the ocean was presented in the Dam-Atoll concept. In this concept ocean waves sweeping towards a floating atoll diffract around it resulting in a system of waves which crashes over the atoll from all sides. A vertical channel at the centre of the atoll carries the water from the waves downward, diverting the wave energy onto a turbine. A study has shown an optimum size of 80 - 100 m diameter for waves of 3 - 6 m high. A 1/100 scale model has been successfully tested and a 1/50 model is being planned.

The Seminar also discussed technical details of devices such as solar box cooker, solar pond, MIS solar cells, solar pumps for irrigation, solar powered refrigeration cycles, sodium sulphur batteries for energy storage, windmill technology, integrated food-energy approach to an Indian rural community, hydrogen as replacement for gasoline and devices using

muscle power.

Underlying the whole discussion was a feeling of urgency. An Indian delegate felt that with all the development effort India would still barely be able to double her energy supply by the turn of the century. The Indonesian delegate bluntly stated that none of the energy options discussed would solve the present and near-term energy problem of the least developed countries. The only solution was to import more oil! The Malaysian delegate pointed out that although the renewables are certainly important energy options, they are not expected to supply the bulk of the energy requirement both in the short and the long term. The U.S., Japan and India have set what are regarded as optimistic goals for total contribution by renewable sources but these goals amount to less than 20%, 10% and 15% respectively targeted for the year 2000. With a conservative projected annual energy demand increase rate of 3%, by the middle of the next century, the total fossil, fissile and renewable resources would not be able to sustain the increase in energy demand necessary to enable the world community at large to progress towards a universal reasonable standard of living. The solution is to develop a limitless energy source such as fusion. Developing countries like India, burdened with a huge population five-sixth of whom depend for their energy requirement on cow-dung and nearly depleted wood, are in a desperate position and need to develop energy options as rapidly as possible for the short-term requirement. On the other hand other developing countries, like Malaysia and Indonesia, are more fortunate and are able to formulate adequate energy policies to optimize the usage of their energy reserves. They are in a position to look at energy options more calmly for the near, middle and long term. This is reflected for example in Malaysia's energy research programme which range from renewables like bio-waste and solar energy to long term energy research like plasma fusion.

The Seminar closed with the formulation of a list of recommendation to be presented to the forthcoming United Nations Conference in Nairobi. The list presents the energy options which the Seminar has agreed that the U.N. should support for research and development programmes in

developing countries. The recommendations emphasized the potential of bio-technology related energy options and also included solar, wind, wave and fusion as areas of research to be supported.

The Seminar also recommended the establishment of an 'Energy Company' and research networks in developing countries. The functions of the 'Energy Company' include the evaluation of energy options and energy devices and the negotiation for purchase and distribution of these devices to developing countries. The research networks will link up existing centres of research, further strenghtening cooperation among the energy researchers of the developing countries.

PERFORMANCE AND OPTIMIZATION OF A LASER INITIATED VACUUM SPARK

C.S. Wong, MIPM and S. Lee, FIPM
Plasma Physics Laboratory
Physics Department
University of Malaya
Kuala Lumpur

Introduction

The vacuum spark has been developed initially as a pulsed x-ray spectroscopic source[1-3] in which some very highly ionized states of elements like copper, iron, nickel etc. can be obtained. It was later on established that the x-ray spectra emitted by the vacuum spark show some degree of resemblance to the solar flare phenomenon[4]. Recently, there has been some interest in the possibility of obtaining plasmas of low Z elements, in particular deuterium, by using the vacuum spark discharge. It has been shown[5] that by using an anode embedded with $(CD_2)_n$ in a vacuum spark device of about 3.5 kJ input energy, neutron yield of the order of 10^4 to 10^5 neutrons per discharge can be obtained. The energy of these neutrons has been estimated to be about 2.5 MeV indicating that fusion reaction has occured in this plasma. In an independent effort, Lee and Conrads[6] have measured neutron yield of the order of 10^7 from a similar device with input energy of 3 kJ.

In this note, effort to improve the performance of the vacuum spark system is described. The holding voltage of the system is increased thus increasing the discharge energy. An optimum electrode separation for the working voltage regime of 20 kV to 30 kV is also established.

Characteristics of the vacuum spark

The principle of operation of the vacuum spark discharge can be described as follows:-

A pair of electrodes (usually with sharp pointed anode) which is separated by about 1 cm is located in a chamber evacuated to a pressure of less than 10^{-5} torr (Figure 1). These electrodes are connected

directly to a high voltage storage capacitor so that when the capacitor is charged up, the high voltage is maintained across the inter-electrode gap. A 60 MW pulsed ruby laser beam is focussed onto the tip of the anode to initiate a discharge across the inter-electrode gap. Plasma spots with linear dimensions of a few micron are observed in such discharges. The electron temperature and density of this plasma have been estimated[7] to be of the order of 8 keV and 10^{21} per cm^3 respectively.

The mechanism operating in this discharge is still unclear. Some of the possible theories proposed are the constricted pinch affect[8]; the bombardment of mircoparticles ejected from the anode by electron beam[9,10]; plasma heating by two-stream instability or turbulence[7].

The vacuum spark system

The latest design of the vacuum spark system in the Physics Department, University of Malaya is shown schematically in Figure 1. Referring to the former design[6] the following modifications have been made:-

a) The outer chamber has been eliminated to increase the ease of obtaining vacuum of $<10^{-5}$ torr. In the new design, the small aluminium chamber is used for holding the cathode and also serves as the vacuum chamber. The chamber volume required to be pumped is thus reduced by at least 10 times. Furthermore, it has been pointed out[11] that long-path discharge may occur between the inner surface of the outer chamber and the anode which will decrease the holding voltage of the system. Hence the elimination of the outer chamber will also help to improve the voltage holding capability of the system.

b) A 60 MW giant pulse ruby laser is used instead of the sliding spark to trigger the discharge. This greatly enhances the accuracy of anode material evaporation so that evaporation is confined to a small area at the anode tip only. This condition is important in the case where LiD is fused in a narrow channel (diameter < 1 mm) through the center of the anode in order to minimize the amount of high Z impurities.

c) The backwall surface breakdown path has been lenghtened by cutting grooves on the perspex insulator.

With these modifications, the pressure of the present system can now be pumped to $\leq 10^{-5}$ torr quite easily; and the holding voltage has been tested to 35 kV. This means that with the present system, the maximum input energy is 13.6 kJ instead of 3 kJ.

The ruby laser

The ruby laser used to trigger the vacuum spark discharge is the System 2000 designed by JK Lasers Limited, England. It can be operated in two modes: the multiple-transverse-mode (MTM) and the single-transverse-mode (STM). In the MTM operation, the nominal power output is 60 MW (1.5 J in 25 ns) and the coherent length is only a few mm. If a better spatial coherence is required (as in the case of holographic interferometry), the laser can be converted to operate in STM. In this case, the power output is reduced to 1.2 MW (30 mJ in 25 ns), but the coherent length is now 1 m.

For the application here where power is the more important factor, the laser is operated in MTM. The laser beam is guided by three dielectric mirrors and then focussed by a lens with 7 cm focal length onto the tip of the anode. The alignment of the laser focussing is done by using a Virtually Pivoted Beam (VPB) Laser Alignment System.

System performance of the vacuum spark

The performance of the present system is assessed using the following diagnostics:-

a) Measurement of the discharge current is obtained by using a Rogowski Coil operated as a current transformer[12]. The calibration constant of the coil used here is 24.7 kA/V.

b) The x-ray image of the plasma spot formed in the vacuum spark is observed through a 800 μm pinhole and recorded by Polaroid film type 667 (ASA 3000). The pinhole is covered by a layer of 2-thousandth inch thick mylar foil.

c) The time-resolved x-ray pulses are measured by a pair of SSR PIN diodes.

The current oscillogram and the x-ray signal of a typical vacuum spark discharge are shown in Figure 2. The electrode separation in this discharge is 5 mm and the capacitor is charged to a voltage of 20 kV. The current oscillogram shows a very severe dip at the current maximum which corresponds to a large x-ray pulse recorded by the PIN diode. During this current-dip, the discharge current has dropped abruptly to almost zero current in a time of less than 100 ns with 70% of the drop occuring in less than 10 ns. This drop may be attributed either to a sudden increase of inductance of the system or to a sudden increase in plasma resistivity. Both these effects can result from a very strong electro-mechanical interaction[13]. It is clear from comparison of the current oscillograms of the vacuum spark to that of the plasma focus[13] that the electro-mechanical interaction in the vacuum spark is even more severe.

The system has been operated at electrode separation of 5 mm, 8 mm, 10 mm, 13 mm and 22 mm and at each separation, the discharge voltage has been varied from 8 kV to 20 kV. In general, the system seems to perform better at smaller electrode separations. So far, large x-ray pulses and severe current dips have been observed for more than 80% of discharges for the separation of 5 mm to 10 mm; and for the case of 22 mm separation, no plasma spot has been observed by the pinhole camera for all the discharges fired. The current oscillogram for a discharge at 22 mm electrode separation also shows different characteristics as compared to a typical shot which produces a plasma spot(Figure 3). The starting portion of its discharge current is observed to be flattened for about 500 ns and in the pinhole picture, it is evident that x-ray is emitted only from the surface of the anode corresponding in time with the flattened part of the current. This x-ray is probably produced by the bombardment of the anode by runaway electrons.

Table 1 lists the optimum discharge voltages of various electrode separations for a vacuum spark system using sharp-pointed stainless steel anode. The base pressure of the chamber is $\sim 10^{-5}$ torr. However, it must be pointed out that there does not exist a clear-cut boundary for the range of discharge voltage which is 'optimum' to any particular separation.

The value of the optimum voltage has been fixed based on observation of the probability of getting good pinching shots. Nevertheless, the electrode separation of 22 mm has been confirmed to be not suitable for the operation of this system.

Conclusion

From the above studies, it can be concluded that the performance of the present vacuum spark system has been fairly well optimized. It is now possible for us to predict the behaviour of the system and to a certain extent control it to achieve the required conditions for obtaining a very hot and dense plasma consistently.

References

1. S.K. Handel, Arkiv for Fysik, 28(27), 303 (1964)
2. Leonard Cohen, Uri Feldman, Marvin Swartz and J.H. Underwood, J. Opt. Soc. America, 58(6), 843 (1968)
3. S.V. Lebedev, Sov. Phys. JETP, 37(2), 248 (1960)
4. T.N. Lie and R.C. Elton, Phys. Rev. A, 3(3), 865 (1971)
5. T.N. Lee and F.C. Young, Bull. Am. Phys. Soc., Ser.II, 19, 944 (1974)
6. S. Lee and H. Conrads, Phys. Lett., 57A(3), 233 (1976)
7. T.N. Lee, Astrophy. J., 190, 467 (1974)
8. T.N. Lee, Proc. 2nd Topical Conf. on Pulsed High Beta Plasmas, (1972)
9. C.R. Negus and N.J. Peacock, J. Phys. D, 12, 91 (1979)
10. R. Jones, preprint
11. C.G. Morgan, Private Communication
12. C.S. Wong, M.Sc. Thesis, Physics Department, University of Malaya, (1978)
13. S. Lee, Proceedings of Symposium on Physics, University of Malaya, (1977)

Table 1

Optimum discharge voltage at various electrode separation

Electrode Separation	Discharge Voltage
5 mm	20 kV
8 mm	15 kV
10 mm	12 kV
13 mm	10 kV
22 mm	-

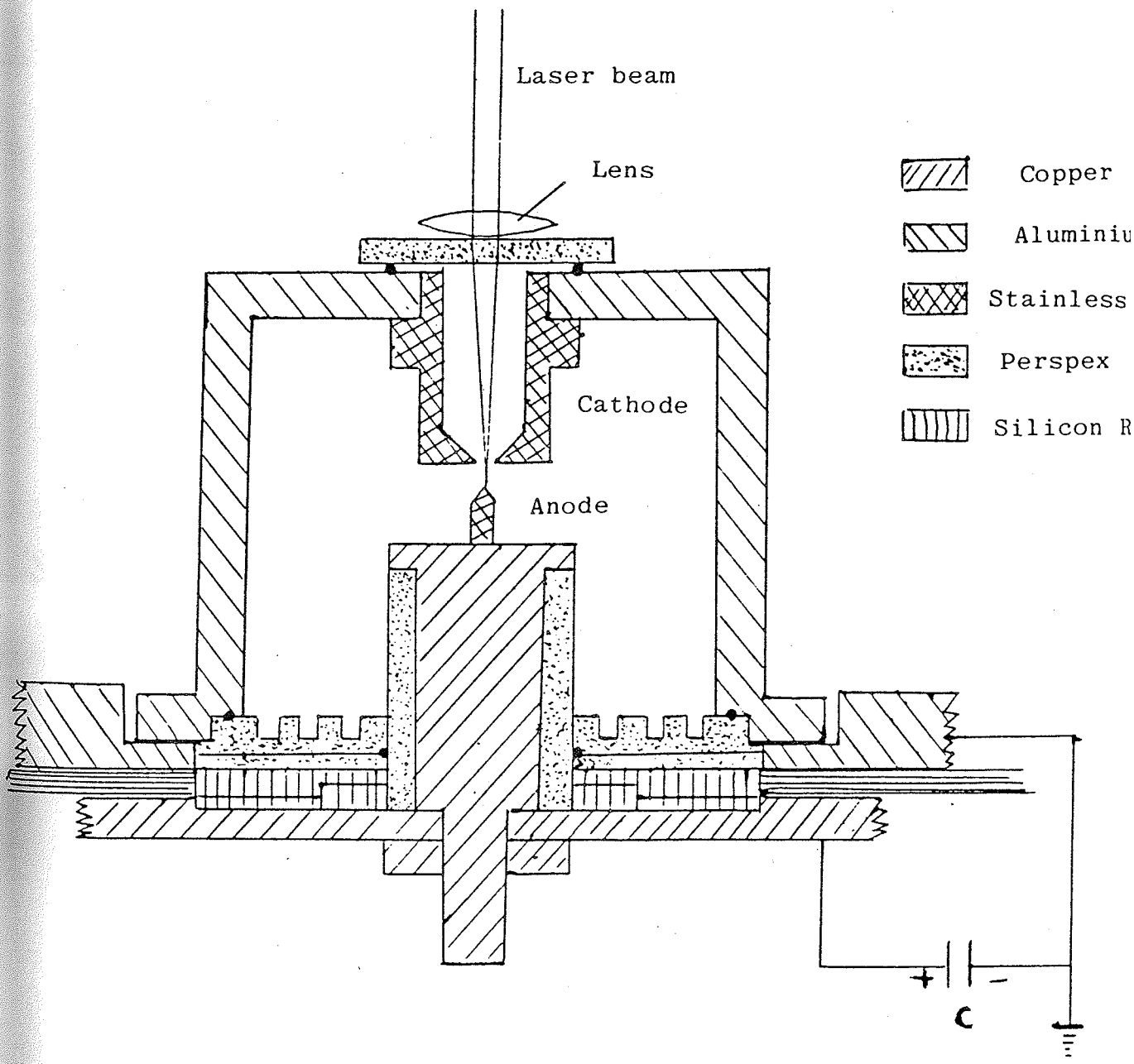

Figure 1: Schematic Diagram of the Vacuum Spark System

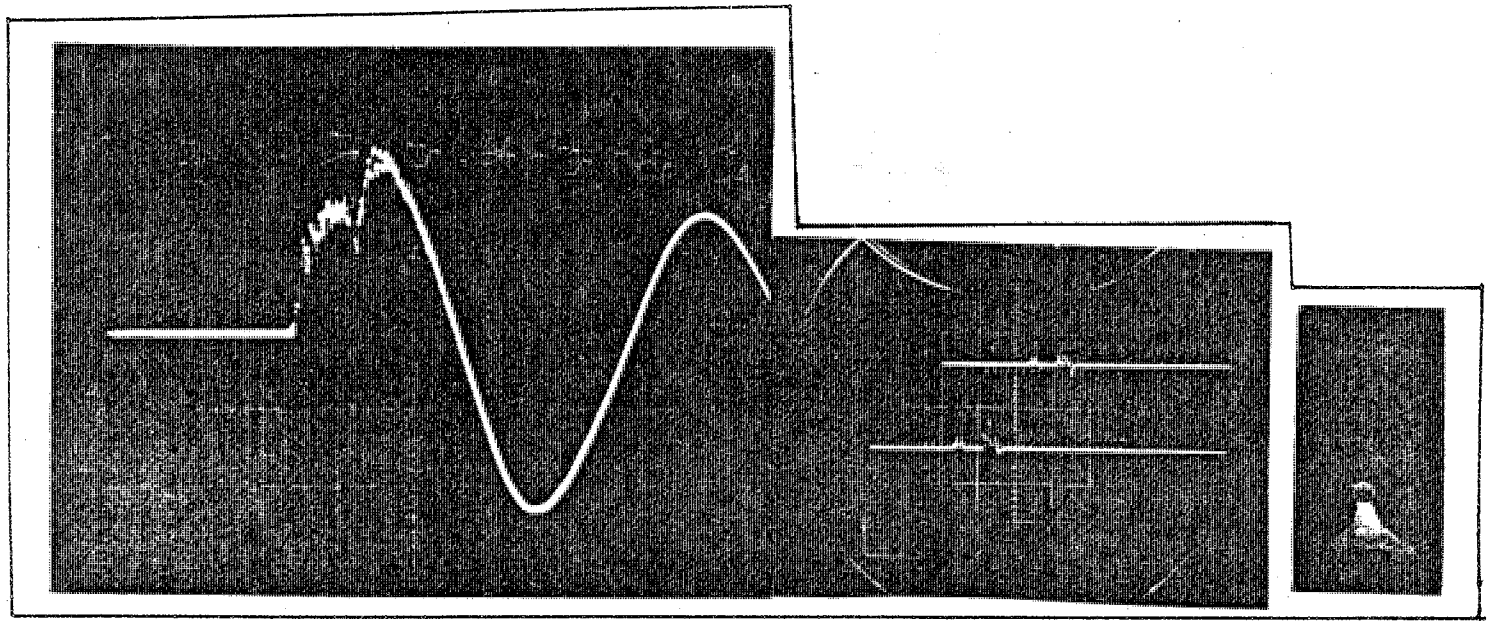

Figure 2: Current Oscillogram, X-ray diode signals and Pinhole picture of a typical vacuum spark discharge.

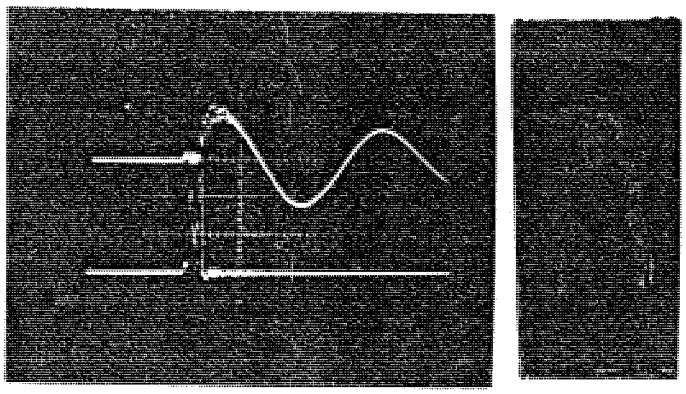

X-ray
Pinhole
picture

Upperbeam: Current
Lowerbeam: X-ray diode
signal

Figure 3: Current Oscillogram, X-ray diode signal and X-ray Pinhole picture of a vacuum spark discharge with 2.2 cm electrode gap

LASER SHADOWGRAPHIC TECHNIQUE APPLIED TO A PLASMA FOCUS

S. Lee, FIPM and Y. H. Chin
Plasma Research Laboratory
Universiti Malaya
Kuala Lumpur

Introduction

The shadowgraph method is suitable for visualising structures in gases in which the index of refraction changes over short distances. The development of the method is usually attributed to Dvorak[1] who in 1880 used it to photograph air disturbances. This method has been widely used in many fields of research e.g. for investigating air jets, air flow around bodies in high speed wind tunnels, turbulence and shock waves produced by high speed projectiles.

With the advent of the pulsed ruby laser, shadowgraphy, as well as the related methods of schlieren photography, interferometry and holographic interferometry, has become a powerful tool for the visualisation of transient plasma structures. For example, plasma turbulence and instabilities have been clearly revealed by applying the shadowgraph method to a theta pinch[2], whilst in 1976 Morgan[3] has taken shadowgraphs of Rayleigh-Taylor instabilities during the collapse phase of the dense plasma focus. The present work extends our range of plasma focus results[4] to laser diagnostics.

The Method

It is well-known that in a deuterium plasma focus, which is fully ionized, the electron refractivity at optical wavelength is dominant[5]. The deuterium plasma optical refractivity for ruby laser light of 6943 Å, may be written as $\mu = 1 - 2.16 \times 10^{-22} n_e$ where n_e is the electron density per c.c.

If an uniform beam of light is travelling along the y-axis and passes through a test region of uniform refractive index then a screen placed beyond the test region in the x-z plane will be uniformly illuminated. If in the test region there exists non-uniform gradients $\frac{\partial \mu}{\partial x}$, $\frac{\partial \mu}{\partial z}$, then the screen will not be uniformly illuminated. There will be variation of illumination ΔI about the original illumination I. It can be shown that for a fully ionized

deuterium plasma, the shadow patterns are governed by:

$$\sum \frac{\Delta I}{I} = -2.16 \times 10^{-22} \ell \int_o^L \left(\frac{\partial^2 n_e}{\partial x^2} + \frac{\partial^2 n_e}{\partial z^2}\right) dy$$

where ℓ = distance of screen from test section

L = length of test section through which the laser light traverses,

and provided $\frac{\partial \mu}{\partial x}$ and $\frac{\partial \mu}{\partial z}$ are much smaller than unity.

Control and timing technique

The ruby laser used as a light source for the shadowgraphs in this experiment has a nominal pulse width at half-maximum of 25 nsec, and a maximum light energy of 1½ joules. Precision in synchronising the giant laser pulse with the plasma focus is important because the implosion phase of the focus lasts only 100 ns after an axial acceleration phase of 3 μs. The dense focus itself lasts about 30 ns. The laser requires to be pumped for 1.25 ms before it is Q-switched. The synchronising scheme adopted is shown in Figure 1. With both the laser and focus tube systems charged and ready, the laser flashlamp is triggered by the manual start pulse. The triggering pulse also triggers a delay unit DU1 with delay time set at 1.25 ms. The delayed output pulse from DU1 is then used to trigger the 2D21 thyratron of the ignitron triggering circuit[6]. The output pulse of the 2D21 thyratron constitutes a master synchronising pulse triggering all diagnostic oscilloscopes. This master synchronising pulse triggers at the same time a second delay unit DU2 set initially at 3 μs. The delayed output of the DU2 is then used to trigger the pockell cell Q-switch of the ruby laser. The ruby laser pulse passes through a pulse chopper (Figure 2), for pulse width reduction, before being expanded to a parallel beam which passes through the test section to arrive finally at the photographic camera.

For the final synchronising, the current and voltage waveforms of the focus tube are monitored on 'centre-aligned' CRO traces. A fast photodiode is suitably located to pick-up stray reflection of the laser pulse. The photodiode output is displayed on a third trace 'centre-aligned' to the voltage trace. Initially the focus and laser are fired repetitively (about 1 minute interval) and the delay time of DU2 is adjusted so that the laser pulse coincides with time to the peak of the focus voltage spike. We define

the time of the peak of the focus voltage spike as t = 0. The time t at which a shadowgraph is taken is specified from the photodiode pick-up in reference to t = 0. For example a shadowgraph taken at time t = -50 ns indicates that the laser pulse passed through the test section 50 ns before the time of the peak of the focus voltage spike. By varying the delay time of DU2 and after firing a large number of shots, a composite sequence of shadowgraphs was obtained showing the focus in its various stage of formation. Figure 3 shows an example of a laser pulse at t = 10 ns.

Laser pulse width

In early experiments it was found that the laser pulse width at half-maximum was 50 - 70 ns and that the collapsing current sheet could not be resolved with this long exposure time. The laser pulse chopper was then used to provide better time resolution. This chopper was initially adjusted for a laser pulse width of 20 - 30 ns.

Results with laser pulse width of 20 - 30 ns

A series of shadowgraphs was then taken with the focus operating at 8 torr deuterium and with 20 kV on the 60 μF capacitor bank. A composite sequence is shown in Figure 4.

The sequence from t = -160 ns to t = +40 ns shows the current sheet sweeping around the anode (t=-160 ns), collapsing inwards (t = -50 ns to t = -20 ns) to a dense focus (t = 0), and breaking up (t = +20 ns) due to m=0 instabilities to form a column of large radius (t = +40 ns). From our earlier neutron measurements[7] it appears that this large column plasma may well be related to the production of fusion neutrons. The post-focus sequence is shown from t = 220 ns (when there is no sign of the current column carrying the current from the anode to the current sheet) to t = 950 ns which shows a plasma with a 'spear-head' feature apparently ejected from the anode with an average velocity of 3 cm/μs. The 'spear-head' feature has a granular appearance which is consistent with the appearance of a cloud of sputtered material.

Results with laser pulse width of 5 - 10 ns

From these shadowgraphs it was concluded that the dynamic compression

phase from -50 ns to -20 ns was not properly resolved in time due to too long a laser pulse. Photographic smearing was evident. The laser pulse chopper was then re-adjusted to provide a shorter pulse width of between 5 - 10 ns. Figure 5 shows the improved results for 6 shots, between t = -70 ns and t = +50 ns. The improved resolution is particularly evident in the radially collapsing phase at t = -40 ns, where the velocity is of the order of 10 - 20 cm/μs giving a smear of up to 1 mm.

Conclusion

This series of experiments has shown that the timing sequence and the chopped laser pulse width of 5 - 10 ns are adequate to time-resolve the plasma focus in its various stages of formation and breaking-up. It has also revealed, for the first time, a post-focus plasma-jetting effect with a consistent 'arrow-head' shape probably of sputtered anode material. This 'arrow-head' appears to jet out from a slower moving dense plasma which envelopes the anode. This dense plasma envelope is conjectured to arise from the 'current-shedding' effect[8].

The results indicate that for shadowgraphy and schlieren, our optics, particularly the mirrors and windows, have to be improved to reduce the effect of stray fringes. For holographic interferometry, the optical quality of components are of no consequence; but the time resolution may become more critical than for shadowgraphy.

Acknowledgement

We acknowledge the Alexander von Humboldt Foundation of West Germany for the gift of the ruby laser system which has made possible the introduction of laser diagnostics to our plasma research laboratory. We also acknowledge the technical help of Jasbir Singh and T.S. Toh in the project and of C.S. Wong and other members of the Plasma Research Group.

References

1. V. Dvorak, Ann. Phys, Lpz. 9, 502 (1880)
2. U. Ascoli-Bartoli, S. Martellucci, E. Mazzucato, 6th Conference on Ionization Phenomena in Gases, Section VIII, 23 (Paris 1963)

3. P.D. Morgan, 'Optical Refractivity Studies of a Plasma Focus' Ph.D. thesis, Culham (1976)

4. S. Lee, 'Review of Plasma Research in Malaysia', Symposium on Plasma Research, Theory and Experiment, ICTP Trieste (1981) - to be published in Procs.

5. R.H. Huddlestone & S.L. Leonard, 'Plasma Diagnostic Techniques' Chapter on Optical Interferometry by R.A. Alpher and D.R. White pg.441

6. S.P. Thong, S. Lee, Mal. J. Science, 2(B), 157-169 (1973)

7. S. Lee, Y.H. Chen, Mal. J. Science, 3(B), 159-163 (1975)

8. S. Lee, Y.H. Chen, S.P. Chow, B.C. Tan, H.H. Teh, S.P. Thong, Int. J. Electronics, 33, 85-90 (1972)

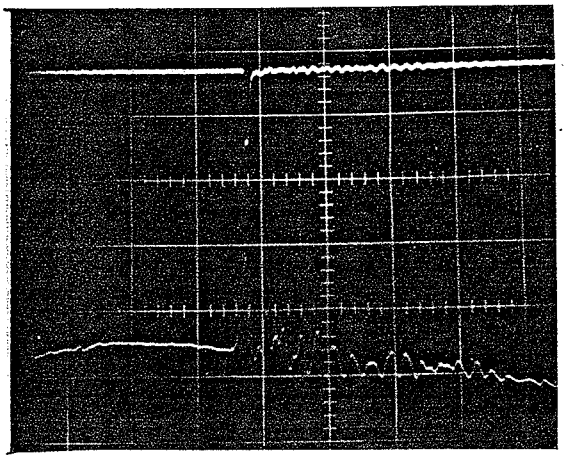

Figure 3: Oscillogram for fixing time of shadowgraphic exposure

Upper trace: photodiode signal of laser pulse
Lower trace: voltage probe signal
Both trace are centre-aligned and linearity optimized. Time scale: 500 ns/cm.

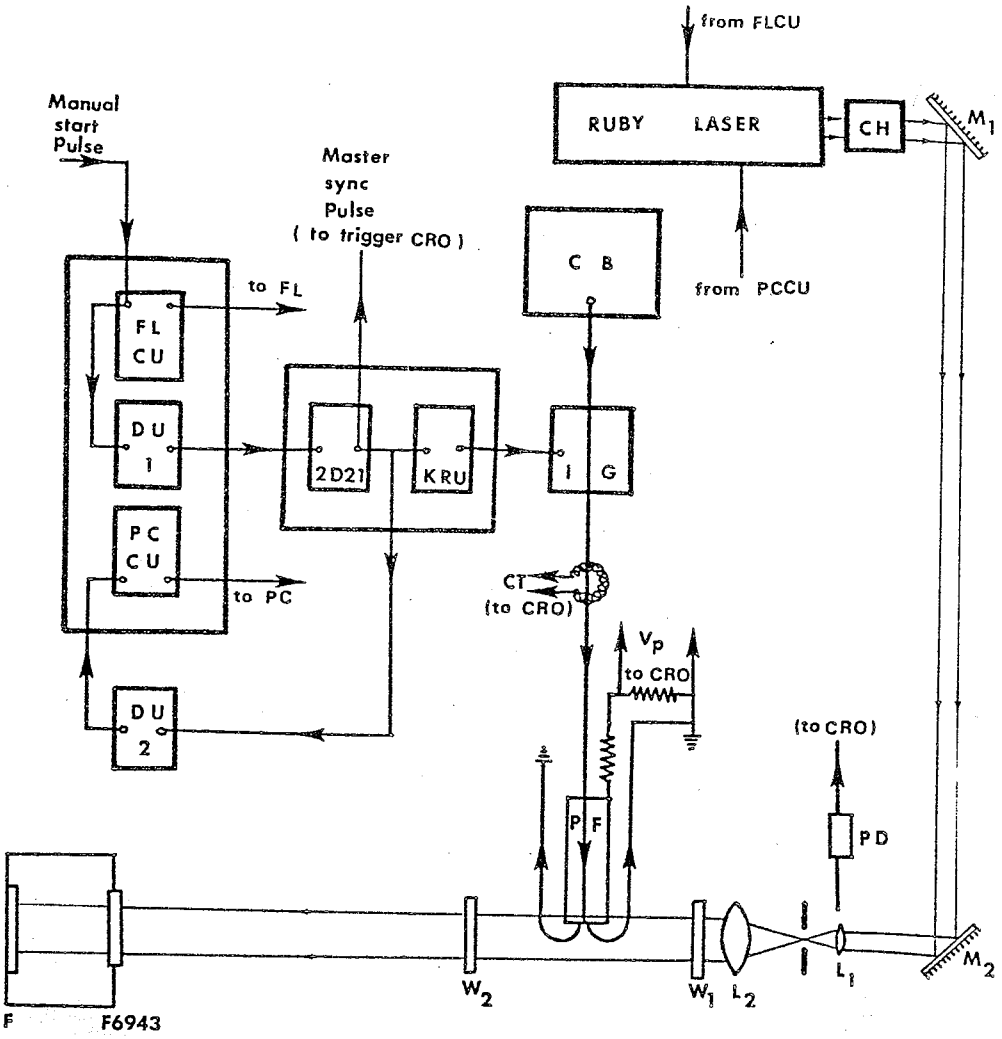

Figure 1: Synchronising circuit and optical set-up for shadowgraphy (not to scale)

FLCU = Flash lamp control unit
CH = Pulse chopper
2D21 = Thyratron 2D21
CB = 60μF capacitor bank operated at 20 kV
L = Lens
M = Laser mirror
PF = Plasma focus tube
VP = Voltage probe
F6943 = Narrow band filter centred at 6943 Å
DU = Delay unit
PCCU = Pockel cell control unit
KRU = Krytron trigger unit
IG = ignitrons switching the capacitor bank
W = Window
F = Polaroid film
CT = Current transformer
PD = Photodiode

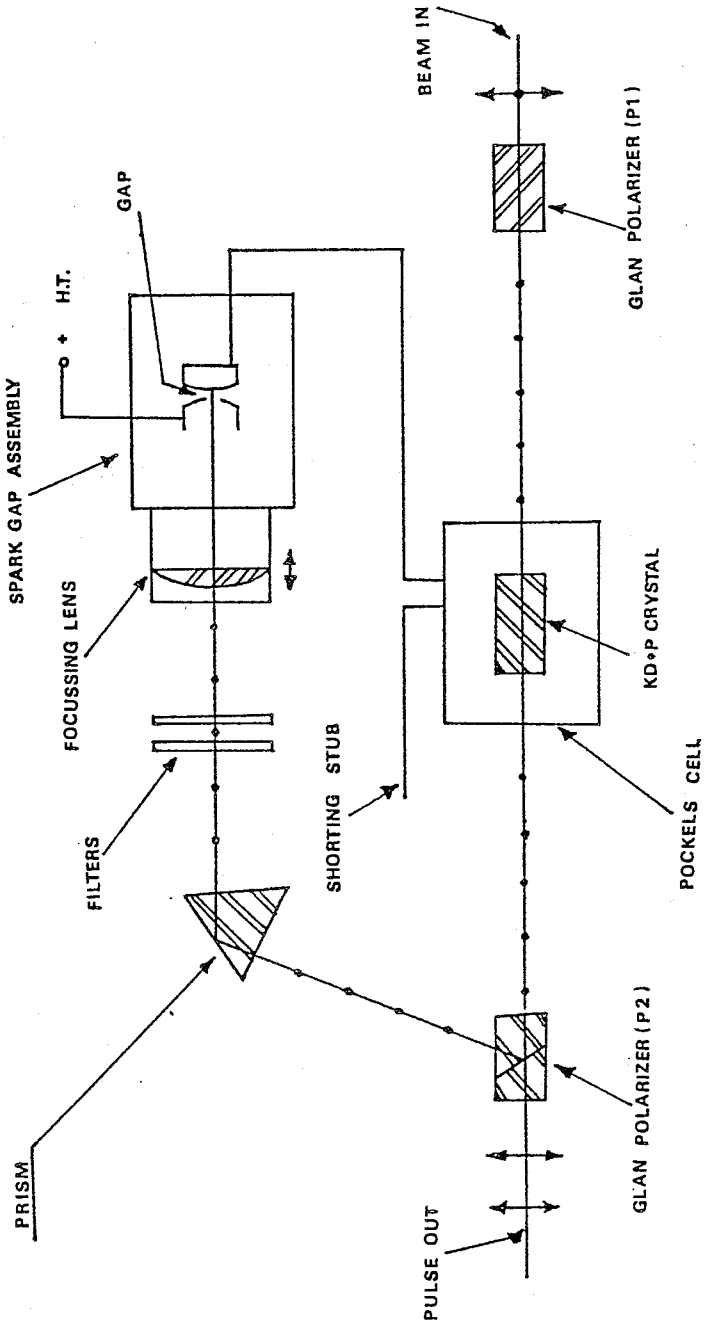

Figure 2: Schematic of the laser pulse chopper

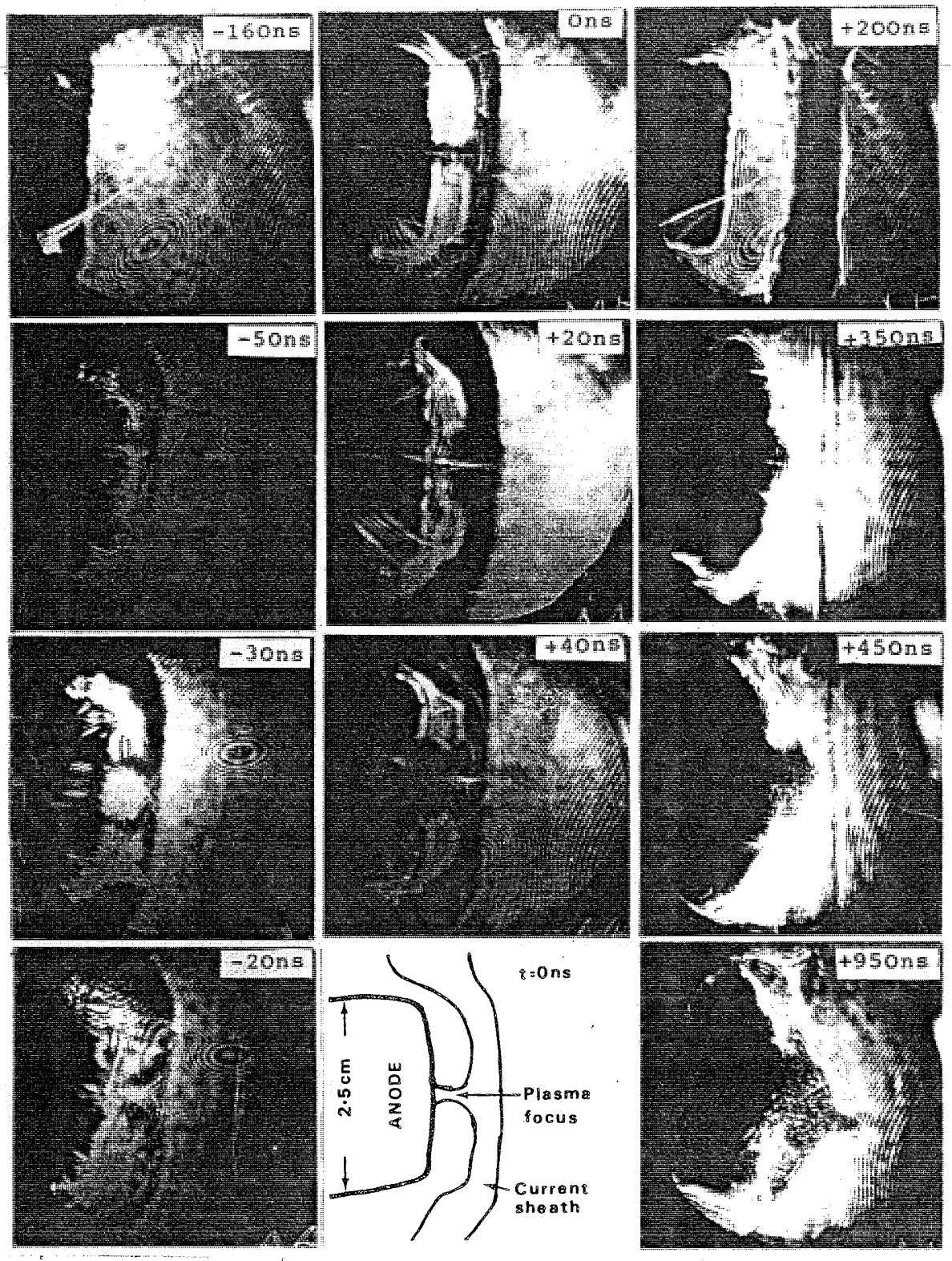

Figure 4 Side-on shadowgraphs of the plasma focus
20 kV, 60 μF, 8 torr deuterium
Shadowgraph exposure time: 20-30 ns. The line drawing corresponds to the shadowgraph at 0 ns.

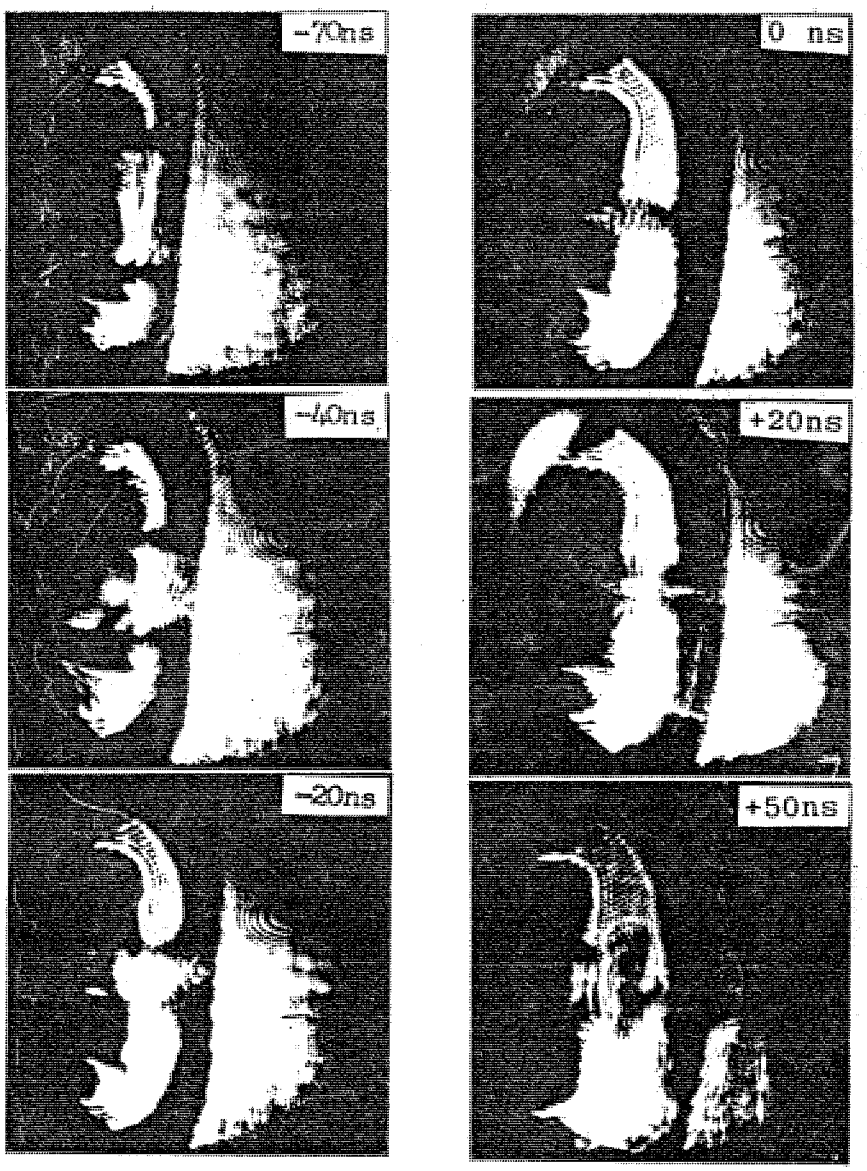

Figure 5 Side-on shadowgraphs with improved time resolution of 5-10 ns 20 kV, 60 μF, 4 torr deuterium

FUSION ENERGY - 1981, IAEA-SMR-82
International Centre for Theoretical Physics, Trieste, 1982.

REVIEW OF PLASMA PHYSICS RESEARCH IN MALAYSIA

S. LEE
Plasma Laboratory, Physics Department,
University of Malaya,
Kuala Lumpur, Malaysia

Abstract

The energy trends of Malaysia projected for the next few decades are briefly discussed as a background to the rationale for Malaysian research into new forms of energy including plasma fusion. The planning of this research started nearly two decades ago. Today research facilities at PLUM centre on two capacitor banks, one rated at 40 kV, 48 kJ, 2 MA short circuit current and the other at 60 kV, 40 kJ, 2MA. Other equipment include several smaller capacitor banks, vacuum systems, oscilloscopes, diagnostic systems, a screened room, a transient digitizer, an Imacon camera and a 100 MW pulsed ruby laser for discharge initiation and diagnostics. The research devices include two plasma focus machines, one vacuum fusion spark, a shock tube and minor experiments like the glow discharge. The main focus facility, the UMDPF1, was designed and built entirely by indigenous effort, using 40 kV capacitors donated by Britain under the Colombo Plan. Difficulties were encountered especially in the need to adapt what is locally available or readily importable to all phases of the design, construction, testing and measurement. Nevertheless, the focus group has achieved the following results: measurement, in 1973, of neutrons produced in the deuterium focus; current, voltage, magnetic field and pressure measurements to interpret plasma dynamics and focus mechanism and to compare with computer simulation of plasma trajectory and configuration; soft x-ray measurements to determine electron temperature; study of the effect on the focus of rotation and multiple ionization up to Argon XVIII; and optimuzation of focus performance as judged from neutron yield.

In 1977 PLUM acquired the Julich DPF1 which was reassembled as a fast focus, the UMDPF2. This device has been converted to operate as a vacuum spark with the aim of demonstrating the spark as a neutron source when using a deuterided anode. We have measured temperatures of 8 keV in the dense plasma spots.

Plasma research work here has produced some interesting results and postgraduate theses including a Ph.D. thesis. A small low-cost Tokamak is being planned to extend the scope of the work.

Introduction

At the Seminar on Energy Options for Developing Countries held in Madras in February 1981 it was pointed out that despite all conservation measures that may be taken the rate of increase of energy consumption world-wide would result in a doubling time in energy consumption of about 20 years It was also pointed out that renewable resources could only be planned, and optimistically at that, to provide 10-20% of the world's energy needs towards the early part of the 21st Century.

These conclusions together with estimates of the logistic production curves of fossil and fissile ores give us a scenario as depicted in Figure 1. Inexorable social and economic pressures dictated by an increasing population and an innate world-wide demand towards an universal reasonable standard of living compatible with the average human intelligence require the energy consumption curve to rise at a minimum rate of 3% towards a point some 20 times above present consumption. However, well before this 20 times point is reached, a critical point is reached when the total of all energy supplies, fossil, fission (with breeding) and renewables, is insufficient to support any further increase in consumption [1].

This would be a critical point in human history at which human hopes would forever by extinguished unless a limitless source of energy such as fusion were to be developed. The present increasing international effort to built a fusion reactor is primarily motivated by such a scenario. Realising that this problem is crucial to all humanity, developing countries inclusive, many scientists in developing countries must have pondered as we did in Malaysia how we may attempt to play a role at least firstly in carrying out some experiments to enable us to understand, at first hand, some of the problems regarding the physics of fusion.

Energy trends in Malaysia

The energy trends in Malaysia [1] have been extrapolated to the middle of the next century by 'soft-energy' proponents as shown in Figure 2. It is certain that a study of the land area and the construction materials required to support the energy-plantations and the hundreds of square miles of solar collectors will result in large gaps in these 'soft-energy' proposals from early in the 21st Century. But a proposed package such as shown in Figure 2 does indicate that despite the projected phenomenal growth in energy consumption, 7% per annum, Malaysia does have a breathing space to plan her energy policy and research without the strangle-hold of immediate energy crisis. The result is that a fairly comprehensive range of energy research now thrives in Malaysia including solar energy research and plasma fusion research.

Plasma Research in Malaysia

Plasma research at the University of Malaya started in the early 1960's with the studies of oscillations in the glow discharge [2]. At the same time components for a 40 kV, 60 μF capacitor bank, including capacitors, transformers, thyratrons and other electrical parts were secured from the U.K. government through the Colombo Plan. Assembly of the capacitor bank was started but progress was slow because of inadequate understanding of the technical aspects of capacitor bank switching and associated timing and synchronising problems. During this time shock wave research was carried out [3-6].

Capacitor bank

These problems were resolved in 1970 when a decision was made to use ignitrons to switch the bank. A modular design was adopted [7,8] dividing the 60 μF bank into four modules each with 25 capacitors. Each module was switched by two 7703 ignitrons as shown in Figure 3, with all 8 ignitrons controlled by one master krytron. A novel feature of this bank was the confinement of the full capacitor voltage to the capacitor terminals by means of auxilliary spark gaps so that although the capacitors were charged at 40 kV, only 20 kV appeared on the ignitrons until the ignitrons are switched. This reduces the problem of corona and also enables the use of 7703 ignitrons (rated at 20 kV) to switch the 40 kV bank. Discharged into a short-circuit load, the bank delivered a measured current of 1.93 MA on 23rd March 1972. The inter-ignitron jitter was determined to be ±50 ns and synchronisation jitter between the start of the current and the master trigger pulse was of the same order. Since 1972 the 8 ignitrons have switched in excess of 10000 times between 15 to 30 kV. The maintenance was minimal until the end of 1980. The ignitrons need to be replaced now.

Plasma Focus

In late 1970 with the capacitor bank partially operational a decision was made to operate a plasma focus as this device appeared to be the most promising, given our limited facilities, for the production of a plasma hot and dense enough for detectable plasma fusion. A Mather-type focus was designed [9] with suitable parameters so that focus could occur at or slightly after peak current. Considering a snow-plow model and taking into account the effect of the dynamic impedance of the focus tube on the circuit current the tube parameters were provisionally fixed at: diameter of inner electrode = 5 cm, length of inner electrode = 25 cm, operating pressure = 1 torr in deuterium for an operating voltage of 20 kV generating a plasma current of 500 kA. The outer electrode was interchangeable using either a copper cylinder of 8.2 cm diameter or a glass cylinder of 10 cm in diameter to facilitate photography.

Diagnostics

By early 1971 this focus tube was operational with the partially completed capacitor bank. Magnetic probes were used systematically to establish the symmetry, structure and dynamics of the current sheath in the accelerator region. Voltage and current probes were used to establish focus dynamics and energetics. These probes were all of the simplest designs. We also proceeded to develop soft x-ray techniques for the estimation of electron temperatures. For neutron measurements we designed indium foil activation counters and also time-of-flight systems in order to measure the energy of the neutrons. The time-of-flight systems included two detectors spaced 10 m apart. Each detector consisted of a plastic (NE102) scintillator and a fast photomultiplier. The sensitivity of each detector to neutrons was estimated and then compared with a calibration using a standard polonium-berylium neutron source. In this way the time-of-flight system could also give information on the neutron yield.

Results

By late 1971 the gross dynamics of our plasma focus had already been established both in the run-down region and in the focus region. Trajectories of the luminous plasma were obtained using the Imacon in framing and streak modes. Trajectories of the current sheath were obtained using magnetic probes [9]. Soft x-ray pictures of the focussed plasma were obtained and using a multiple foil technique the plasma electron temperature was estimated to be between 0.8 - 2.5 keV [10].

In October 1973 from a deuterium plasma focus we measured a burst of neutrons with an energy of 2.2 ± 0.1 MeV (see Figure 4) in the backward direction [11]. In the forward direction the neutron energy was measured to be 2.6 ± 0.1 MeV. Thus the evidence indicated that the neutrons were produced from the D-D reaction (neutron branch) from a plasma with a centre-of-mass moving in the forward direction. The distribution of neutrons from the focus was later studied [12] with a view of relating the distribution to one of the three popular models namely the beam-target, the moving boiler and the converging-ion model. A typical distribution is shown in Figure 5. The conclusion of this study was that these models were not adequate to explain the neutron production.

An attempt was made to further understand focus dynamics by the measurement of its mass flow in the run-down region and by constructing a 1-D radial compression model for the focus. The mass flow measurement was made with a piezoelectric probe (Fig. 6) in the run-down region and concluded that only 4-7% of the ambient mass swept up by the current sheath arrives in time to participate in the focussing action [13]. The 1-D radial collapse model which

we developed [14] has an equation of motion of the form:

$$\frac{d}{dt}\{m_o+\pi\rho_o(r_o^2-r_s^2)\}\frac{dr}{dt} = -\frac{\mu_o I^2}{4\pi r} + f(P)$$

where the LHS represents the rate of change of momentum per unit length of the focussing plasma and the first term of the RHS represents the corresponding focussing force supplied by the self-magnetic field of the cylindrical focus current sheath. The term f(P) represents a retarding force exerted by the kinetic pressure of the plasma. This retarding force is calculated using a shock wave-current sheath model; and divides the collapsing region into 3 phases, the incident shock phase, the reflected shock phase followed by a phase of adiabatic compression. The trajectory computed from the model, using initial values of m_o and dr/dt consistent with experimental observations, agrees with high speed photography of the inward-collapse and with soft x-ray estimates of minimum focus radius. However the current sheath rebound predicted by the model was not observed experimentally. Indeed, voltage and current measurements were used to show that as the focus diameter approached the minimum value, the current sheath abandoned its snow-plow cylindrical configuration, rapidly diffused through the plasma and flowed on-axis. This is a necessary consequence of the large electron Hall parameter as the radius decreases. For example the electron Hall parameter is estimated as 500 for a typical focus radius of 1 mm. The plasma conductivity of the focus is therefore reduced by a factor of 250000 from its Spitzer value.

Together with the development of the 1-D radial collapse model, two projects were also carried out, one to investigate plasma focus rotation in the presence of an axial bias field[15] and the other to compute the degrees of ionization in an argon focus [16,24].

The next major project was the optimization of the focus. We had already observed earlier that attempts to increase the neutron yield by a reduction of operating pressure so as to enhance plasma speeds resulted in very erratic operation and to shattering of the back-wall insulator. This had led to the conclusion that the focus seems to operate best at a speed of 6 cm/μs to 9 cm/μs. The detailed optimization procedure adopted by us [17,18] eventually enabled reproducible neutron production in a high-pressure neutron optimised regime, as distinct from a low-pressure beam optimised regime. A comparison of the neutron yield of various DPF devices reported in the literature is shown in Figure 7.

Currently we are developing laser diagnostics of the plasma focus. We started with laser shadowgraphy [19] and are now proceeding to laser holographic interferometry. Figure 8 shows some shadowgraphs of our plasma focus.

Laser-initiated vacuum spark

In 1975 a link was developed with the Institut fuer Plasmaphysik of the Nuclear Research Centre (KFA) Juelich, Federal Republic of Germany, which resulted in the transfer of the Juelich DPFI facility to our laboratory under the sponsorship of the Alexander von Humboldt Foundation post-fellowship programme. This is a 60kV, 40kJ machine originally operated as a fast focus but converted in its last year at the Institute for Reactor Development Juelich into a vacuum spark [20] . A 100 MW pulsed ruby laser was also donated by the AVH Foundation.

With the vacuum spark we have obtained a high density point plasma having a measured temperature of 8 keV. We are currently attempting to generate fusion neutrons in this device by using an anode with a LiD insert [21].

Tokamak

Since 1977 our Group has been in discussion to build a small Tokamak [22] with the aim of enabling us to develop measurement techniques of a plasma which is less transient than a plasma focus. We have been encouraged by the 1978 Report of the IAEA Consultants' Meeting on Fusion Programme for Developing Countries [23] , and recently we are completing a design for a small Tokamak specifically to operate from our existing capacitor banks.

With this constraint we shall be using our 40 kV bank to provide about 21 kJ to the stabilizing field of the Tokamak. This limits severely the energy we can supply to the plasma heating current for which we could not use more than 1 kJ from a 10 kV, 100 μF bank, in order not to exceed the Kruskal-Shafranov limit for the plasma current. Despite this energy limitation the scaling laws show that we should still be able to obtain a plasma for the purpose of diagnostic development. The design parameters for our small Tokamak are shown in the following table.

Design Parameters of PLUM Tokamak

Major radius	0.25 m
Minor radius	0.05 m
Aspect ratio	5
Toroidal field	2 T
Plasma current	40 kA
Safety factor	2.5
Ion temperature	0.1 keV
Electron temperature	0.1 keV
Confinement time	1.4 ms
Particle density	3×10^{13} cm^{-3}

Stabilization Bank	
Capacitance	60 μF
Coil Inductance	63 μH
Number of turns	100
Coil current	25 kA
Rise time	100 μs
Charging voltage	26 kV

Plasma Heating Bank	
Capacitance	100 μF
Coil inductance	360 μH
Number of turns	20
Coil current	2 kA
Rise time	300 μs
Charging voltage	4 kV

Conclusion

Much of the work reviewed in this paper would not have been possible without the material support given in the early 1960's by the British Government through the Colombo Plan and more recently by the Nuclear Research Centre (KFA) Juelich and the Alexander von Humboldt Foundation. The projects have also been given added momentum by the collaboration between individual members of the PLUM Group and members of the Institut fuer Plasmaphysik of KFA Juelich and the Institut fuer Plasmaforschung of Stuttgart University. We hope that we can extend our international contacts in this research. We also hope that we at PLUM may be able to play a role in the strengthening of plasma research and plasma research collaboration in the developing countries. The goal is ever before us - infinite energy through plasma fusion.

References

[1] LEE S., 'Conventional Energy Supplies and Non-Conventional Energy Research in Malaysia', COSTED Seminar on Energy Options for Developing Countries, Madras (1981).

[2] LEE K.W., 'Current Oscillations in Glow Discharges', M.Sc. Thesis, Universiti Malaya (1972).

[3] LEE S., 'Some Shock Wave Phenomena in a Ring-Electrode System', M.Sc. Thesis, Universiti Malaya (1966).

[4] PANG C.K., 'Shock Wave Studies in a Ring-Electrode Shock Tube', M.Sc. Thesis, Universiti Malaya (1969).

[5] TEH H.H.,LEE S., Int. J. Electronics, 22 (1967) 193.

[6] LEE S., Malaysian J. of Science, 3B (1975) 165

[7] LEE S., CHEN Y.H.,CHOW S.P.,TAN B.C.,TEH H.H.,THONG S.P., 'High Current Discharge in Plasma Focus Experiment, Procs. Symp. on Phys., Singapore (1971) 182.

[8] THONG S.P.,LEE S., Malaysian J. of Science, 2B (1973) 157.

[9] CHOW S.P.,LEE S.,TAN B.C., J. of Plasma Phys, 8 (1972) 21.
CHOW S.P., 'Current Sheath Studies in a Coaxial Plasma Focus Gun', M.Sc. Thesis, Universiti Malaya (1972).

[10] CHEN Y.H.,LEE S., Int. J. of Electronics, 35 (1973) 341.
CHEN Y.H., Study of Coaxial Plasma Guns in Mode I Operation', M.Sc. Thesis, Universiti Malaya (1972).

[11] LEE S.,CHEN Y.H., Malaysian J. of Science, 3B (1975) 159.

[12] WONG C.S.,LEE S.,MOO S.P., 'Distribution of Neutrons from a Plasma Focus' - accepted for publication Malaysian J. of Science.
WONG C.S., 'Some Neutron Measurements of the Plasma Focus', M.Sc. Thesis, Universiti Malaya (1978).

[13] LEE S.,TAN T.H., 'Dependence of Focus Intensity on Mass and Field Distribution' Procs. of Seventh European Conf. on Controlled Fusion and Plasma Phys., Lausanne (1975) 65.

[14] LEE S.,CHEN Y.H., 'A Radial Trajectory Computation of the Plasma Focus', Procs. of Twelfth Int. Conf. on Phenomena in Ionized Gases, Eindhoven (1975) 353.

[15] CHEW A.C., 'The Plasma Focus in an Axial Magnetic Field', M.Sc. Thesis, Universiti Malaya (1974).
[16] YONG Y.C., 'Multiple Ionization in an Argon Plasma Focus', M.Sc. Thesis, Universiti Malaya (1978).
[17] CHEN Y.H., 'Parametric Study of Focus Optimization', Ph.D. Thesis, Universiti Malaya (1978).
[18] LEE S.,CHEN Y.H., 'Geometrical Optimization of the Dense Plasma Focus', Paper in Symposium on Plasma Research, Theory and Experiment, Trieste (1981).
[19] CHIN Y.H., 'Shadowgraphic Studies of a Plasma Focus', M.Sc. Thesis, Universiti Malaya, to be submitted.
[20] LEE S.,CONRADS H., Phys. Lett., 57A (1976) 233.
[21] WONG C.S., 'Vacuum Spark as a Fusion Device', Paper in Symposium on Plasma Research, Theory and Experiment, Trieste (1981).
[22] LEE S., Bulletin of the Malaysian Institute of Physics, 1,2 (1980) 14.
[23] Report of the IAEA Consultants' Meeting on Fusion Programme for Developing Countries (1978).
[24] LEE S., Ed., Procs. Symp. on Plasma Focus Work in Kuala Lumpur (1976).

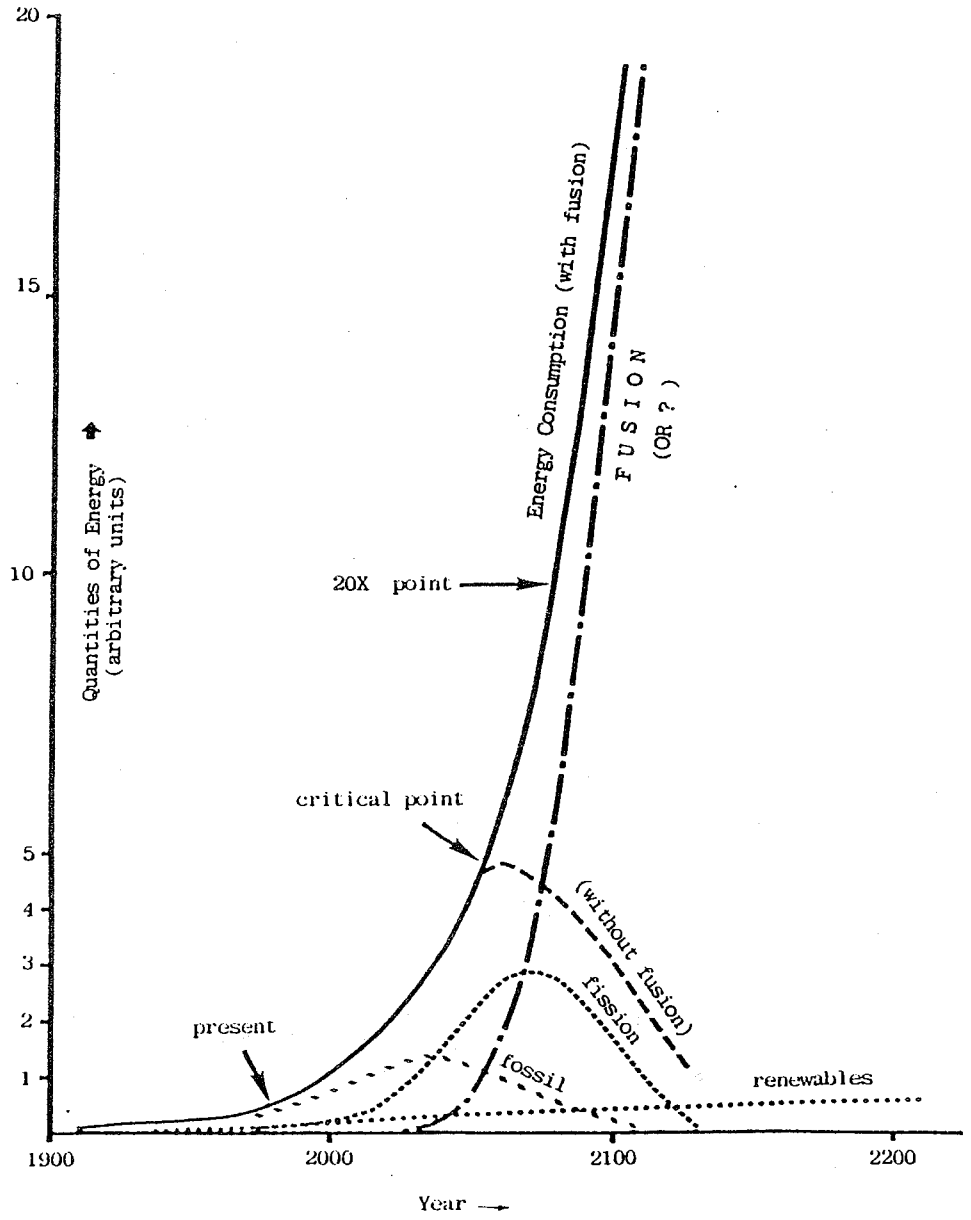

Figure 1: Impact of Fusion Energy on Future of Civilisation.

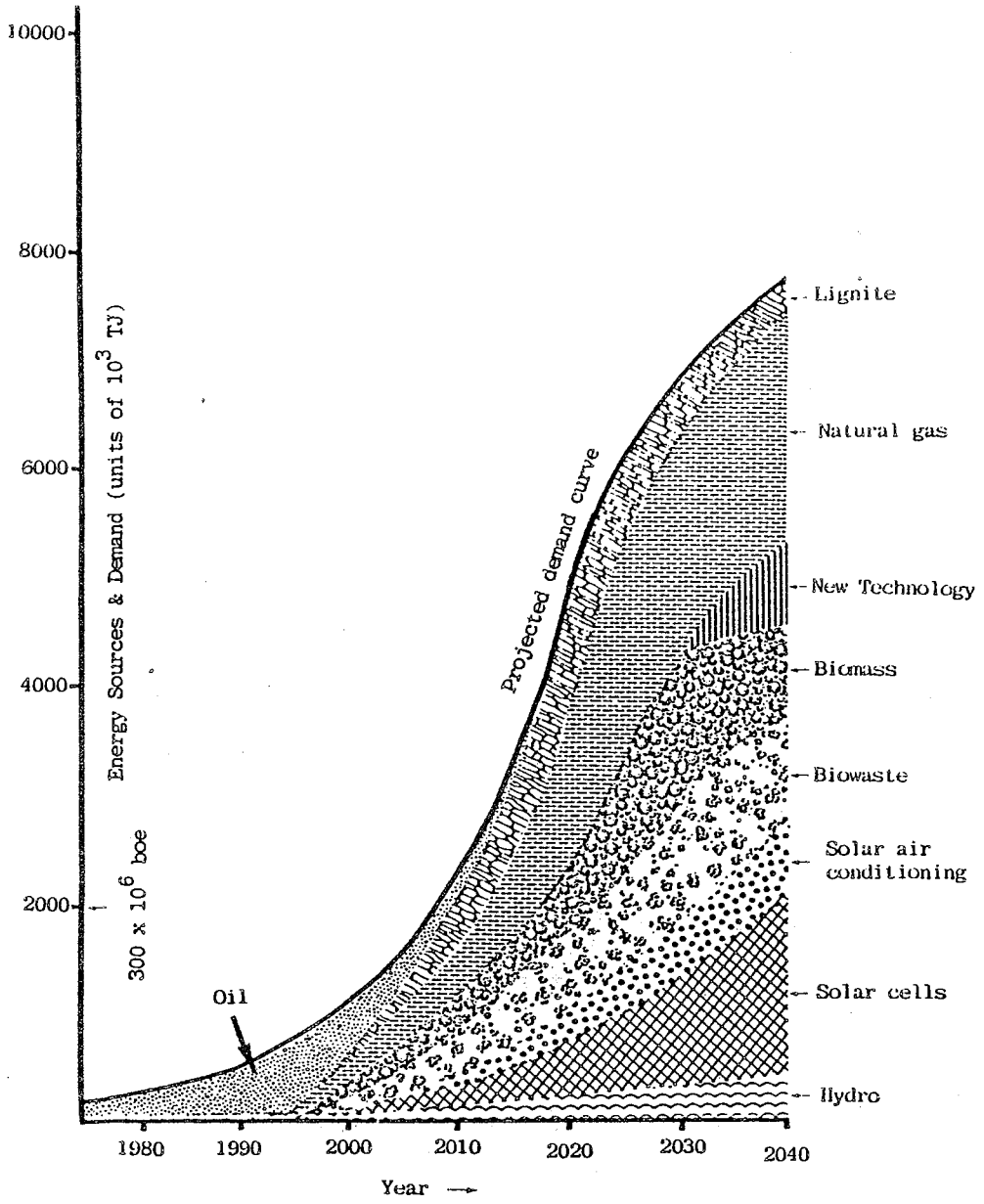

Figure 2: Energy Supply Sources for Malaysia till 2040.
(after Wong Kien Keong)

293

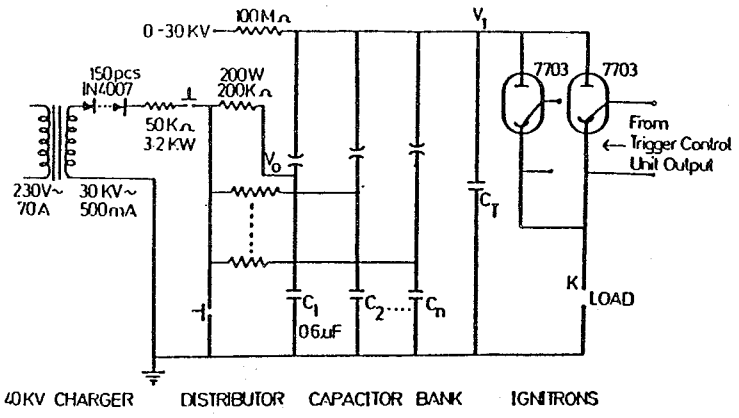

Figure 3: Circuit diagram for a module of 25 capacitors, showing charging circuit, distributor, capacitor bank, voltage division spark-gaps, ignitrons and load.

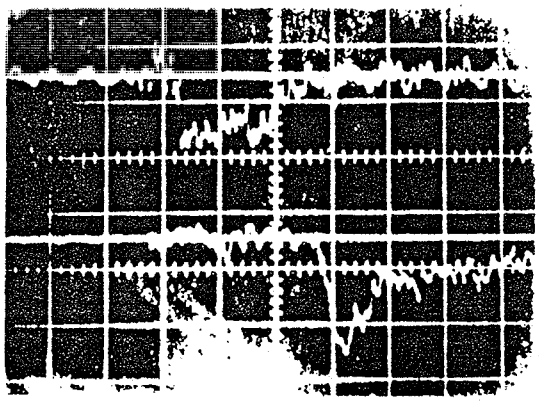

Figure 4: Time-of-flight oscillogram obtained in the measurement of neutron energy. Top trace records output from near detector. Bottom trace records output from far detector placed 10.2 m behind near detector. Horizontal scale 200 ns per cm.

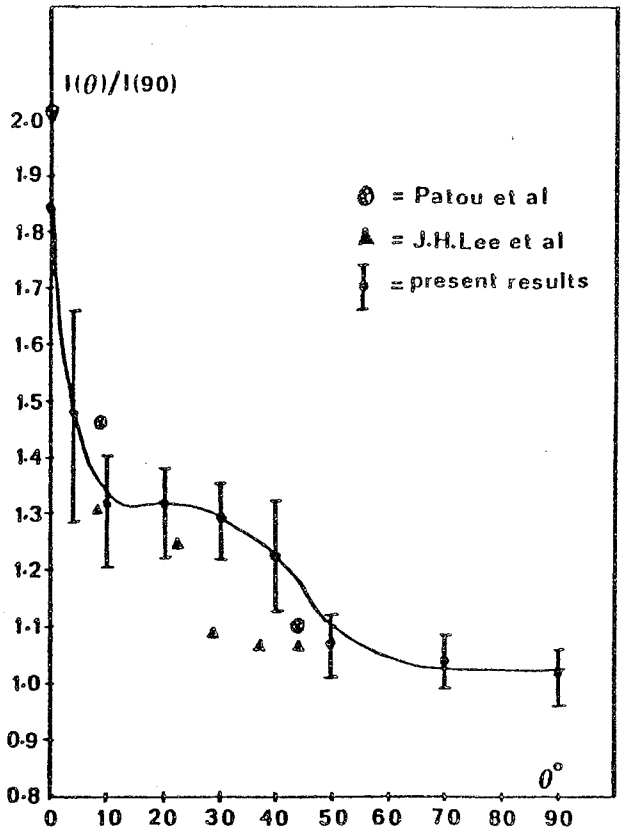

Figure 5: Results of angular distribution of neutrons from plasma focus.

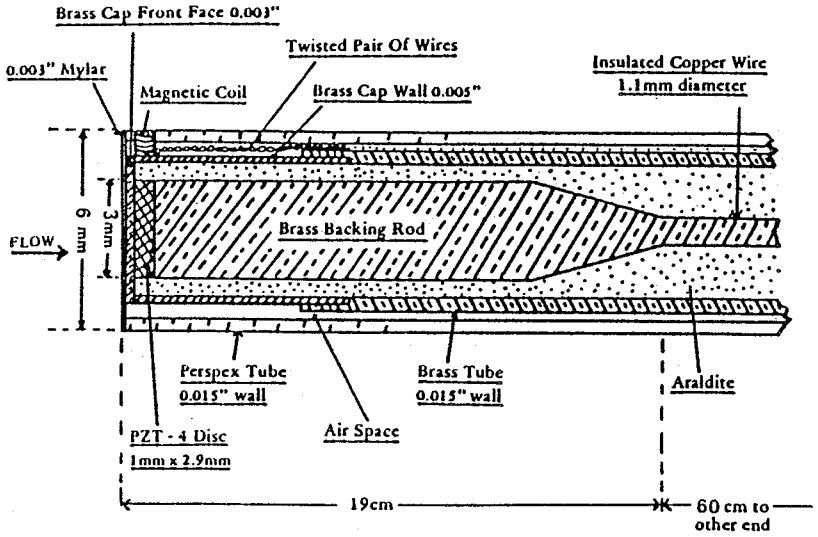

FIGURE 6. Combination probe for measuring plasma total pressure and magnetic field.

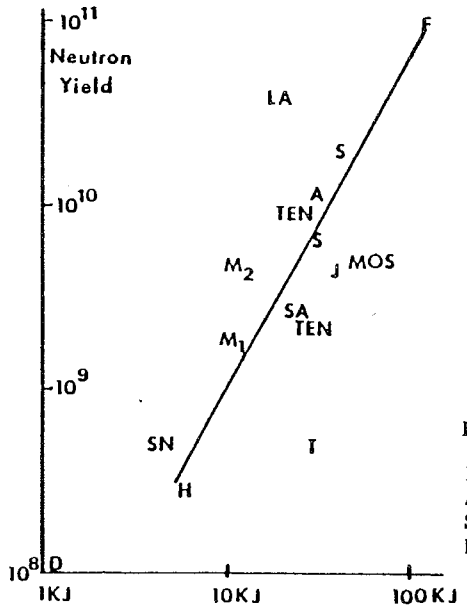

Figure 7: Neutron production as a function of energy.

F=Frascati; LA=Los Alamos; S=Stuggart; A=El Sequnda Aerospace; TEN=Tennessee; MOS=Moscow; J=Julich; SA=Sandia; SN=Steven; T=Texas; M_1=UMDPF1; M_2=UMDPF2; H=Hoboken; D=Darmstadt.

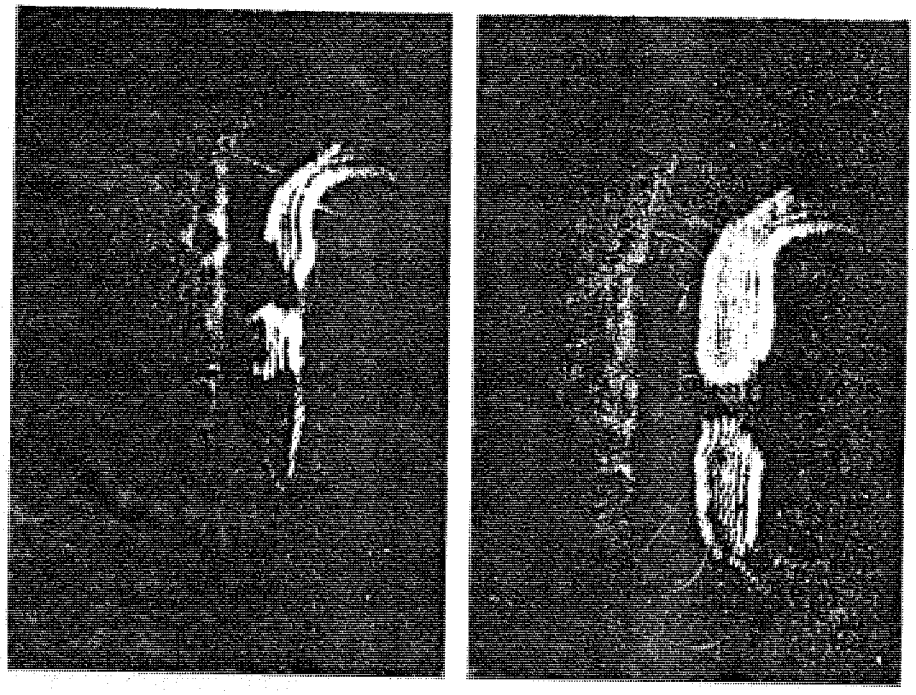

Figure 8: Shadowgraphy of the Plasma Focus

Left: 50 ns before minimum radius
Right: Just before minimum radius

FUSION ENERGY - 1981, IAEA-SMR-82
International Centre for Theoretical Physics, Trieste, 1982.

GEOMETRICAL OPTIMIZATION OF THE DENSE PLASMA FOCUS

S. LEE, Y.H. CHEN
Plasma Laboratory, Department of Physics,
University of Malaya,
Kuala Lumpur, Malaysia

Abstract:

A 12 kJ DPF device with a periodic time of 12μsec, UMDPF1 has been optimized geometrically to produce a higher neutron yield of 1.5×10^9 at 10 torr filling pressure than from the same device before optimization. With the same optimization procedure a faster DPF device with a periodic time of 3.7μsec, UMDPF2, of the same energy has also been optimized to give a peak neutron yield of 6.3×10^9 at 16 torr filling pressure. Experimental evidence shows that over and above the increase in neutron production due to an increase in current according to the $I^{3.3}$ scaling law, a faster current rise time may have an additional effect of enhancement in neutron production.

The outcome of this project is that a new high pressure regime of 16 torr with an enhanced neutron yield of 6.3×10^9 and improved yield reproducibility for an input energy of 12 kJ has thus been established.

There is every reason to believe that this optimization procedure can be extended to other DPF devices.

I Introduction

Considerable effort has been made to enhance the neutron yield in middle-energy DPF devices in the attempt to develop a reproducible and reliable pulsed neutron source {1}. In this paper, the results obtained in optimizing two middle energy DPF devices, UMDPF1 (Universiti Malaya Dense Plasma Focus 1) with a periodic time of 12 μsec and UMDPF2 (Universiti Malaya Dense Plasma Focus 2) with a periodic time of 3.7 μsec are presented. The geometrical influence and the effect of the current rise time on neutron production are also discussed.

The DPF devices used in this project are of Mather-type. A DPF device is a coaxial plasma accelerator but with a truncated inner electrode as shown schematically in figure 1. In this optimization project, the outer electrode consists of evenly spaced rods.

II Experimental Procedure

In this optimization program, the effect of the seven operational parameters of DPF devices on neutron yield has been investigated in detail. These seven parameters are inner electrode diameter, inner electrode length, outer electrode diameter, outer electrode length, insulator length, breakdown gap and filling pressure.

The neutron flux is measured with an indium activation counter and a silver activation counter. All data on neutron yield presented in this paper are the average of more than 20 shots each. After every experiment, the neutron detectors are calibrated in situ with a neutron source of known strength. In calculating the calibration factor, the abundance of excited atoms, the half time of the decay schemes as well as the dead time correction were taken into account. The accuracy of the calibration factor is estimated to be better than 5%.

The hard x-ray and neutron pulses are measured by a NE102A scintillator-photomultiplier detecting system. The current is measured by a Rogowski coil operated as a current transformer.

In the procedure, we first optimize the inner electrode length for a fixed inner electrode diameter with variation of the filling pressure. This, in effect, is to shift the focussing action so that the focussing action occurs at the time of the peak current in order to have maximum efficiency in utilizing the stored capacitor energy {2,3}.

The optimum inner electrode length is achieved when the neutron yield versus pressure curve is symmetrical and the neutron yield is reproducibly the maximum. Then the outer electrode diameter, outer electrode length, insulator length and breakdown gap are optimized with variation of filling pressure, one by one sequentially until the peak neutron yield is the maximum. After that the inner electrode diameter is varied and the above optimization procedure is repeated until the inner electrode diameter has also been optimized. This is indicated by the maximum neutron yield and the symmetry of the neutron yield versus pressure curve. The optimization procedure is summarised in figure 2.

III Optimization of the UMDPF1 and results

The geometrical parameters and the characteristic of UMDPF1 at various stages of optimization are shown in table 1. It was found that the filling pressure, the inner electrode

length, the inner electrode diameter and the outer electrode diameter are the strong parameters. They have great influence on the neutron production and have to be optimized properly for high reproducibility and maximum neutron yield. The other parameter like the outer electrode length, the insulator length and the breakdown gaps are weak parameters because their effect on neutron production is less significant than that due to the strong parameters.

The optimization results are summarised in figure 3 and figure 4. Figure 3 shows the dependence of the neutron yield on the inner electrode length. At the optimum inner electrode length of 16 cm, the curve is symmetrical and the peak neutron yield is the highest. Figure 3 also shows that with a reduction in the inner electrode diameter at the optimized inner electrode length, the neutron yield remains unchanged but the optimum filling pressure is shifted from 2.0 torr to 10.0 torr. The influence of the outer electrode diameter on the neutron production is also shown. At the optimum outer electrode diameter of 85 mm, the peak neutron yield is 1.5×10^9 with no shift in the optimum operating pressure. For an optimized device, the neutron yield variation for more than 10 shots on the same filling is less than 10%. With a single gas filling neutron production has been obtained for more than 30 shots consistently. These results are similar to those already reported earlier {1,4}.

IV Geometrical influence on neutron production

It has been reported that at all operating conditions the product of the filling pressure and the optimum inner electrode length is a fixed constant for a particular DPF device and they can compensate each other in optimization {3,5}. Our optimization results show that this constant product rule needs to be qualified once the inner electrode diameter is varied, which involves a variation in the axial acceleration force of the current sheath due to the 1/r dependence of the magnetic field. Experimental evidence shows that the effect of the variation of the inner electrode diameter on the time of focussing action is not capable of being compensated by the variation of the filling pressure alone. Hence the inner electrode length as well as the filling pressure need to be adjusted for maximum neutron production. This leads to a new constant for the same device. The optimum product of the filling pressure and the inner electrode length changes from 36 torr-cm for inner electrode diameter of 50 mm to 160 torr-cm for that of 25 mm.

Experimental results indicate that there exists an optimum inner electrode diameter and an optimum ratio of the outer and inner electrode in order to have an optimum operating condition

at which the neutron yield is resproducibly the maximum. On reviewing the total body of experimental results including framing photographs and magnetic probe measurements it appears that the existence of an optimum inner electrode diameter is related to the dependence of the azimuthal self magnetic field to the inner electrode diameter. Thus when the inner electrode is too large, the magnetic field is too small for effective driving. On the other hand with decreasing inner electrode diameter the time for the radial compression stage has also been reduced correspondingly. The dynamics of this stage has been found to be significant for the formation of the final focus and hence the total neutron yield {6,7,8}.

Similarly, it appears that the existence of an optimum ratio of the outer to the inner electrode diameters also depends on two conflicting conditions. The smaller the ratio the larger the pinch current tends to be from the impedance point of view. This factor encourages a higher neutron yield. However, experimental observation of radial restrikes indicate that for a given inner electrode diameter and a fixed capacitor voltage, it is necessary to have a minimum interelectrode gap to minimize the occurance of radial restrikes which invariably leads to current shedding {9,10,11,12}, resulting in a lower pinch current. Thus the optimum ratio of the two diameters is that ratio which gives the largest drive current without incurring significant radial restrikes.

An optimum ratio of 3.4 was observed in these experiment on UMDPF1 as opposed to a factor of 2 as suggested by Mather {2}.

V. Effect of the current rise time on neutron yield

The UMDPF2, formerly the DPF1 {13} in Jülich, Federal Republic of Germany, is one of the fastest DPF devices available in middle energy range. The operating parameters of this device have also been optimized using the experimental procedure discussed in Section III. The seven optimized parameters and the characteristic of UMDPF2 at 27 kV and 33 kV after optimization are shown in table 2.

Experimental result shows that when the charging voltage increases from 27 kV to 33 kV, the peak neutron yield increases from 3.5×10^9 to 6.3×10^9 with a shift of the optimum filling pressure from 13.5 torr to 16 torr as shown as figure 4. The increase in neutron yield obeys the $I^{3.3}$ scaling law. However the neutron yield of 6.3×10^9 for UMDPF2 is more than 4 times that from UMDPF1 at the same input energy of 12 kJ.

Comparing the neutron yield obtained from UMDPF1 at 20 kV and that from UMDPF2 at 27 kV, the neutron yield of 3.5×10^9 at 620 kA from the UMDPF2 is too high for the $I^{3.3}$ scaling law in

order to be in agreement with that of 1.5×10^9 at 520 kA from the UMDPF1. If the $I^{3.3}$ scaling law is employed, a neutron yield of 2.7×10^9 instead of 3.5×10^9 is expected. This reproducible 30% increase in the neutron yield is most probably due to the effect of the faster current rise time of 0.9 μsec for the UMDPF2, compared with that of 3 μsec for the UMDPF1. This enhancement effect could be related to an increased ratio of focus current to total tube current.

VI Conclusion

This project shows that the total neutron yield can be increased by optimizing the geometrical dimensions of the DPF devices. The inner electrode length, inner electrode diameter, outer electrode diameter and filling pressure are the strong parameters that have greater influence on the neutron production and need to be optimized with great care for high reproducibility and maximum neutron yield. The other parameters such as outer electrode length, insulator length and breakdown gap are weak parameters, whose influence on neutron yield is insignificant as long as they are within reasonable limits.

The outcome from this project is that the operating pressure has been extended from 2 torr with a neutron yield of 1.0×10^9 to 16 torr with a higher yield of 6.3×10^9 operating with the same amount of input energy, 12 kJ. A new high pressure regime of focus operation with enhanced neutron yield and improved yield reproducibility has thus been established.

VII Acknowledgement

One of the authors, Y.H. Chen acknowledges the original suggestion of G. Decker for the start of the optimization program during his stay at the Institut für Plasmaforschung, Stuttgart. The optimization program was repeated and extended using UMDPF1 and UMDPF2 at the Plasma Laboratory, Universiti Malaya, Malaysia. He is also grateful to German DAAD fellowship for the financial support during his stay in Stuttgart.

We are indebted to the Kernforschungsanlage (Nuclear Research Establishment) Jülich and the Alexander von Humboldt Foundation, Federal Republic of Germany for the gift of the Jülich DPF1 which has been reassembled in Plasma Laboratory, Universiti Malaya, Malaysia as UMDPF2, on which part of this work was done.

VIII References

{1} CHEN Y.H.,DECKER G.,FLEMMING L.,KIES W.,OPPENLÄNDER T., PROSS G.,RUECKLE B.,SCHMIDT H., SHAKHATRE M., TRUNK M., 8th European Conf. Controlled Fusion and Plasma Physics, Prague (1977), Paper 65.

{2} MATHER J.W. in Griem H.A. and Loveberg R.H. "Methods of Experimental Physics Vol. 9 Part B" Academic Press (1970).

{3} TRUNK M., Plasma Phys. 17 (1975) 237.

{4} KIES W., "Experimentelle Parameterstudien am Plasmafokus Minifokus", Stuttgart University, Institut für Plasmaforschung, Internal Report (1977).

{5} RAPP H., Phys. Let. 43A 5 (1973) 420-421.

{6} SCHMIDT H., NAHRATH B., RÜCKLE B., 7th European Conference on Controlled Fusion and Plasma Physics, Proceedings (1976) pp 57.

{7} TOEPFER A.J.,SMITH D.R.,BECKNER E.H., Phys. Fluids 14 (1971) 52.

{8} PEACOCK N.J.,HOBBY M.G.,MORGAN P.D., 4th IAEA Conf. on Plasma Physics and Controlled Nuclear Fusion Research, Tokyo, IAEA-CN-28 (D-3) (1972).

{9} LEE S.,CHEN Y.H.,CHOW S.P.,TAN B.C.,TEH H.H.,THONG S.P., Int. J. Electronics, 35 (1972) 85.

{10} CHEN Y.H.,LEE S., Int. J. Electronics, 3 (1973) 341-352.

{11} Pross G 1975 "Zuordnung von Neutronenausbeute und Zuverlässigkeit Zur Wahl Experimentaller Parameter bei einer Plasmafokus - Maschine", Ph.D. Thesis, IPF, Universität Stuttgart, Federal Republic of Germany.

{12} LEE S.,TAN T.H., 7th European Conference on Controlled Fusion and Plasma Physics, Proceedings (1975) pp 65.

{13} CLOTH P.,CONRADS H., Nuclear Science and Engineering, 62 (1977) pp 591-600.

Table 1

Parameters of UMDPF1 at various stage of optimization.

Parameters of UMDPF1			
$D_{i.e.}$	50 mm	25 mm	11 mm
$l_{i.e.}$	18 cm	16 cm	13 cm
$l_{o.e.}$	18 cm	16 cm	13 cm
$D_{o.e.}$	115 mm	85 mm	65 mm
l_{in}	40 mm	43 mm	43 mm
l_{eff}	14 cm	11.7 cm	8.7 cm
Characteristic of UMDPF1 at 20 kV			
C	60 μF	60 μF	60 μF
T	12.4 μsec	13 μsec	14 μsec
E	12 kJ	12 kJ	12 kJ
I	550 kA	520 kA	450 kA
P	2.0 torr	10 torr	13.5 torr
Y	1.0×10^9	1.5×10^9	8×10^8

Table 2

Parameters of UMDPF2 after optimization.

Parameters of UMDPF2

$l_{i.e.}$	8.5 cm
$l_{o.e.}$	15 cm
$D_{i.e.}$	25 mm
$D_{o.e.}$	65 mm
l_{in}	2.8 cm
l_{eff}	5.7 cm
d	3 mm

Characteristic of UMDPF2 at 27 kV and 33 kV

V	27 kV	33 kV
C	22 μF	22 μF
E	8 kJ	12 kJ
T	3.7 μsec	3.7 μsec
I	620 kA	760 kA
P	13.5 torr	16 torr
Y	3.5×10^9	6.3×10^9

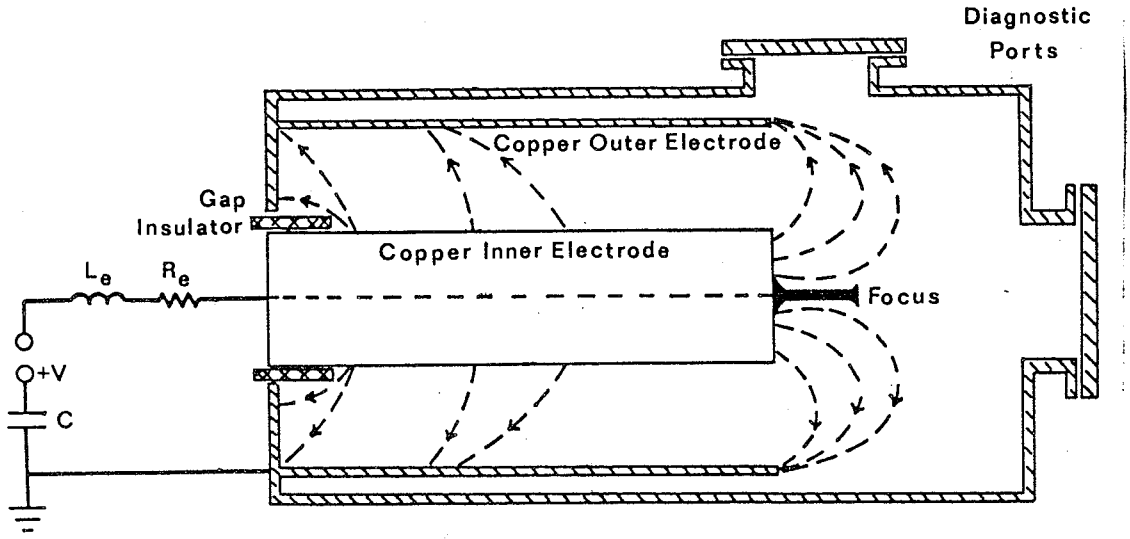

Figure 1: Schematic representation of a dense plasma focus (DPF) device

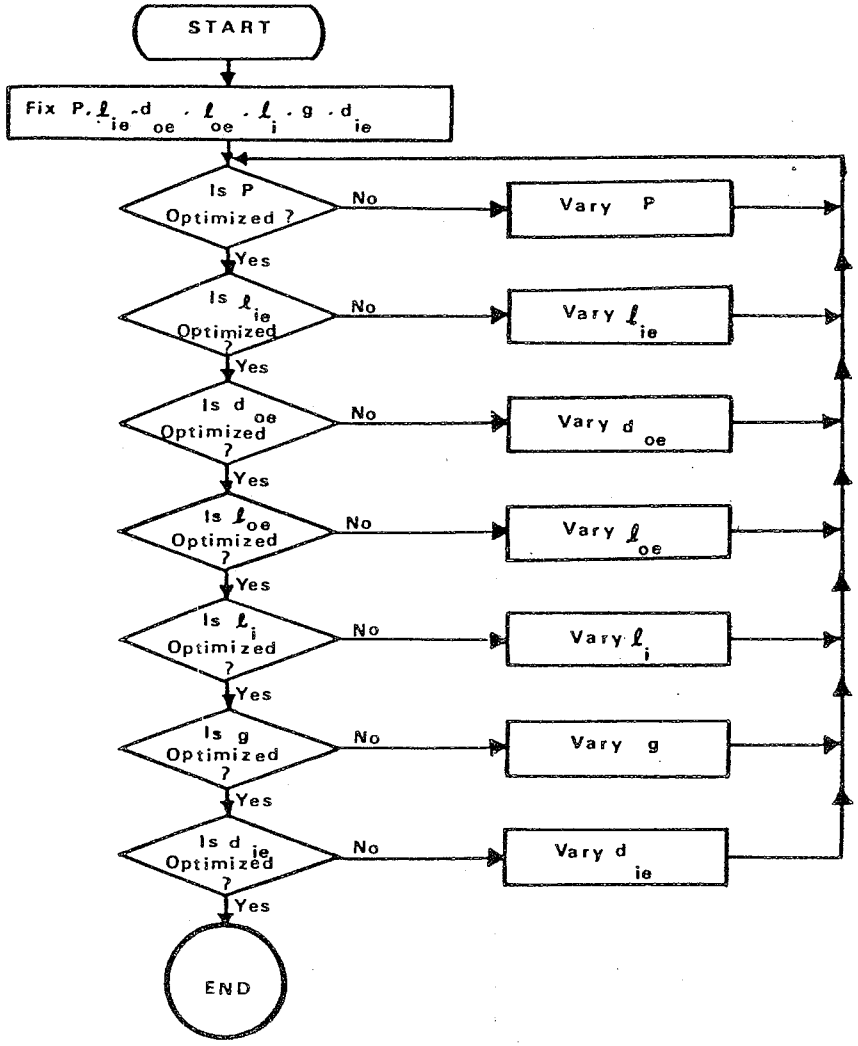

Figure 2: Flow-chart of the Optimization Procedure

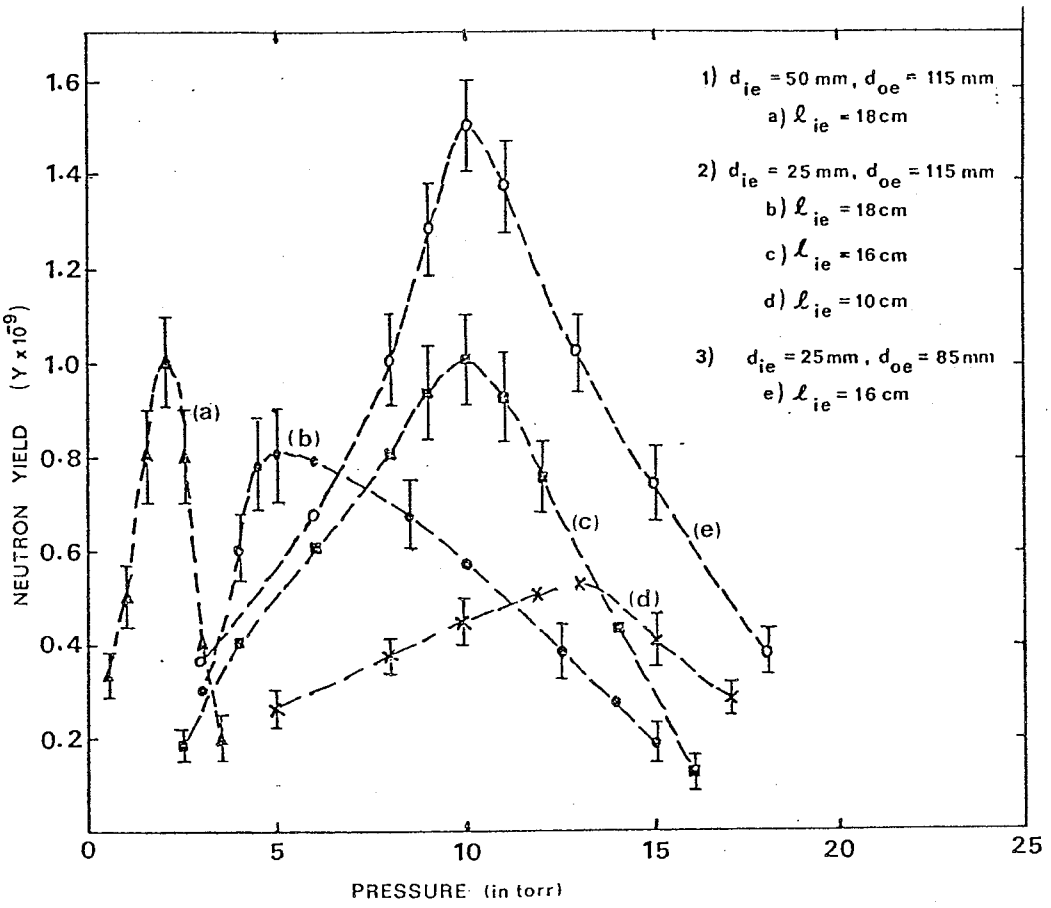

Figure 3: Experimental curves of neutron yield versus filling pressure at various inner electrode diameter, outer electrode diameter and inner electrode length.

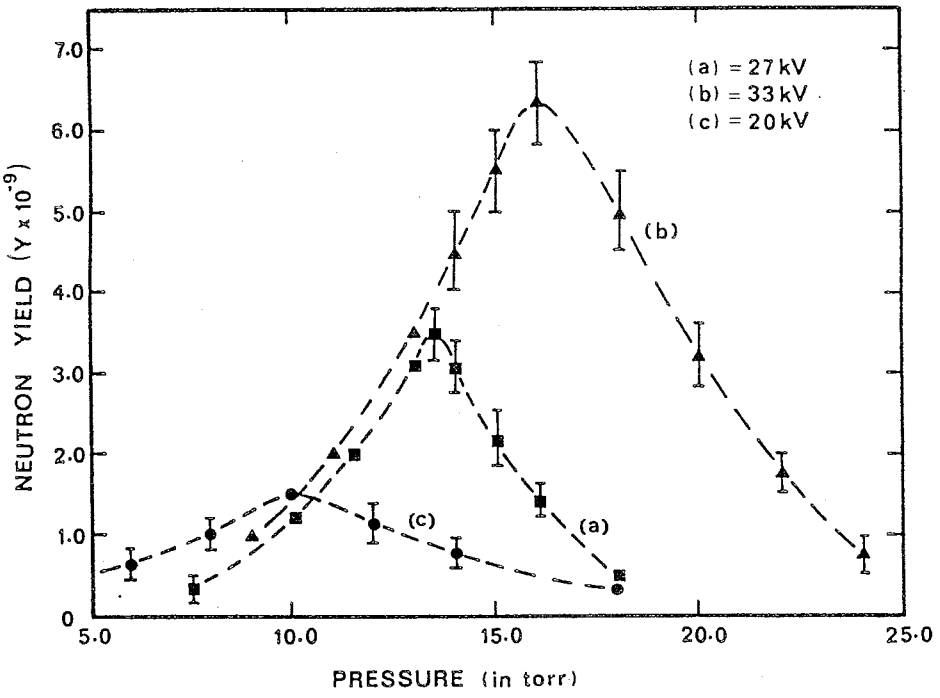

Figure 4: Experimental curves of neutron yield versus filling pressure at various charging voltages for operation with optimized parameters for UMDPF2.

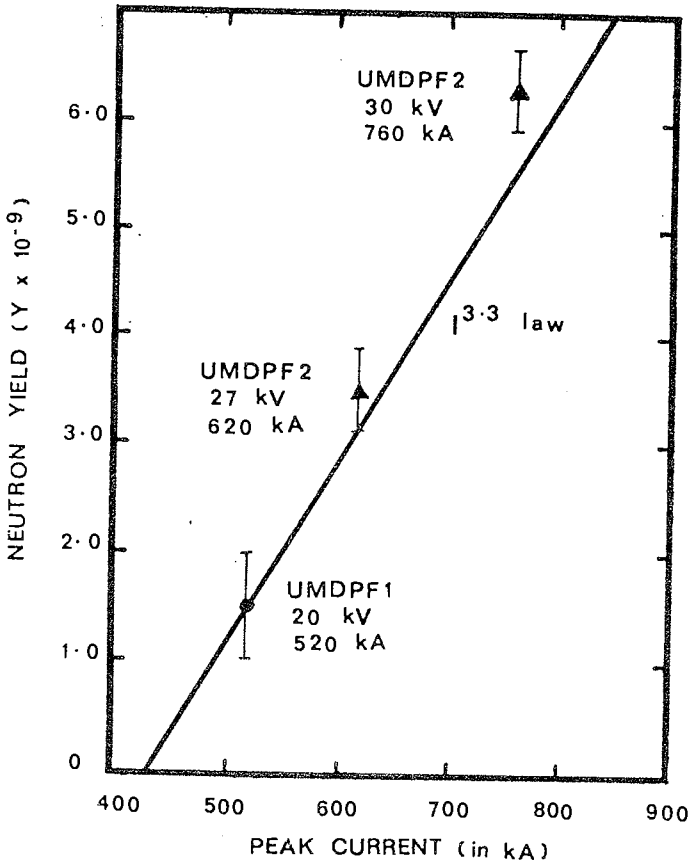

Figure 5: The $I^{3.3}$ Scaling Law

FUSION ENERGY - 1981, IAEA-SMR-82
International Centre for Theoretical Physics, Trieste, 1982.

VACUUM SPARK AS A FUSION DEVICE

C.S. WONG, S. LEE
Plasma Physics Laboratory,
Physics Department,
University of Malaya,
Kuala Lumpur, Malaysia

Abstract

The existence of extremely hot and dense plasma state in a vacuum spark has inspired the investigation of the possibility of developing it as a fusion device. Effort to achieve this aim has been carried out in the Plasma Physics Laboratory, University of Malaya and this is presented in this paper. A reproducible and consistent vacuum spark system with input energy of 13 kJ has been built and tested. The electron temperature of the plasma produced in this vacuum spark system has been estimated to be about 4 to 10 kev. Attempt to introduce LiD into the system in order to achieve fusion is also described.

1. Introduction

The vacuum spark is considered to be one of the simplest device that is capable of producing in the laboratory hot dense plasma with highly stripped ions such as Fe-XXVI, Cu-XXVIII and Ti-XXII[1]. Research on this device is mainly concentrated in two areas: Firstly, it is being utilised as a pulsed x-ray source for spectroscopic study of high Z materials[2-6]. In this case, the material being studied is made into the anode. Secondly, there has been considerable effort in trying to relate the vacuum spark discharge to the solar flare phenomenon[7,8]. It has been shown that the x-ray spectrum observed in the vacuum spark shows great resemblance to that of the solar flare.

During the vacuum spark discharge, there is extremely high concentration of energy in plasma spots with diameter of approximately 10 μm. This results in the compression and heating of the plasma to very high density and temperature. Typical values[9] of the plasma parameters of the vacuum spark are: $T_e \sim 8$ kev, $N_e \sim 10^{21}$ cm^{-3}, $T_i \sim 20$ kev and $N_i \sim 10^{19}$ cm^{-3}.

The above mentioned plasma conditions have been obtained from a vacuum spark device using high Z anode materials such as Fe, Cu, Ni and so on. However, due to the existence of these plasma conditions, it is reasonable for us to consider the feasibility of developing the vacuum spark as a fusion device. This immediately imposes two crucial questions: (i) can the same value

of $N_e \sim 10^{21}$ cm^{-3} be achieved in a deuterium plasma produced by the vacuum spark ? (ii) if so, can the ion temperature of 20 kev as in the case of high Z plasma be maintained ?

These questions have initiated the present project which is aimed at developing the vacuum spark as a fusion device. The preliminary experiments on this project have been performed in Jülich of the Federal Republic of Germany[10]. By using an anode with a central channel of LiD, neutron yield of the order of 10^7 per burst had been obtained and the neutron energy had been measured to be about 2 to 3 Mev[10]. In order to increase the neutron yield of this device, several modifications have been made[11]. These include the increase of maximum input energy from 3 kJ to 13 kJ and the use of high power pulsed ruby laser for the initiation of the discharge. The latter modification will improve the selectivity of anode material vaporisation so that the amount of high Z impurities in the deuterium plasma formed can be reduced.

2. The vacuum spark system

A schematic diagram of the vacuum spark device used in this project is shown in Fig.1(a). It consists of a sharp pointed cylindrical anode separated from the cathode by 5 mm. The anode is screwed on a brass cylindrical holder which is mounted onto the positive plate of the capacitor bank. This anode holder is insulated from the earth plate by perspex and silicon rubber. The cathode, which is cylindrical and has a one inch diameter channel through its center, is mounted on the aluminium vacuum chamber which also provides the return path of the discharge. The perspex window above the cathode is provided to allow transmission of laser light into the chamber. Laser beam focussing is achieved by using a 7 cm focal length biconvex lens.

To operate the vacuum spark device, the capacitor bank is first charged up to 20 to 35 kV. Since the electrodes of the system are connected directly to the capacitor bank, and the chamber is evacuated to a low pressure ($< 10^{-5}$ torr), the voltage will be held across the electrodes until some form of triggering is activated. Conventionally this is done by introducing a third electrode into the system and a high voltage pulse is applied across a ceramic surface between this electrode and the cathode[1-6]. The surface discharge produces electrons which are accelerated towards the anode tip. The main discharge will then start. Recently, the vaporisation effect of high power pulsed laser on metallic surface has been utilised for this purpose[11,12,13].

In this project, a 60 MW ruby laser pulse is used to initiate the vacuum spark discharge. It is focused onto the tip of the anode to a spot size of approximately 2 mm in diameter[14].

This corresponds to a laser irradiance of the order of 10^9 watts per cm^2 at the anode tip. The discharge is powered by a 22 μF capacitor bank which can be charged to a maximum voltage of 60 kV. However, due to the limitation imposed by the insulation, the system can only hold a maximum voltage of 35 kV which corresponds to an input energy of 13.5 kJ. The overall inductance of the system is estimated to be about 40 nH.

3. Experimental results

3.1. System performance of the vacuum spark device

In the effort to develop the vacuum spark as a fusion device, it is important to ensure that the system performs consistently and reliably. It is required to investigate several mechanical and electrical parameters such as the inter-electrode separation and the discharge voltage to establish an optimum system configuration at which the desired plasma conditions can be obtained consistently.

The performance of the vacuum spark system is studied with reference to the measurement of the discharge current, the time-resolved x-ray signals and the x-ray pinhole imaging. The discharge current is measured by a Rogowski coil operated as a current transformer. This measurement provides information concerning the electromechanical behaviour of the vacuum spark discharge. The time-resolved x-ray signals are measured by a pair of double-diffused silicon PIN diodes which have risetime of about 2 nsec. In order to obtain the x-ray image of the plasma formed in the vacuum spark, a covered pinhole of diameter of 600 μm or 300 μm is employed and the image formed is recorded on Polaroid Film Type 667.

The current and x-ray signals together with the x-ray image recorded simultaneously for a typical vacuum spark discharge with solid stainless steel anode are shown in Fig.2(a). Current dips are clearly observed at the time of ∿ 400 nsec after the start of the discharge and near the peak of the current. These dips usually correspond to strong bursts of x-ray from the vacuum spark. Meanwhile, bright plasma spots and clouds are observed on the pinhole picture indicating that intense x-ray fluence is being emitted from a small region between the electrodes. X-ray is also observed to be emitted from the surface of the anode tip. The anode tip is thus visible in the x-ray photograph and is taken as reference to locate the position of the plasma spot.

The macroscopic behaviour of the vacuum spark discharge as visualised from the current and x-ray observations is as follows:

On hitting the anode tip with laser irradiance of ∿ 10^9 watts/cm^2, some of the anode material will be vaporised and
338 resulting in a blowoff from the anode surface. This is further

heated by the laser light energy to form a plasma consisting of electrons, ions, neutral atoms as well as some small particles of the molten material. This plasma will soon expand to fill the inter-electrode gap and discharge will then occur. Since the electrons are moving much faster than the ions, we may consider the discharge current to be carried mainly by a beam of electrons accelerating towards the anode in a background of ions, atoms and micro-particles.

As the current-carrying electron beam is accelerated towards the anode, it may either interact with a cloud of plasma during which Bremsstrahlung x-ray is emitted; or it may impinge onto a micro-particle upon which a large portion of the beam energy is deposited to heat the micro-particle to form a hot dense plasma spot. This may cause the sharp decrease of the discharge current as observed from the current oscillogram.

The consistency of the vacuum spark discharge has been observed to be dependent on the inter-electrode separation. Generally, by refering to the current and x-ray signals and the x-ray pinhole image, the system seems to have a better reproducibility at inter-electrode separation of less than 1 cm. At a separation of 2.2 cm, the effect of increasing the discharge voltage will enhance the possibility of electron beam hitting the anode instead of interacting with the micro-particle. It can be seen from Fig.2b that the current signal obtained from the discharge of a vacuum spark system with such configuration is different from those obtained from typical discharge as shown in Fig.2a. The starting portion of such current signal is flattened indicating that energy of the system is being dissipated through electron-anode bombardment which results in the emission of x-ray from the whole surface of the anode as shown in the x-ray pinhole picture of Fig.2b. On the other hand, the system is observed to be very reproducible at separation of 0.5 and 0.8 cm, with over 80 % of the shots fired being able to produce the plasma spot.

3.2. Estimation of electron temperature

The electron temperature of our vacuum spark has been estimated by the foil-absorption technique[15]. Although it has been shown that[16,17] the error incurred by neglecting the contribution due to free-bound transition can be as high as 50 % for a high Z plasma, an estimation of the electron temperature can be obtained by taking into account the classical Bremsstrahlung continuum only. The classical x-ray Bremsstrahlung continua at various electron temperatures are shown in Fig.3.

In our experiment, the x-ray flux is measured by two PIN diodes which face the vacuum spark through identical windows covered with two thousandth inch of mylar sheet. Additional aluminium foil of 60 μm thickness is added so that only x-ray

with wavelength shorter than 1.65 Å will contribute to the diode signal.

To estimate the electron temperature of the vacuum spark plasma, the ratio of the amplitudes of the two detectors, with one of them having additional aluminium foils of thicknesses 20 μm, 40 μm, 60 μm and so on, are obtained for a series of discharges. These data are then compared with the theoretical curves as shown in Fig.4. It is concluded from this comparison that the electron temperature of our vacuum spark plasma is of the order of 4 to 10 kev.

3.3. Neutron production from the vacuum spark

The feasibility of operating the vacuum spark as a neutron producing fusion device has already been demonstrated[10]. It is believed that both the reactions $^{1}D(D,n)^{3}He$ and $^{7}Li(D,n)^{8}Be$ are responsible for the neutron yield if LiD is used[10]. This is mainly based on two facts: (i) It has been observed that particle energy of above 1 Mev is possible in the vacuum spark plasma[7]; and (ii) in experiments where particle beams of ^{7}Li and ^{1}D are bombarded at deuterium targets, the neutron yields for the reaction $^{7}Li(D,n)^{8}Be$ are more than an order of magnitude higher than that of the D-D reaction at particle energy range above 1 Mev[18]. Hence in any realistic estimation of neutron yield from this device, both reactions have to be taken into account.

The main difficulty that is confronting us at present is the fabrication of the deuterided anode. In the original design[10], LiD is fused into a small capillary of diameter 0.2 mm at the tip of the anode. During the process of fusing the LiD, it is required that the handling of LiD be carried out in an environment of dry nitrogen to prevent oxidation of the LiD crystals. It is also necessary to heat the LiD to a temperature of 700°C at which it will melt. Finally, it is allowed to cool down and solidify in deuterium. The use of only 0.2 mm diameter channel of LiD will also increase the possibility of high Z contamination of the deuterium plasma.

Several other anode designs have been tried in order to eliminate the difficulty in fusing the LiD and also to enhance the purity of the deuterium plasma. These are shown in Fig.1(b). Design A is the original design which has produced the neutron yield of 10^{7} neutrons per burst when LiD is fused into the central channel. In design B, the anode is a solid piece with a hole of diameter and depth of 3 mm each which is filled with LiD crystals. Experiments using this anode has not been sucessful mainly due to the throwing out of the LiD crystals during the discharge. This is evident from the fact that after just one discharge using this anode, no more LiD is found in the hole at the anode tip and pieces of LiD crystals are observed inside the aluminium chamber. In order to prevent this, design

C is proposed which consists of a central channel of diameter 3 mm. The lower part of this channel can be filled with LiD crystals or pellets. This will prevent discharge current to flow through the central part of the anode. This design will be tested in the very near future.

4. Conclusion

From the data we have obtained so far, it is reasonable to believe that the vacuum spark is feasible to be developed into a fusion device which may be able to find its application as a pulsed neutron source which may be useful in the design of a fusion reactor. Our present tasks are to simplify the process of anode fabrication so that the system can be set up easily, and to investigate the possibility of increasing the neutron yield from such a device.

Acknowledgement

The capacitor bank and the pulsed ruby laser used in this project are presented to the Physics Department, University of Malaya by the Alexander von Humboldt Foundation and Kernforschungsanlage Juelich of the Republic of Germany.

References

[1] Lie,T.N. and Elton,R.C., Phys. Rev.A 3 3(1971)865.
[2] Handel,S.K.,Ark. Fys. 28 27(1964)303.
[3] Beier,R. and Kunze,H.J., Z. Phys. A 285(1978)347.
[4] Fraenkel,B.S. and Schwob,J.L.,Phys. Lett. 40A 1(1972)83.
[5] Turechek,J.J. and Kunze,H.J., Z. Phys. A 273(1975)111.
[6] Cillier,W.A., Datla,R.U. and Griem,Hans R., Phys. Rev. A 12 4(1975)1408.
[7] Elton,R.C. and Lie,T.N., Space Sci. Rev. 13(1972)747.
[8] Gol'ts,E.Ya., Zhitnik,I.A., Kononov,E.Ya., Mandel'shtam,S.L. and Sidel'nikov,Yu.V., Sov. Phys. Dokl. 20 1(1975)49
[9] Lie,T.N., Proc. 2nd. Topical Conf. on Pulsed High Beta Plasmas(1972), ed. Lotz,W., paper G-7.
[10] Lee,S. and Conrads,H., Phys. Lett. 57A 3(1976)233.
[11] Wong,C.S. and Lee,S., Bul. Fizik Malaysia, 2 1(1981).
[12] Lee,T.N., Astrophys. J. 190(1974)467.
[13] Negus,C.R. and Peacock,N.J., J. Phys. D: Appl. Phys.12(1979)91.
[14] Wong,C.S. and Lee,S., Bul. Fizik Malaysia 2 2(1981).
[15] Jahoda,F.C., Little,E.M., Quinn,W.E., Sawyer,G.A. and Stratton,T.F., Phys. Rev. 119 3(1960)843.
[16] Seka,W., Breton,C., Schwob,J.L. and Minier,C., Plasma Phys, 12(1970)73.
[17] Sinha,B.K., J.Phys.D: Appl. Phys. 13(1980)1253.
[18] Burrill,E.A., "Neutron Production and Protection", Report of High Voltage Engineering Corporation, Burhington, Massachusetts.

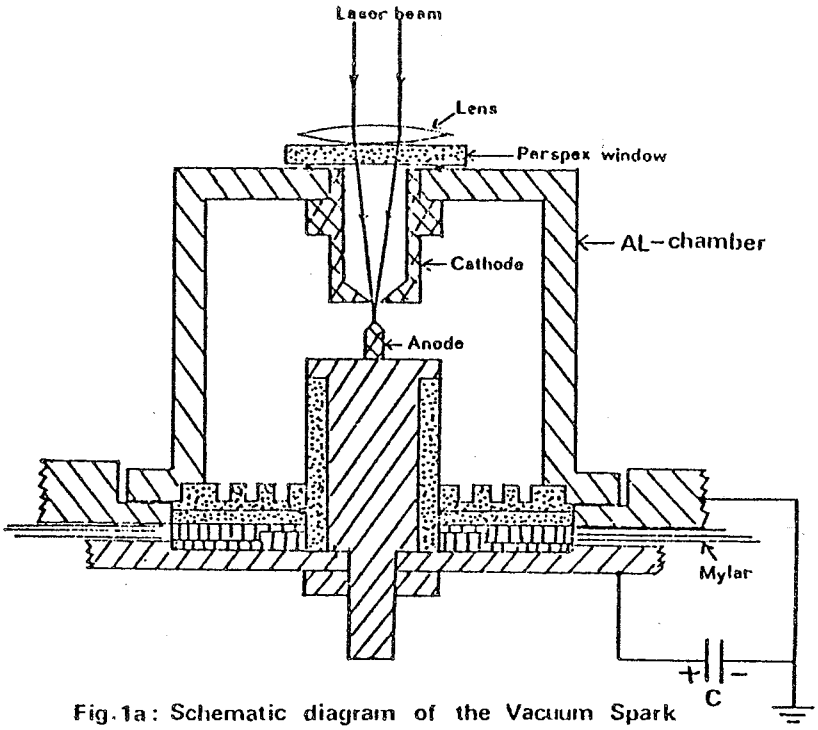

Fig.1a: Schematic diagram of the Vacuum Spark

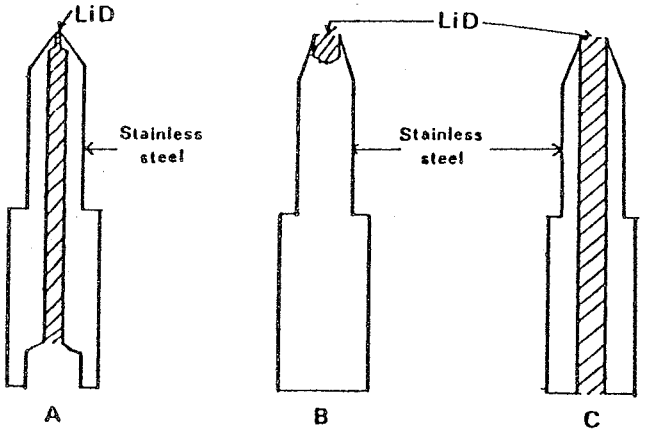

Fig. 1b: Anode designs

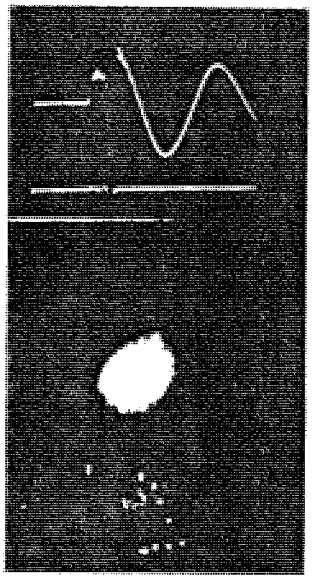

Fig. 2a: Current, x-ray oscillograms and x-ray pinhole picture of a typical vacuum spark discharge; electrode separation = 5 mm

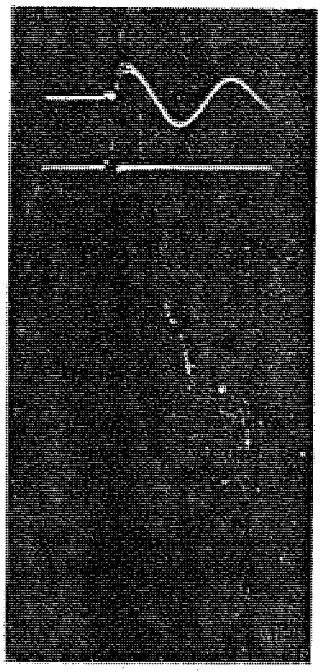

Fig. 2b: The same at electrode separation of 2·2 cm

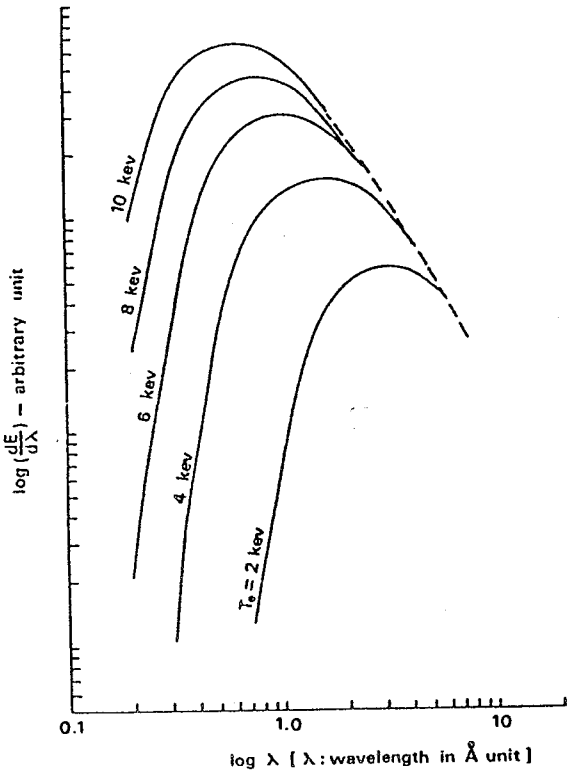

Fig. 3: X-ray Bremsstrahlung continua

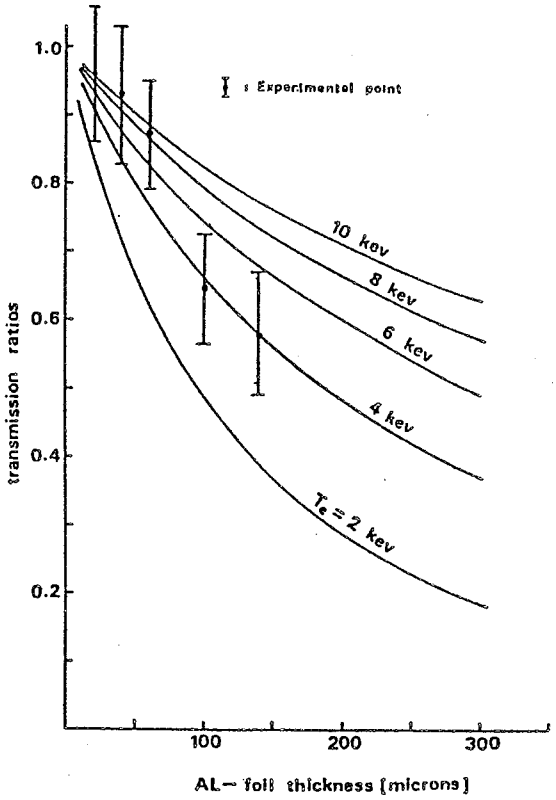

Fig. 4: Transmission of x-ray through AL-foils

341

Malaysian J. Sci. 6(B): 167–174(1980).

Neutron measurements of a 12 kJ plasma focus

C.S. WONG, S. LEE AND S.P. MOO

Abstract

The neutron yield of a 12 kJ plasma focus has been measured by indium-foil activation detector to be within the range of 10^7 to 5×10^8 neutrons per burst for more than 80% of the discharges. The neutron emission is found to be anisotropic and the neutron intensity in the forward direction ($\theta = 0°$) is about twice that in the radial direction ($\theta = 90°$). For discharges where more energy is injected into the plasma during focussing, the neutron yields are generally observed to be higher.

INTRODUCTION

The plasma focus has been the subject of intensive research since the first reports of Filippov, Fillipova and Vinogradov (1962) and Mather (1964). Although until today, no one theoretical model has been found successful in explaining the phenomenon precisely, several conclusions have been drawn from experimental results obtained so far. It is now understood that most of the neutrons produced from the plasma focus, if not all, are of nonthermal origin (Bernstein and Hai, 1970; Krompholf, Michel, Schonbach and Fischer, 1977). However, the device can be considered to be sufficiently well-behaved with respect to neutron yield taht it is possible to optimise a plasma focus device to obtain consistently high neutron yields (Chen, 1978; Chen and Lee). It has also been shown (Michel, Schonbach and Fischer, 1974) that an empirical neutron scaling law with respect to the discharge energy can be established from results obtained in various laboratories. This is of the form $N \sim E^{2.1}$, where E is the input energy of the plasma focus device. These well-behave characteristics, as well as the high neutron intensity (about 10^8 to 10^{11} neutrons in 100 nsec), of the plasma focus make it very feasible as a pulsed neutron source for neutronic investigations in controlled thermonuclear reactor blanket and material studies (Cloth and Conrads, 1977).

In this paper, the measurements of neutrons produced from the plasma focus device in this laboratory will be described. These utilise two indium-foil activation detectors and the absolute yield as well as the angular distribution of the neutrons has been measured. The energy injected into the focused plasma and its correlation with the neutron yield is also discussed.

EXPERIMENTAL SET-UP

The plasma focus device in this laboratory is of the Mather type and is shown schematically in Fig. 1. Powering the discharge is a capacitor bank which in this series of experiments is set at 20 kV delivering 12 kJ. The switching of this capacitor bank has been described elsewhere (Thong and Lee, 1973). The discharge current is measured by a Rogowski coil acting as a current transformer while the transient voltage across the electrodes during the discharge is measured by a resistive voltage divider. Typical current and voltage oscillograms are shown in Fig. 2.

The neutrons produced from the plasma focus is measured by two indium-foil activation detectors each consisting of an EMI 6097 photomultiplier tube coupled to a NE 102 plastic

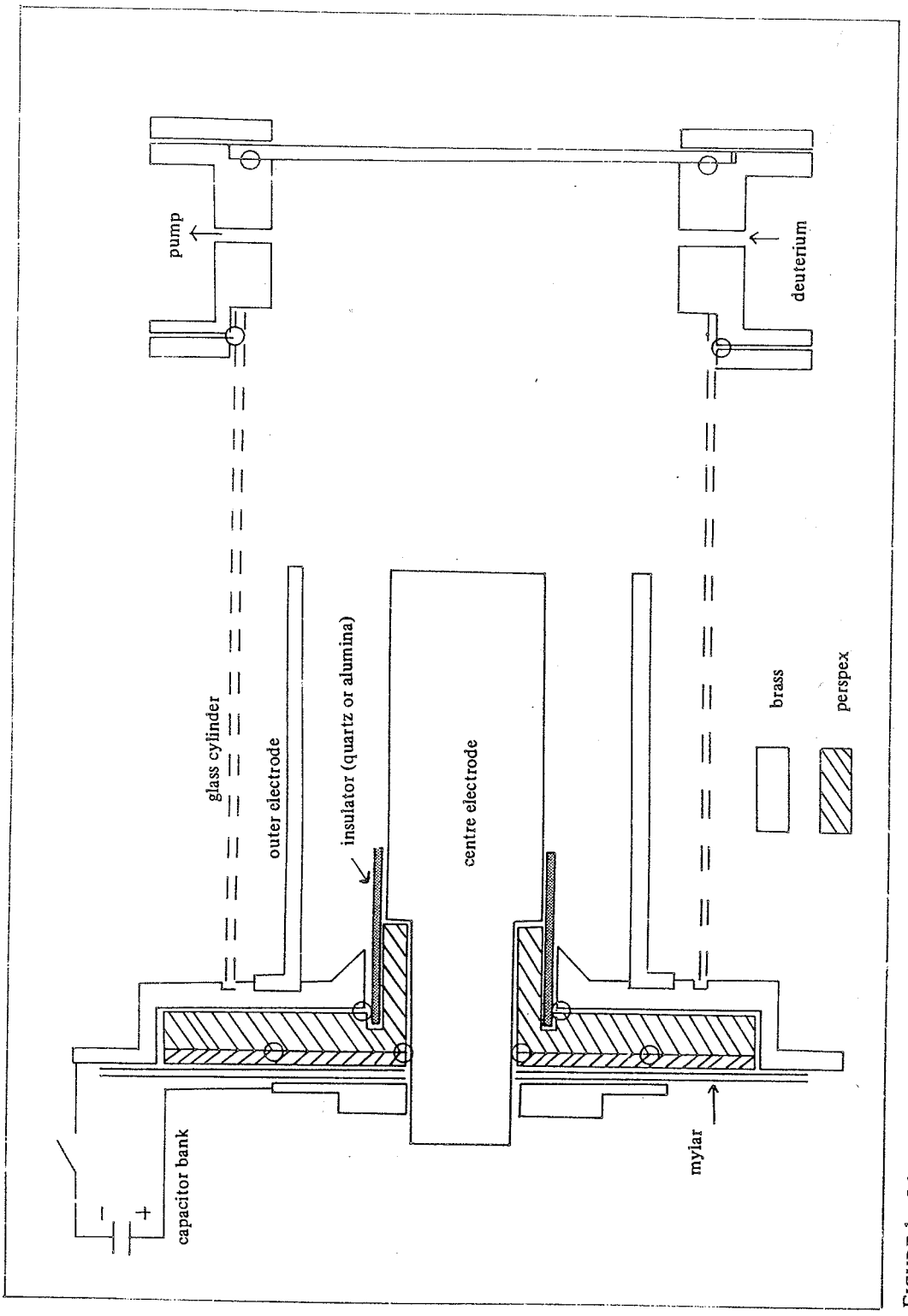

FIGURE 1. Schematic diagram of the plasma focus tube.

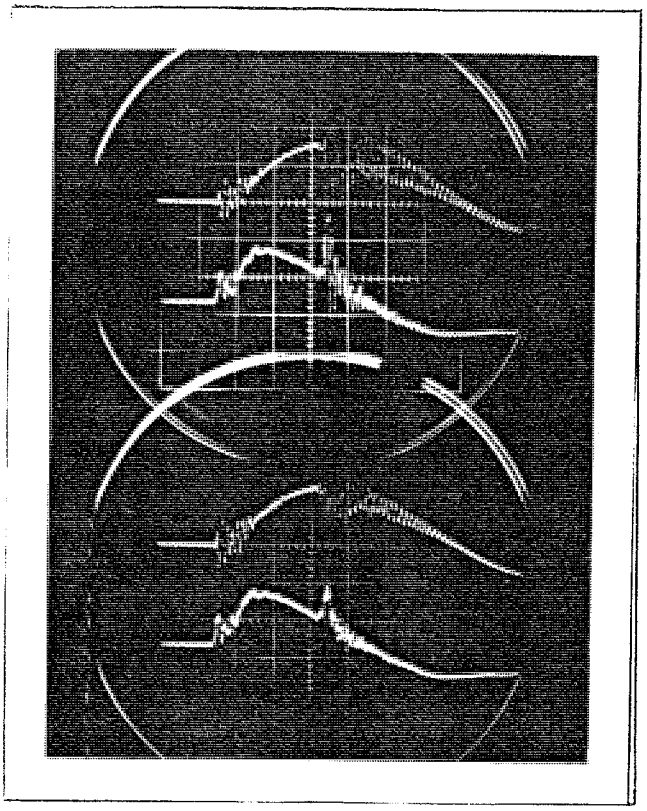

Display 1
Upper: I (t)
Lower: V (t)

Display 2
Upper: I (t)
Lower: V (t)

FIGURE 2 Two typical displays of current and voltage wave-forms of the focus tube on a double beam oscilloscope. In display 1, the focusing is more severe.

scintillator as shown in Fig. 3. Indium-foils of thickness 0.2 mm are used and the neutrons are thermalised by paraffin blocks before arriving at the indium-foil. At the indium foil the reaction of interest is

$$^{115}\mathrm{In} + \mathrm{n} \longrightarrow {}^{116}\mathrm{In} \longrightarrow {}^{116}\mathrm{Sn} + \beta^{-}$$

with a halflife of 14s for the ^{116}In. The betas have a maximum energy of 3.29 Mev.

Using this system, the betas are counted for a period of 40 seconds immediately after the neutron pulse. The number of counts gives an indication of the number of neutrons incident on the paraffin block. One advantage of such a system over a system that counts the plasma focus neutrons in real time is that the difficulty of high speed counting is eliminated.

These detectors have been calibrated with a ^{228}Th-Be neutron source. With one of these detectors fixed at the radial position of the focus tube and the other placed at various angular positions, the angular distribution of the neutron emission was obtained.

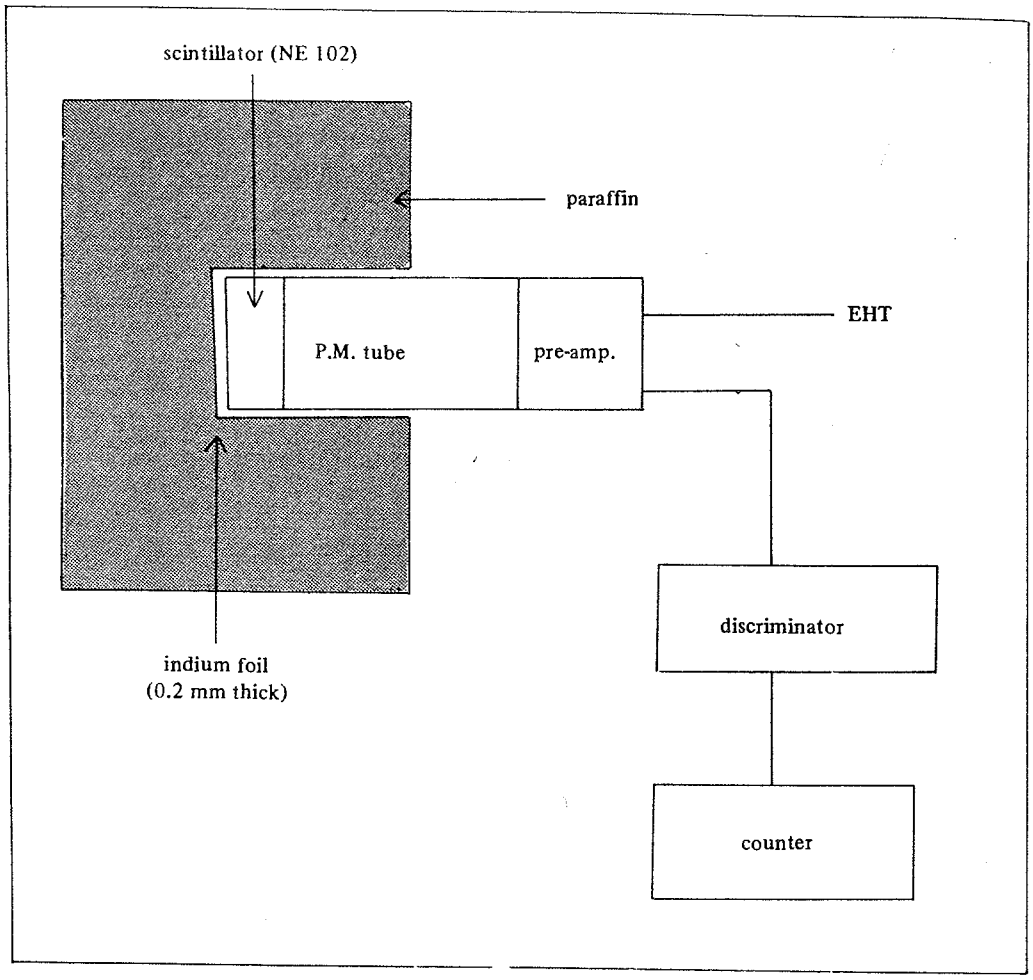

FIGURE 3 Schematic set-up of an indium foil activation detector.

RESULTS AND DISCUSSIONS

The neutron yield of the plasma focus device can be optimised by adjusting the electrical and mechanical parameters as well as the ambient gas pressure. An optimised focus neutron source not only produces high neutron yield (above 10^9 neutrons per burst), but should also be able to produce consistently the same yield under the same conditions. In this experiment, where the main aim is to study the characteristic of neutron production, a device with fixed electrical and geometrical parameters is used. The ambient deuterium gas pressure is varied to obtain a situation where the neutron yield is consistently within 10^7 to 5×10^8 neutron per burst. With yield of this order of magnitude, the counting statistics can be kept reasonably good and an average of ten to fifteen shots can be fired before it is necessary to refill the tube with deuterium.

The electrical and geometrical parameters of this focus device are listed in Table 1. The optimum ambient gas pressure is found to be between 1.0 to 1.5 torr, at which the neutron

TABLE 1

Electrical parameters and geometrical parameters of focus tube

discharge voltage	20 kV
maximum discharge current	590 kA
periodic time of current	11 μs
diameter of inner electrode	5 cm
diameter of outer electrode	10 cm
length of inner electrode	20 cm
length of outer electrode	25 cm
length of insulator	5 cm

yield is within the range of 10^7 to 5 x 10^8 neutrons per burst for more than 80% of the discharges.

The angular distribution of the neutrons emitted from the plasma focus device in this laboratory is shown in Fig. 4 as a graph of intensity against the angular position θ. The intensity shown is normalised against the radial direction (θ = 90°). From this graph, it can be seen that the neutron intensity is peaked at the forward axial direction (θ = 0°) with the ratio I(O)/I(90) equal to 1.84. Although this result cannot be compared directly to those obtained by Patou, Simonnet and Watteau (1969) and Lee, Shomo and Kim (1972) due to the differences in focus tube parameters, however, it shows the same feature of anisotropy as reported by them (Fig. 4). Rcently, the existence of an extended neutron source from the plasma focus has been reported (Cloth and Conrads, 1977). From these observations, it is evident that the deuterons which produce the neutrons are moving in the forward axial direction, with an average velocity of about 250 keV as estimated from results obtained in earlier experiments in this laboratory (Lee and Chen, 1975).

In order to investigate the injection of energy into the plasma during focusing, the variation of input power of the system is computed from the current and voltage oscillograms as shown in Fig. 5. The shaded area represents the extra energy injected into the plasma during focusing. This energy E_f is found to be generally less than 2.5% of the total input energy of the device. However, it is observed that this energy is generally higher for discharges of higher neutron yield (Fig. 6). This is in agreement with the fact that a more effective focusing action can be achieved by arranging the focus to occur near the maximum of the discharge current (Mather, 1971) which corresponds to a more effective compression of the plasma, thus resulting in more energy injected into it.

CONCLUSIONS

From the above experiments, it has been shown that the neutrons are emitted from the plasma focus anisotropically with a forward peaking feature similar to those reported by other workers. From the shape of the angular distribution curve, it is believed that there are more than one kind of neutron production mechanism operating in the plasma focus; and

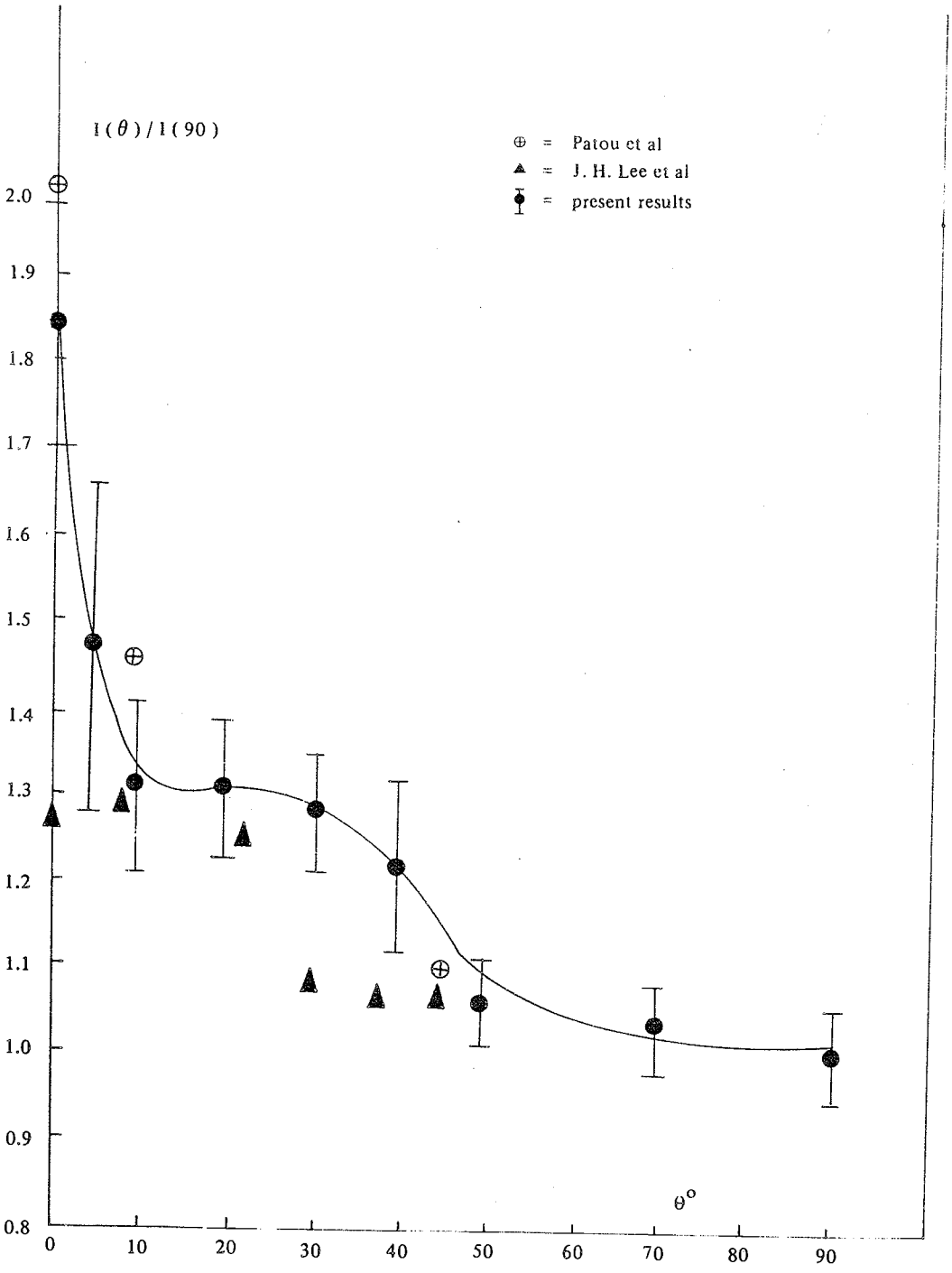

FIGURE 4. Results of angular distribution of neutrons from plasma focus

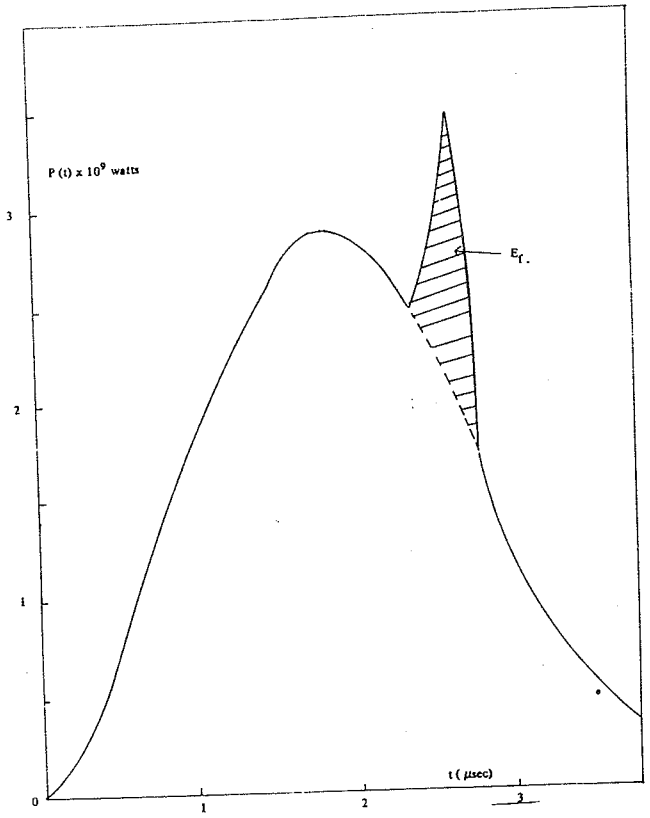

FIGURE 5. Graph of power against time

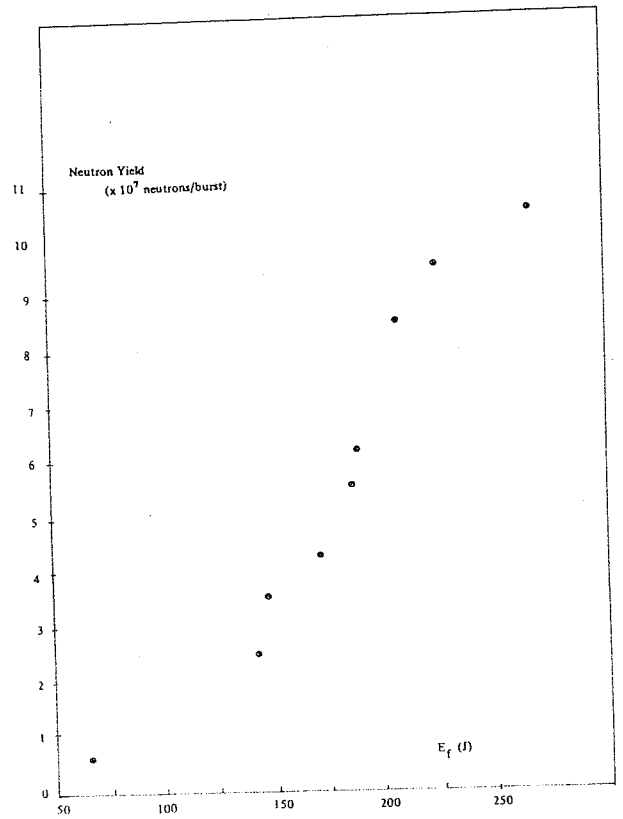

FIGURE 6. Graph of neutron yield against the energy injected into the plasma during focusing.

that not one of the models proposed (the beam-target, the moving-boiler and the converging-ions model) is adequate to explain the neutron production phenomena in the plasma focus. However, the fact that a higher neutron yield is obtained for a discharge with higher energy injected into the plasma during focusing indicates that the focus device can be considered to be well-behaved with respect to neutron yield. Hence in a system which has been tuned to the correct pressure regime, an estimation of energy injection can provide a rough relative measurement of the neutron yield without the use of a neutron detection system.

REFERENCES

FILIPPOV, N.V., FILLIPOVA, T.L. & VINOGRADOV, V.N. (1962). Dense, high-temperature plasma in a noncylindrical Z-pinch compression. *Nuclear Fusion Suppl.* Pt. 2; 577.

MATHER, J.W. (1964). Investigation of the high energy acceleration mode in the coaxial gun. *Phys. Fluids Suppl.;* 528.

BERNSTEIN, B.J. & HAI, F. (1970). Evidence of nonthermonuclear neutron production in a plasma focus discharge. *Phys. Letters* **31A**; 6.

KROMPHOLZ, H., MICHEL, L., SCHONBACH, K.H. & FISCHER, HEINZ. (1977). Neutron-, ion-, and electron-energy spectra in a 1 kJ plasma focus. *App. Phys.* **13**; 29–35.

CHEN, Y.H. (1978). *Parametric study of focus optimization.* Ph. D. thesis, Physics Department, University of Malaya.

CHEN, Y.H. & LEE, S. (1979). Geometrical optimization of DPF devices (to be published).

MICHEL, L., SCHONBACH, K.H. & FISCHER, HEINZ. (1974). Neutron emission from a small 1 kJ plasma focus. *App. Phys. Letters* **24(2)**; 57.

CLOTH, P. & CONRADS, H. (1977). Neutronics of a dense plasma focus – an investigation of a fusion plasma. *Nucl. Sci. and Engineering* **62**; 591-600.

THONG, S.P. & LEE, S. (1973). A simplified method of switching a 2 mega-ampere capacitor bank using a voltage division technique. *Mal. J. Sci.* **2(B)**; 157–169.

PATOU, P.C., SIMONNET, A. & WATTEAU, J.P. (1969). Measured anisotropies of the plasma focus neutron emission compared with proposed mechanism. *Phys. Letters* **29A(1)**; 1.

LEE, J.H., SHOMO, L.P. & KIM, K.H. (1972). Anisotropy of the neutron fluence from a plasma focus. *Phys. Fluids* **15(B)**; 2433.

LEE, S. & CHEN, Y.H. (1975). Measurement of neutrons from a plasma focus. *Mal. J. Sci.* **3(B)**; 159–163.

MATHER, J.W. (1971). Dense plasma focus. *Methods of experimental Phys.*, Vol. 9, pt. B, Chapter 15; Academic Press, Ed. Lovberg, R.H. and Griem, H.R.

THE PINCH PHASE OF A PLASMA FOCUS

S. Lee, FIPM
Plasma Research Laboratory
Physics Department, University of Malaya
Kuala Lumpur 22-11, Malaysia

Introduction

Research work on the pinch has been generally handicapped by a lack of understanding of the plasma structure both during the dynamic collapse phase and the quasi-equilibrium phase. For example, the classical snow-plow collapse model predicts a collapse of the plasma column to zero radius. On the other hand, the Bennett treatment is for a purely static column whereas as observed experimentally the dynamic phase is of great importance in determining the structure of the final quasi-static pinch. Thus, neither the snow-plow nor the Bennett model could predict even the radius of the quasi-equilibrium pinch.

Recently, a collapse model with inclusion of a collapse retardation pressure term has been developed[1] which, with the help of two adjustable parameters, has given pinch radii for the plasma focus in agreement with experimental results. It is only in 1978, however, that Potter[2] has treated a constant current pinch in an entirely self-consistent manner and derived plasma dynamics and plasma structures. One of his important results was that for a constant current pinch, the pinch ratio, defined as the pinch radius r_p (Figure 1a) divided by the original radius r_o, is dependent only on γ, the specific heat ratio of the plasma, and is given by:

$$r_p = r_o \left(\frac{\gamma}{\gamma + 1}\right)^{\frac{\gamma}{\gamma - 1}} .$$

In this paper, it is shown that a simple consideration based on energy and pressure balance gives an expression for the pinch ratio comparable with Potter's more comprehensive computation. Furthermore, the simplicity of the method based on energy and pressure balance enables the argument to be extended to pinches with non-constant currents; and non-constant length, the latter property being particularly applicable to

the pinch phase of a plasma focus (Figure 1b). The interest in the pinch phase of a plasma focus arises because in certain regimes of operation in a plasma focus machine a well-defined pinch with a stable phase may be obtained. In these 'pinch-optimised' regimes the plasma focus machines does not exhibit the intense electro-plasma interactions that occurs when the machine 'focusses' as in both the 'beam-optimised' as well as the 'neutron-optimised' regimes. However, these plasma-focus pinches show features similar to the finite-Larmor-radius (fLr) stabilised pinches[3,4] currently being studied with high-voltage constant current Marx generators as power sources. Plasma focus devices utilize a simple capacitor discharge and thus may prove to be simple method of generating fLr stabilised pinches.

Some experimental results are shown of these plasma-focus pinches and it is concluded that the difference in observed pinch ratios between a constant current pinch and a plasma-focus pinch is due to the non-constant length of the plasma-focus pinch which increases from zero at the start of the pinching process towards a maximum value, ℓ_p[5].

Theory

Energy and pressure balance

Constant current pinch of constant length

We consider the following model. On initiation, the current, I, flows axisymmetrically in a thin sheath of radius r_o (Figure 1a). The current interacts with its self-magnetic field B_θ and implodes inward. The implosion may be described as a magnetic piston travelling at a highly supersonic speed preceded by a shock wave. Starting at radius r_o the magnetic piston compresses the plasma sheath which collapse into a plasma column when the shock wave has imploded onto the axis. The magnetic piston continues moving inwards until the temperature of the column becomes sufficiently high to eventually stop the motion of the piston. A phase of quasi-static equilibrium is achieved at pinch radius r_p.

The magnetic piston exerts a magnetic pressure $P_m = B_\theta^2/2\mu$

where the magnetic induction $B_\theta = \mu I/2\pi r$. I is the current flowing through the plasma-magnetic field boundary at radius r. The work done by the piston in moving from position r_o to position r_p is:

$$W' = \int_{r_p}^{r_o} \underset{\sim}{F}.\underset{\sim}{dr} = \int_{r_p}^{r_o} \frac{\mu^2 I^2}{4\pi^2 r^2 (2\mu)} 2\pi r dr \qquad (1)$$

per unit length of the plasma column.

If the pinch density is ρ, the mass per unit length is $\rho\pi r_p^2$ and the work done per unit mass by the magnetic piston in moving from r_o to r_p is

$$W = \frac{\mu I^2}{4\pi^2 \rho r_p^2} \ln\left(\frac{r_o}{r_p}\right) . \qquad (2)$$

Assuming that this work is subsequently converted into the enthalpy of the pinched plasma without loss we may write the plasma enthalpy per unit mass as:

$$h = \frac{P}{\rho}\frac{\gamma}{\gamma-1} = \frac{R_o}{M} Tz \frac{\gamma}{\gamma-1} \qquad (3)$$

where P is the plasma pressure, R_o the universal gas constant, M the molecular weight, T the pinch temperature and z the departure coefficient due to real gas effects, if any.

Equating the enthalpy to the work done we have:

$$\frac{R_o}{M} Tz \frac{\gamma}{\gamma-1} = \frac{\mu I^2}{4\pi^2 \rho r_p^2} \ln\left(\frac{r_o}{r_p}\right)$$

giving a pinch temperature of:

$$T = \frac{I^2}{4\pi^2 \rho r_p^2} \ln\left(\frac{r_o}{r_p}\right) \frac{M}{R_o} \frac{1}{z} \frac{\gamma-1}{\gamma} . \qquad (4)$$

We may also obtain independently another equation for the pinch temperature from pressure balance i.e. by equating the magnetic pressure at r_p constraining the static pinch to the contained plasma pressure

$P = \rho \frac{R_o}{M} Tz$. Thus we write:

$$\frac{\mu^2 I^2}{4\pi^2 r_p^2 (2\mu)} = \rho \frac{R_o}{M} Tz$$

and obtain

$$T = \frac{\mu I^2}{8\pi^2 \rho r_p^2} \frac{M}{R_o} \frac{1}{z} \quad . \tag{5}$$

Combining the independently derived equations (4) and (5) for pinch temperature T, we obtain:

$$r_p = r_o \exp\left\{\frac{-\gamma}{2(\gamma-1)}\right\} \quad . \tag{6}$$

The pinch ratio expressed in equation (6) agrees with Potter's pinch ratio in the limit $\gamma = 1$ corresponding to an infinite number of degrees of freedom for the pinched gas in which case the pinch ratio is zero. For $\gamma = 5/3$, corresponding to a gas of 3 degrees of freedom typical of fully ionized gases, equation (6) gives a pinch ratio of 0.29 compared to one of 0.31 from Potter's theory.

From Potter's theory it is not readily apparent what the effects are on the pinch ratio of deviations from the constant current, constant length model. From the above theory of energy and pressure balance, the effects of any such deviations are easily seen.

Current rising during pinch

This case is particularly applicable to classical pinch experiments in which the current may rise from low values of the order of a few kA at the start to tens of kA or greater at the time of the static pinch. In this case the I in equations (4) and (5) may be taken as the current flowing at the time of peak compression with the pinch radius at r_p; and in equation (4) there should be an additional factor f with $f < 1$ resulting from the integration in equation (1) because of the rising current. The resulting pinch ratio is seen to be reduced.

Conversely, if the current drops during the pinch the pinch ratio would be increased.

Axial loss of mass

This case may be more applicable to the plasma focus pinch because of the axial velocity inherent in the plasma-focus pinch formation. An examination of equations (1) to (6) shows no change in the situation unless the axially ejected mass carries away a substantial amount of energy. The effect then could be to reduce the pinch ratio. From shadowgraphy[5], there is no evidence of substantial axial ejection of mass out of the plasma-focus during the pinch phase and it is our conclusion that this is not the major cause of the reduced pinch ratio observed in the case of the plasma-focus pinch when compared to the constant current, constant length pinch.

Initial mass

The presence of an 'initial mass' in the case of the plasma-focus pinch[6] is not expected to change the pinch ratio because of its low energy content.

Increasing length during the pinch

This case is peculiar to the plasma-focus pinch. As the current sheet sweeps around the anode to start the pinch its length may be considered to be zero. As the pinch progresses its length increases to a maximum value of ℓ_p. The relationship between the current sheet radius r and the pinch length ℓ may be written as:

$$\ell = \frac{\ell_p}{(r_o - r_p)} (r_o - r).$$

Then the work done for the whole pinch may be written as:

$$\int_{r_p}^{r_o} \frac{\mu^2 I^2}{4\pi^2 r^2 (2\mu)} 2\pi\, r\ell\, dr$$

and the work per unit mass m be written as:

$$W = \frac{\mu I^2}{4\pi^2 \rho} \frac{r_o}{(r_o - r_p) r_p^2} \{\ell n(\frac{r_o}{r_p}) - (1 - \frac{r_p}{r_o})\} .$$

Thus, from energy balance we have

$$T = \frac{\mu I^2}{4\pi^2 \rho r_p^2} \frac{r_o}{(r_o - r_p)} \{\ell n(\frac{r_o}{r_p}) - (1 - \frac{r_p}{r_o})\} \frac{M}{R_o} \frac{1}{z} \frac{\gamma - 1}{\gamma} . \qquad (7)$$

Combining this with equation (5) gives for $\gamma = 5/3$

$$\ell n(\frac{r_o}{r_p}) = 2.25 \ (1 - \frac{r_p}{r_o})$$

with a solution for the pinch ratio of $\frac{r_p}{r_o} = 0.14$.

Experimental observations

Some experimental observations will be noted here for comparison with the above theory.

Argon focus versus deuterium focus

A plasma focus in argon is observed to exhibit more intense electro-plasma interactions than a plasma focus in deuterium[7]. This may be ascribed to the fact that in a typical argon focus $\gamma = 1.14$ giving a reduction in the pinch ratio of more than 10 when compared with a $\gamma = 5/3$ gas like deuterium. This will give rise to more intense electro-plasma interaction from both inductance as well as stability considerations.

Rising current pinches

Experimental observations on classical pinches using rising currents have shown pinch ratios considerably less than 0.3. The measured pinch ratio for the Imperial College constant current pinch is 0.29. Both these observations are in agreement with the theory.

Plasma-focus pinch

In early work on the Universiti Malaya Dense Plasma Focus (UMDPF) it was found that for operation at low pressures a current-shedding effect was observed[8] and a focus phase would be present or absent depending

on the proportion of current participating in the pinch phase[6]. Typically at 0.2 torr D_2, with 19 kV giving a peak current of 430 kA, a strong focus phase is observed whenever 50% or more of the current participates in the compression phase. For cases where current shedding was so severe that only about 20% of the total current arrived in time to participate in the radial compression no focus phase was observed. Instead a well-formed pinch with a sustained stable phase was observed.

A typical example is shown in the inset of Figure 2 which is one of a series of streak photographs taken for the case of 0.2 torr D_2 at an estimated approximately constant current of 80 kA. The anode diameter used was 4 cm and the concentric cathode of the focus device had a diameter of 9 cm, and was slightly tapered towards the anode at its open end. The overall experimental evidence was that this particular shape of the cathode did not affect materially the plasma compression as the current sheet swept off the anode. The streak slit was positioned 3 mm off the end of the anode in a direction perpendicular to the axis of the anode.

Because of the coincidental similarity of these plasma-focus pinches to the constant current pinches recently published by the Imperial College Workers[3,4] these streak photographs have been reconstructed (Figure 2) to the same time and space scale as the published streak photograph of the Imperial College pinch operated at 0.07 torr H_2 at an anode radius of 4 cm and constant pinch current of 60 kA lasting for 100 ns[3].

For the same initial radius the speed of the compression scales as $I/\rho^{\frac{1}{2}}$. Thus, the Imperial College pinch should compress at a speed 1.8 times that of the UMDPF pinch. This is observed experimentally in Figure 2. The Imperial College pinch has a measured pinch ratio of 0.3 which compares with Potter's predicted value of 0.31 and the predicted value of 0.29 from the energy balance equations presented earlier in this paper. The UMDPF pinch (constant current but increasing length) has a measured pinch ratio of 0.13 which compares with a value of 0.14 from our energy balance theory.

The Imperial College pinch has a stable lifetime of 100 ns. Defining a stability enhancement factor M' = lifetime/transit time of small

disturbance speed, the estimated M' for the Imperial College pinch is 20. This value of M' has been ascribed to the effects of fLr stabilisation[3].

The stable lifetime of the UMDPF pinch exceed 300 ns giving a minimum estimated stability enhancement factor M' of 30 in the UMDPF pinch. The line density N for the UMDPF pinch is 10^{19} per m giving a ratio of Larmor radius r_{gyr} to pinch radius[3] of:

$$\frac{r_{gyr}}{r_p} = 8.08 \times 10^8/N^{\frac{1}{2}} = 0.26.$$

This ratio indicates that fLr stabilisation could be the mechanism responsible for the large value of M' observed in the UMDPF pinch.

Conclusion

It is shown that simple theory based on energy and pressure balance is able to predict pinch ratios with results comparable to Potter's more comprehensive computation applied to a constant current, constant length pinch. Morever, this simple theory extends readily to so far untreated cases with non-constant current and non-constant length as well as cases with axial mass ejection out of the pinch during the pinching process. Thus, this energy balance theory is particularly suited to computations for the pinch phase of the plasma focus. The computation and experimental results agree that the increase in length of the pinch during the pinching phase of the plasma focus is the predominat factor resulting in a greatly reduced pinch ratio. This is contrary to the speculation of other authors who have ascribed the reduced pinch ratio of the plasma focus to an axial loss of mass during pinching[2,3].

Finally, results are presented of a stable pinch phase observed in a low pressure plasma focus operated in a heavily current-shedded non-focusing regime. A stability enhancement factor of 30 was estimated for this UMDPF pinch. Work is in progress to demonstrate that a 'pinch-optimised' regime may be clearly defined in plasma focus devices.

Reference

[1]S. Lee and Y.H. Chen, *'The Plasma Focus - A radial trajectory computation'* Procs. of Twelth Int. Conf. on Phenomena in Ionized Gases, Eindhoven, Netherland, I, Paper 353 (1975)

[2]D.E. Potter, Nucl. Fusion, 18, 813 (1978)

[3]M.G. Haines, Phil. Trans. R. Soc. Lond., A300, 649 (1981)

[4]P. Choi, A.E. Dangor, A. Folkierski, E. Kahan, D.E. Potter, P.D. Slade and S.J. Webb, Plasma Phys, and Nucl. Fusion Research II, 69, Vienna IAEA (1978)

[5]S. Lee and Y.H. Chin, *'Shadowgraphic technique applied to a plasma focus'*, Bul. Fiz. Mal., 2-2, 105 (1981)

[6]S. Lee and T.H. Tan, *'Dependence of focus intensity on mass and field distribution'*, Procs. of Seventh Europ. Conf. on Controlled Fusion and Plasma Phys. Lausanne, I, Paper 65 (1975)

[7]Y.C. Yong and S. Lee, *'Multiple ionization in an argon plasma focus'*, Procs. Symp. Phys., Kuala Lumpur, 149 (1977)

[8]S. Lee, Y.H. Chen, S.P. Chow, B.C. Tan, H.H. Teh and S.P. Thong, Int. J. Electronics, 33, 85 (1972)

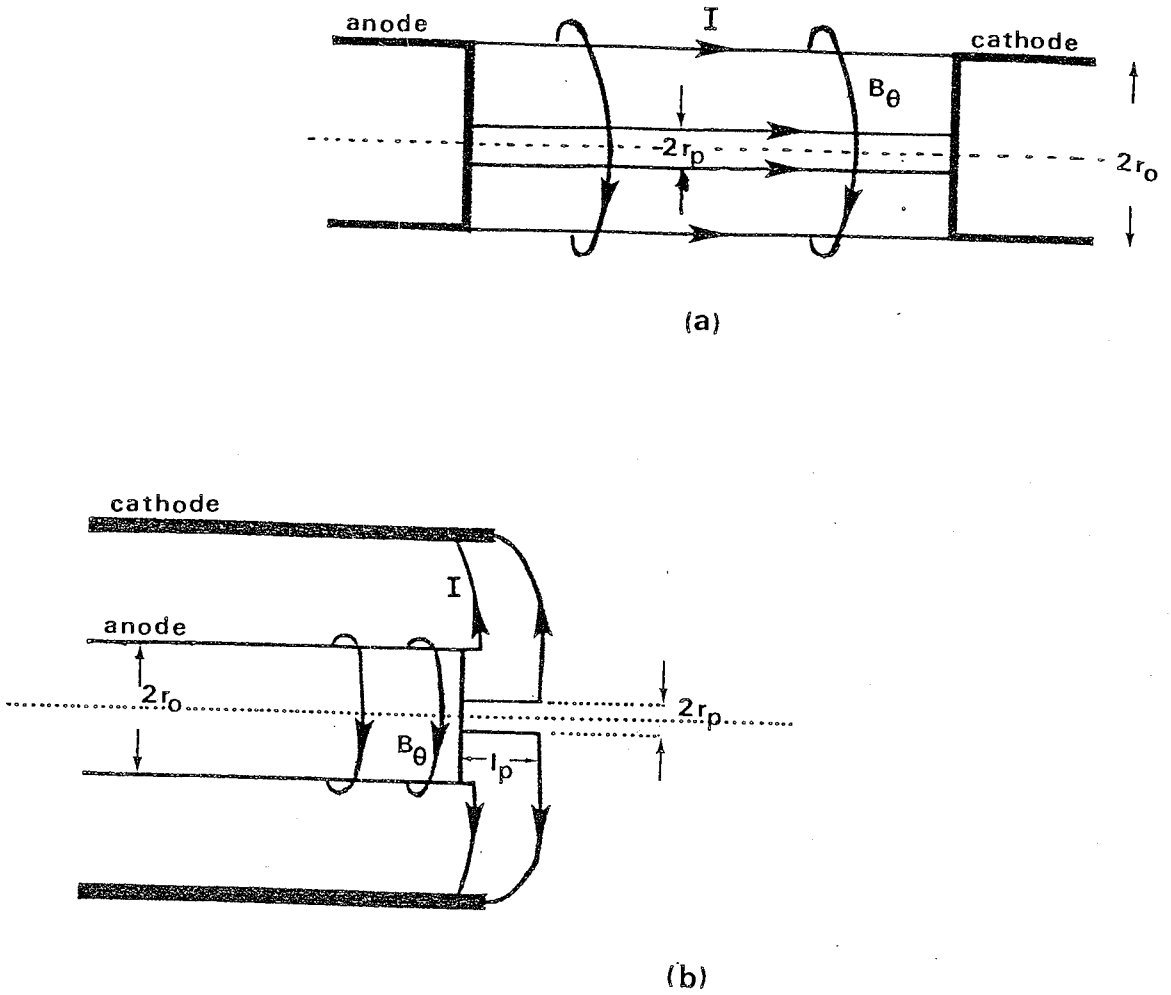

Figure 1: Comparison of linear Z-pinch and plasma focus pinch.
(a) linear Z-pinch
(b) plasma focus pinch

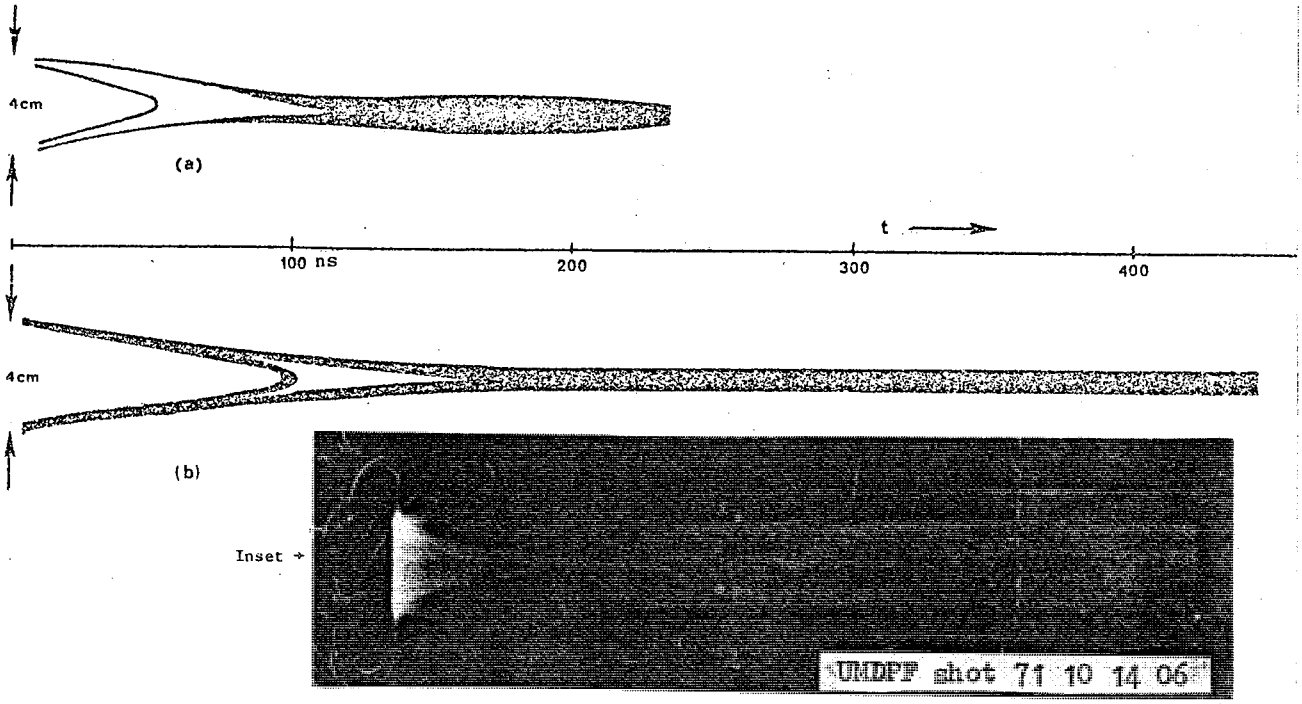

Figure 2: Comparison of Imperial College Mark II Z-pinch and UMDPF pinch-streak pictures

(a) Imperial College Mark II Z-pinch, 0.07 torr H_2, 60 kA constant current.

(b) UMDPF non-focus pinch, reconstructed from Figure 2c. 0.2 torr D_2, approximately constant curent of 80 kA.

Inset: Streak photograph of UMDPF non-focus pinch from which Figure 2b is reconstructed. Streak length 1μs. r_o = 4 cm.

CIRI-CIRI SEBUAH LASER DELIMA DENYUTAN DAN KEGUNAANNYA UNTUK PENYELIDIKAN DALAM BIDANG FIZIK PLASMA

C.S. Wong, MIPM dan S. Lee, FIPM
Makmal Fizik Plasma, Jabatan Fizik, Universiti Malaya
Kuala Lumpur 22-11, Malaysia

Abstract: This paper describes the operational characteristics of the pulsed ruby laser in the Plasma Physics Laboratory, and its usage as a diagonstic tool and for plasma production. The laser is operated in both single and multi-mode and typically has a power of 60 MW with a fwhm time of 50 ns. In chopped mode its pulse width can be reduced to 5 ns making it suitable for 'freezing' high plasma velocities.

Pendahuluan

Laser delima adalah salah satu jenis laser denyutan berkuasa sederhana yang banyak dipakai dalam bidang perindustrian, tentera dan juga penyelidikan saintifik. Jenis laser ini telah menjadi lebih penting semakin hari sebab ianya senang untuk digunakan dan juga dijaga. Harganya juga tidak mahal jika diperbandingkan dengan jenis laser lain yang bertenaga setaraf. Istimewanya dalam bidang Fizik Plasma, laser ini telah digunakan sebagai alat pengukuran dan juga sebagai sejenis sumber tenaga untuk memanaskan plasma.

Di Makmal Fizik Plasma di Jabatan Fizik, Universiti Malaya ini, kedua-dua kegunaan laser delima yang tersebut di atas telah dapat dicubakan[1]; iaitu laser ini telah digunakan sebagi sumber cahaya untuk teknik bayanggrafi[2] dan interferometri holograf[3], dan ia juga ada digunakan sebagai sumber tenaga untuk memanaskan bahan anod bagi memulakan nyahcas spark vakum[4].

Dalam kertas ini, ciri-ciri sistem laser delima yang berada di Makmal kami (JK Laser 2000) akan diperiksa. Kegunaan laser ini untuk penyelidikan dalam projek Fokus Plasma dan Spark Vakum juga dibincangkan dengan ringkasnya.

Sistem laser delima

Satu skim susunan sistem laser delima ada ditunjukkan dalam Raj. 1. Ia mempunyai satu rongga yang terdiri dari sebuah etalon berkepingan tunggal sebagai cermin keluaran (pemancaran separa) dan sebuah cermin cekung sebagai cermin belakang (100% kepantulan). Jejari cermin cekung itu adalah 5 meter dan panjang rongga ialah hampir 1 meter. Komponen terpenting dalam sistem ini adalah pengayun delima (ruby oscillator) yang panjangnya 4 inci dan garispusatnya ialah $\frac{3}{8}$ inci. Batang delima ini dipamkan secara optik dengan menggunakan dua batang lampu-kilat xenon yang diletakkan samada batang delima di dalam sebuah bekas yang disejukkan oleh air-suling.

Ini adalah susunan Q-tetap (fixed-Q) untuk laser tersebut. Dalam keadaan ini, bilangan atom yang ada di tingkat tenaga atas akan bertambah dengan cepatnya sehingga ambang untuk keluaran laser tercapai dan satu denyutan laser pun dikeluarkan. Kejadian ini akan meruntuhkan bilangan atom di tingkat tenaga atas dan keluaran laser terus terhenti. Tetapi, oleh kerana pada masa itu lampu-kilat itu masih berkuasa cukup, keluaran laser itu akan berulang beberapa kali lagi sehingga pendudukan terbalik (population inversion) tidak dapat dicapai lagi. Susunan kejadian ini akan menghasilkan satu rantai denyutan-denyutan laser seperti yang didapati dalam Raj. 2(a). Tempoh kejadian ini adalah lebih kurang 200 μs.

Untuk mendapatkan operasi Q-suis, sebuah pengutub berjenis 'stacked-plate' dan sebuah sel-Pockel berhablur K*DP hendaklah ditambah ke dalam rongga laser. Selepas melalui pengutub, cahaya yang dikeluarkan dari pengayun ruby itu terjadi terkutub linear. Pada mulanya satu voltan-pincang sebanyak 1.6 kV dipasang ke atas sel-Pockel itu supaya sinaran akan dipantul oleh cermin-cekung belakang dan melalui sel-Pockel sekali lagi, menjadikan pengutubannya linear semula tetapi sudut-pengutubannya telah diputar sebanyak 90°. Oleh sebab itu, sinaran yang diasalkan dari pengayun itu tidak dapat melalui pengutub lagi dan akan dihilangkan. Dengan cara ini, kadar kehilangan rongga laser itu telah ditinggikan (ini bermakna nilai Q rendah) dan keluaran sinaran laser menghalang untuk membiarkan bilangan atom di tingkat tenaga atas bertambah sehingga lebih tinggi dari ambang laser itu. Masa tunda di antara permulaan lampu-kilat dan pembukaan

sel-Pockel biasanya ialah lebih kurang 1 ms[5]. Untuk laser kami, masa tunda yang sesuai ialah 1.25 ms. Keluaran laser Q-suis boleh didapati dengan memadamkan voltan-pincang sel-Pockel itu selama ≃ 500 ns pada hujung masa tunda yang perlu. Kejadian ini ada ditunjukkan dalam Raj. 2(b). Dengan operasi Q-suis, keluaran laser terjadi sebagai satu denyutan gergasi (giant pulse) dalam selang masa 30 ns. Kuasa denyutan laser ini adalah 60 MW.

Keluaran laser yang terdapat seperti diterangkan tadi ialah operasi berbilang mod (multimode operation). Dalam kes ini, taburan keamatan laser adalah bukan-gauss dan jarak koherennya ialah lebih kurang 1 cm sahaja. Akan tetapi, kalau laser ini hendak digunakan sebagai sumber sinaran untuk teknik interferometri holograf, bim laser yang bertaburan gauss dengan jarak koheren 1 m akan diperlukan. Ini bermakna bahawa mod pengayun rongga laser mestilah dilaraskan menjadi TEM_{oo} dan sela jarakgelombang pun harus dipendekkan sehingga kurang daripada 0.005 Å. Syarat pertama itu boleh dicapai dengan menggunakan suatu bukaan kecil dengan garispusat 1.8 mm. Untuk syarat kedua, sebuah etalon-dalam-rongga (intracavity etalon) hendaklah ditambah di antara batang delima dan pengutub seperti terdapat dalam Raj. 1. Ini adalah operasi mod-tunggal (single mode operation) laser ini.

Ciri-ciri keluaran laser delima

Denyutan-denyutan keluaran laser delima itu telah diukur dengan menggunakan sebuah diod PIN (masa kenaikan ≃ 2 ns dan masa keruntuhan ≃ 10 ns). Keluaran dari diod ini boleh ditinjau dengan menggunakan sebuah osiloskop TEK 7834.

Satu contoh osilogram denyutan laser yang terdapat ada ditunjukkan dalam Raj. 3(a). Kuasa laser ini boleh dikoncang oleh beberapa faktor seperti suhu batang delima, kelemahan lampu-kilat, kebersihan air penyejuk dan sebagainya. Tetapi dalam tempoh satu jam, koncongan kuasa laser telah dilihat tidak lebih dari 3%. Tempoh-setengah-maksima (fwhm) laser itu pun telah diukur dan didapati bahawa tempoh ini adalah lebih panjang bila voltan nyahcas lampu-kilat itu dikurangkan. Tempoh-tempoh denyutan laser delima ini pada beberapa voltan nyahcas lampu-kilat telah di senaraikan

dalam Jadual 1.

Untuk meninjau taburan keamatan bim laser itu, kertas foto Polaroid 667 telah digunakan. Caranya ialah mengarahkan bim laser itu kemukaan kertas foto. Satu tanda terbakar yang disebabkan oleh bim itu akan terlihat seperti yang ditunjukkan dalam Raj. 4. Bahagian (a) adalah tanda dari operasi Q-suis berbilang mod. Kita boleh dapati bahawa mod melintang (transverse mode) laser itu ialah $TEM_{11,0}$ dalam operasi berbilang mod. Kalau bukaan kecil ditambah, mod melintangnya boleh dikurangkan kepada TEM_{oo} yang bertaburan-gauss seperti dalam Raj. 4(b). Akan tetapi, kuasa laser dalam kes (b) itu adalah banyak kali kurangnya dari kes (a).

Cara memendekkan tempoh denyutan laser

Untuk menggunakan laser delima dalam pengukuran plasma seperti interferometri holograf, denyutan laser dengan tempoh-setengah-maksima yang kurang daripada contoh yang ditunjukkan dalam Raj. 3(a) akan diperlukan. Dalam laser delima kami, tempoh ini boleh dikurangkan ke 5 ns dengan menggunakan sebuah pemotong denyutan (pulse chopper). Susunan komponen-komponennya telah ditunjukkan oleh pekerja-pekerja lain dari makmal ini[2]. Ianya mempunyai 2 buah pengutub Glan, sebuah sel-Pockel K*DP dan sebuah jurang spark (spark gap). Turutan opersainya adalah seperti berikut:

Selepas melalui pengutub pertama, bim laser delima itu akan dijadikan terkutub linear. Oleh kerana pada mulanya voltan-pincang sel-Pockel itu adalah sifar, bim itu dapat melaluinya tanpa perubahan, dan kemudianya dipesong oleh pengutub kedua ke sebuah prisma dan akhirnya dipesong ke jurang spark. Jurang spark ini dipenuhi nitrojen dengan tekanan 45 psi supaya dapat menahan voltan sebanyak 10 kV. Tetapi apabila terkena oleh sinaran laser, peruntuhan jurang spark ini akan terjadi dan voltan 10 kV itu akan dipasangkan kepada sel-Pockel. Selang masa denyutan voltan tinggi itu dikawal oleh kabel pendek yang digunakan sebagai satu 'shorting stub'. Dengan voltan ini, pengutuban sinaran laser itu akan bertukar dan sekarang sinaran laser tidak lagi dipesong ke prisma oleh pengutub kedua tetapi akan melaluinya tidak berubah. Dengan cara ini, satu denyutan laser dengan tempoh yang pendek akan didapati. Satu contoh denyutan laser terpotong

itu adalah ditunjukkan dalam Raj. 3(b).

Kegunaan laser delima dalam Makmal Fizik Plasma

Beberapa teknik pengukuran plasma yang menggunakan laser delima telah dikembang dalam makmal ini. Ini adalah termasuk teknik bayanggrafi[2] dan interferometri holograf[3]. Dalam kertas ini, kami akan membincangkan dengan lebih mendalam lagi tentang kegunaannya sebagai sumber tenaga untuk memanaskan bahan anod bagi memulakan nyahcas di spark vakum[4]. Dalam keadaan ini, irradiance laser yang besar adalah diperlukan dan oleh sebab itu, adalah lebih sesuai sistem laser delima ini dijalankan dalam operasi berbilang mod. Sinaran laser itu dipesong oleh 3 buah cermin dielektrik dan kemudian di fokus oleh sebuah kanta ke atas hujung anod di dalam sistem spark vakum itu (Raj. 5). Bahagian tenaga laser yang hilang selepas melalui cermin-cermin dan kanta adalah tidak melebihi 10%. Dalam operasi biasa tenaga 1.5 J dikeluarkan oleh laser itu dalam selang masa 50 ns. Kuasa yang kami dapat di hujung anod ialah 27 MW. Garispusat bintik laser yang terdapat di atas anod pun telah diukur dan panjangnya adalah lebih-kurang 1.0 mm. Ini bermakna bahawa irradiance laser itu adalah sebanyak 3.4×10^9 W/cm^2. Irradiance laser seperti ini adalah cukup untuk menghasilkan satu plasma dengan ketumpatan elektron yang tinggi ($\simeq 10^{18}$ cm^{-3}) dan suhu setinggi beberapa ev[6]. Apabila nyahcas yang berarus besar berlaku dalam plasma ini, plasma yang amat panas dan rapat dengan $T_e \simeq 4 - 8$ kev[7] dan $N_e \simeq 10^{21}$ cm^{-3} pun akan terhasil. Garispusat plasma ini adalah lebih kurang 50 μm.

Kesimpulan

Ciri-ciri operasi sebuah laser delima denyutan sistem JK2000 telah ditinjau dan diperiksakan dengan rujukan kepada kesesuainnya sebagai alat untuk pengukuran plasma dan sebagai sumber pemanasan plasma.

Pengakuan

Laser delima JK2000 telah dihadiahkan kepada Jabatan Fizik, Universiti Malaya sebagai satu 'Post-Fellowship Award' daripada Yayasan Alexander von Humboldt, Jerman Barat.

Kami ingin mengucapkan terima kasih kepada Cigku Ishak bin Salim dari Pusat Bahasa, Universiti Malaya kerana membaca dan memberi beberapa nasihat yang bernilai untuk membaiki Bahasa Malaysia dalam kertas ini.

Istilah-istilah yang diguna dalam kertas ini adalah mengikuti 'Istilah Fizik' yang dikeluarkan oleh Jawatankuasa Peristilahan Fizik Antara Universiti (JPFAU) pada tahun 1981.

Rujukan

[1]S. Lee, *'Review of Plasma Physics Research in Malaysia'*. Paper presented at the Symposium on Plasma Research, Theory and Experimental, ICTP Trieste (1981 - to be published in the Procs.)

[2]S. Lee and Y.H. Chin, Bul. Fiz. Mal., 2-2, 105 (1981)

[3]K.H. Kwek and Y.H. Chen, Bul. Fiz. Mal., 2-2, 114 (1981)

[4]C.S. Wong and S. Lee, Bul. Fiz. Mal., 2-1, 50 (1981)

[5]W. Koechner, *'Solid State Laser Engineering'*, Chapters 5 & 8, Springer Series in Optical Science, Vol. 1 (1976)

[6]J.F. Ready, *'Effect of High Power Laser Radiation'*, Chapter 5, Academic Press (1971)

[7]C.S. Wong and S. Lee, *'Vaccum Spark as a Fusion Device'*. Paper presented at the Symposium on Plasma Research, Theory and Experimental, ICTP Trieste (1981 - to be published in the Procs.)

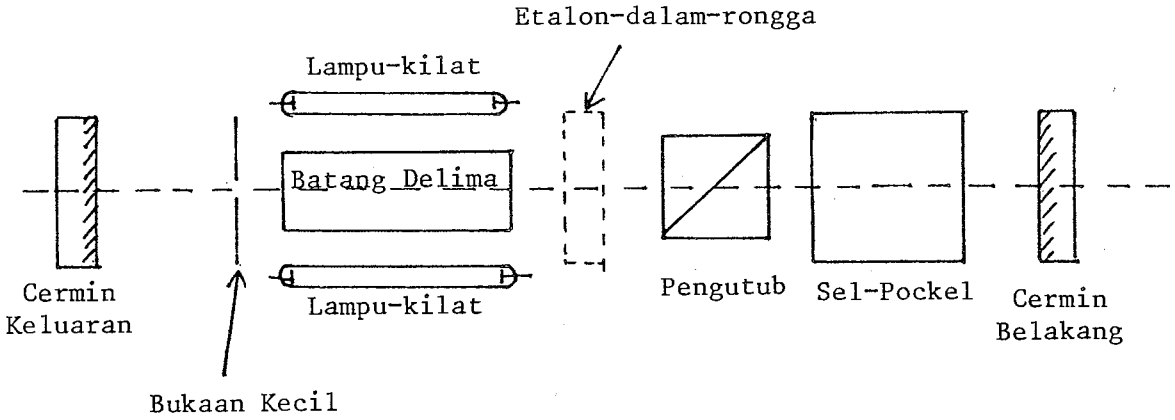

Raj.1: Susunan komponen-komponen di dalam sistem laser delima.

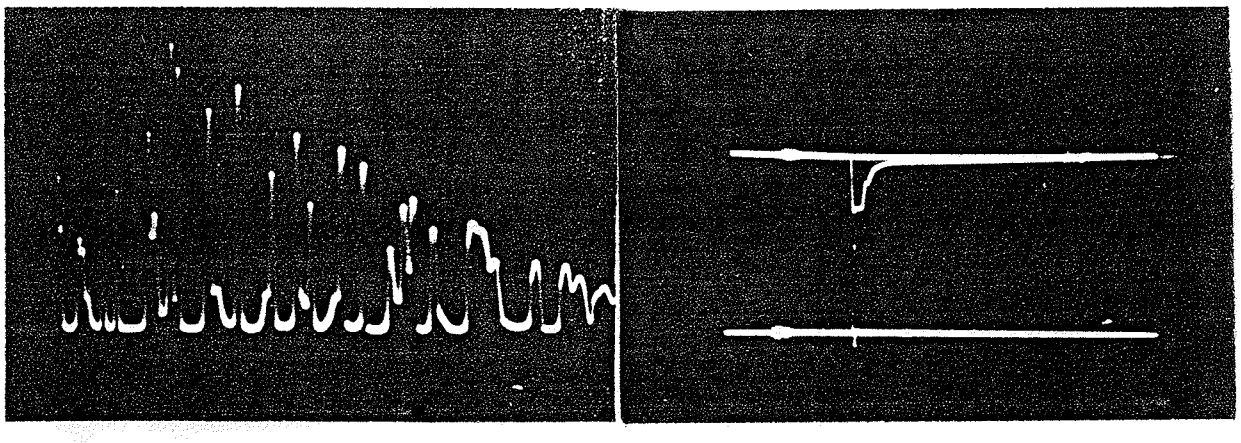

(a)
(20 μs/div.)

(b)
(2.0 μs/div.)

Raj.2: (a)Keluaran laser delima Q-tetap.
(b)Masa pembukaan sel-Pockel(atas) dan denyutan gergasi laser delima(bawah).

Buletin Fizik Vol.2 No.4 1981

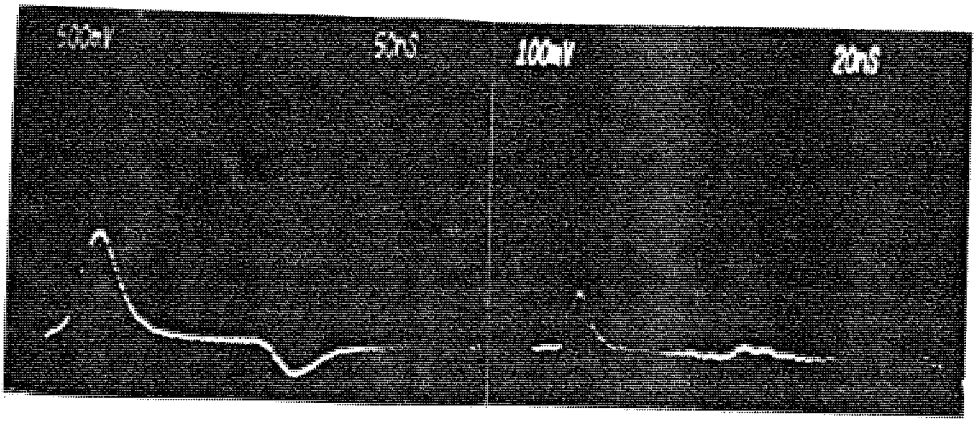

(a) (b)

Raj. 3: (a) Denyutan laser delima secara Q-suis
(b) Denyutan terpotong (chopped pulse)

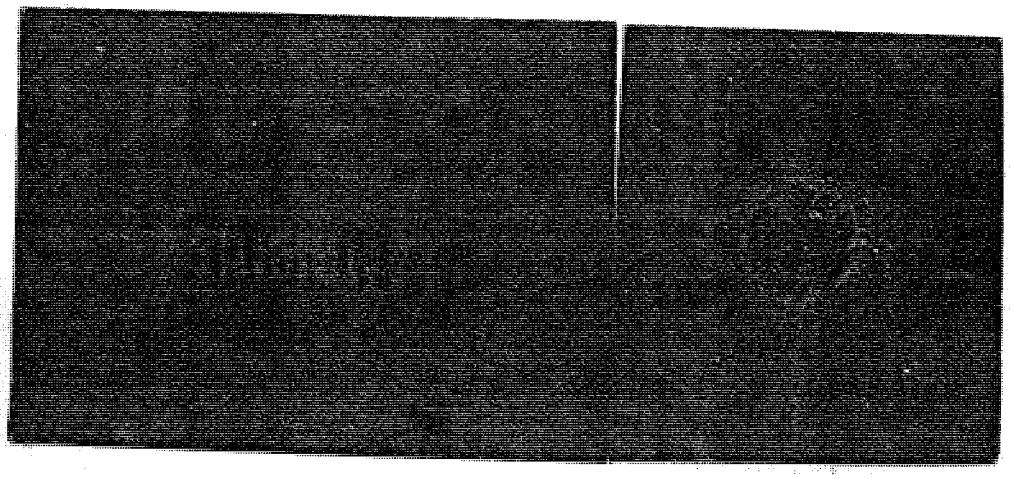

(a) (b)

Raj. 4: (a) Tanda terbakar oleh laser delima di atas kertas foto jenis Polaroid 667 dalam operasi berbilang mod.
(b) Yang sama dengan operasi mod-tunggal.

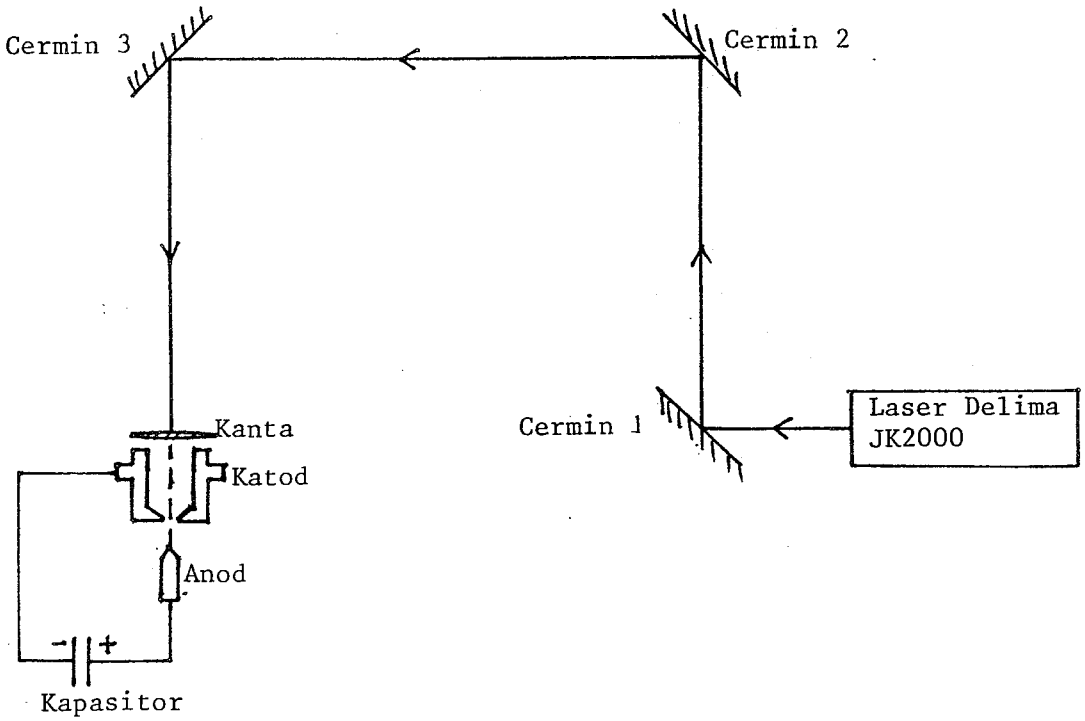

Raj.5: Susunan sistem spark vakum yang menggunakan laser delima untuk memulakan nyahcas.

Voltan (kV)	2.10	2.15	2.20	2.25	2.30
Tempoh (ns)	85	70	60	55	50

Jadual 1: Perubahan tempoh denyutan laser delima dengan voltan nyahcas lampu-kilat.

HIGH DENSITY HIGH TEMPERATURE PLASMA PRODUCTION IN FAST Z-PINCHES

P. F. M. Baldock, A. E. Dangor, M. B. Favre Dominguez, D. Grimsley, J. D. Hares, E. Kahan, S. Lee*

The Blackett Laboratory
Imperial College of Science and Technology
London SW7 2BZ, U.K.

Experiments in two Z-pinch devices are being conducted at Imperial College. The drivers for both pinches are characterised by a very fast current rise time (10 - 30 nsec) obtained by the use of pulse charged and switched water transmission lines.

The smaller device, a laser-initiated gas-embedded pinch, produces a radially stable plasma of radius 100 - 400 μm and density 2×10^{19} to 10^{20} cm^{-3}. The current (50 kA), with the Bennett relation, give a temperature of 600 - 100 eV. Radial equilibrium is obtained during current rise where the increase in plasma pressure due to Joule heating is balanced by an increasing magnetic pressure.

In the high current device ($I \sim 150$ kA) a high density high temperature plasma is produced by the shock compression of a hydrogen or argon gas column. A magnetic piston forms and detaches from the pinch tube (initial radius ~ 1 cm) which drives the plasma to a final radius of $\frac{1}{3}$ - $\frac{1}{6}$ of the initial radius with argon pinching more than hydrogen, as expected.

X-ray and optical measurements indicate a temperature of a few hundred eV and a density of 10^{18} cm^{-3}. No gross instabilities are observed within the duration of the current pulse. This corresponds to several radial Alfvén transit times.

It is envisaged that the equilibrium plasma be driven to higher density by a subsequent adiabatic compression phase.

*Permanent address: Universiti Malaya, Kuala Lumpur.

Bull. Phys. M'sia 3, 197 (1982)

MICROCOMPUTER IMPLEMENTATION OF MAGNETOHYDRODYNAMIC COMPUTATION INCLUDING REAL GAS EFFECTS

S. Lee FIPM
Jabatan Fizik Universiti Malaya, Kuala Lumpur 22-11.

Abstract

Computationsfor the trajectories of electromagnetically compressed gas columns, incorporating real gas effects, are of sufficient complexity to warrant full-scale codes with computer centre facilities. We demonstrate that major parts of such codes may be run,with improvement, on a low-cost microcomputer. A modular approach is proposed to implement the full code. Such an approach has the advantage of greater control over the physics of the problem resulting in a better model for each module and hence also a better over-all code.

Introduction

The role and use of microcomputers (a) in teaching[1,2] and (b) for interfacing to experiments[3,4] has recently been discussed in the Malaysian physics scene. It is proposed to demonstrate here that this role may be widened to include the use of the microcomputer in the implementation of large computer packages, or codes, traditionally the preserve of full-size facilities in computer centres. The microcomputers referred to here are from 16K to 48K in capacity and may cost from below 1000 to 3000 Malaysian Ringgits. It is this very low cost that has made inevitable the introduction of such 'personal' or 'home' machines into many areas of scientific activity including the implementation of large codes, especially in applied physics computations.

We begin by reviewing briefly the computations that we have made earlier using computer centre facilities on radial magnetohydrodynamic flows[5] with the incorporation of real gas effects[6]. The basis of these computations is an equation of motion describing an inward imploding snow-plow type plasma. To avoid the non-physical situation of the plasma piling up on-axis with infinite density a retarding force term due to the kinetic pressure was included. But the method of obtaining structure was not self-consistent, although results could be adjusted to fit experiments or to agree with the final radius as predicted by a self-consistent energy balance model[7]. When argon is used as the test gas all 19 species, from atomic argon to the 18th-ionized argon, have to be considered in the high temperature compression[6]. Such a computation involves storage and generation of energy levels and summation for partition functions and excitation energies and large codes are routinely stored in several computer centres.

We have recently taken a renewed interest in these computations and found that improved control over the physics in our own code is vital in order to make our computations realistic as well as self-consistent. To this end we have used a microcomputer for the implementation of the improved code. Because of the ready access to the microcomputer, numerical experiments could be performed at any time resulting in good continuity in the development of the flow model. The result is an elegant self-consistent model covering both the axial and radial phase of a plasma focus. This will form module I of the code. Further modules will be required for the inclusion of the real gas effects for argon flow.

Module I The flow model for an ideal gas

The following model is developed for a coaxial system with a plasma-focus geometry. In this model the plasma heating is achieved in two phases as depicted in Fig. 1a and Fig. 1b. In the first axial phase an axisymmetric current sheet is propelled from $z = 0$ (Fig. 1a) to $z = z_0$ by the $J \times B$ force (J = radial current density in the current sheet and B = azimuthal magnetic field due to J). This current is discharged from a capacitor C_0 charged to voltage V_0. The circuit inductance is depicted as L_0. When the current sheet reaches z_0, a radial compression starts. This radial compression has an initial length $z_f = 0$ and initial radius $r = a$. In each phase the dynamics is described by appropriate equations of motion and the current is computed from a circuit equation. The equations of motion contain the current I through the magnetic pressure term whilst the circuit equation contains the variable z, for the axial phase, and the variables r and z_f, for the radial phase, through the plasma inductance. In this way the plasma dynamics and the electric current are coupled.

Axial phase

In the axial phase, an infinitesimally thin snowplough model is used. The equation of motion is:

$$\frac{d}{dt}\left[\pi \rho_0 (b^2 - a^2) z \frac{dz}{dt}\right] = \frac{\mu I^2}{4\pi}\left(\ell n \frac{b}{a}\right) \tag{1}$$

The circuit equation is:

$$\left[L_0 + \frac{\mu}{2\pi}\left(\ell n \frac{b}{a}\right) z\right] \frac{dI}{dt} + \frac{\mu}{2\pi}\left(\ell n \frac{b}{a}\right) I \frac{dz}{dt} = V_0 - \frac{1}{C_0}\int I\, dt \tag{2}$$

where ρ_0 = ambient gas density and the inductance of the coaxial tube is taken as $\frac{\mu}{2\pi}\left(\ell n \frac{b}{a}\right) z$.

The following normalization procedure is adopted:

$$\zeta = z/z_0, \qquad \tau = t/t_c \qquad i = I/I_0$$

where $t_c = (L_0 C_0)^{\frac{1}{2}}$ and $I_0 = V_0/(L_0/C_0)^{\frac{1}{2}}$,

The normalized equations are

Motion: $$\frac{d^2\zeta}{d\tau^2} = \left[\alpha^2 i^2 - \left(\frac{d\zeta}{d\tau}\right)^2\right] / \zeta \tag{3}$$

Circuit : $$\frac{di}{d\tau} = \left[1 - \int i\, d\tau - \beta i \frac{d\zeta}{d\tau}\right] / (1 + \beta\zeta) \tag{4}$$

with $\alpha = t_c/t_a$ and t_a is the characteristic axial run-down time

$$t_a = \left[\frac{4\pi^2 (b^2 - a^2)\rho_0 z_0^2}{\mu(\ell_n/b/a) I_0^2}\right]^{\frac{1}{2}}.$$

The parameter α is then an essential scaling factor. The parameter $\beta = [\frac{\mu}{2\pi}(\ell n\frac{b}{a})z_0]/L_0$ is a second essential scaling factor. The starting conditions are:

$$\tau = 0, \quad \zeta = 0, \quad \frac{d\zeta}{d\tau} = 0, \qquad \frac{d^2\zeta}{d\tau^2} = \text{indefinite},$$

$$i = 0, \quad \frac{di}{d\tau} = 1.$$

Radial Compression phase

In the radial compression, a finite-thickness slug model is used. The position of the front of the slug which is a shock front is designated as r_s and the position of the rear of the slug which is the magnetic piston is designated r_p. The position r_s is obtained through shock-jump equations and by linking the shock pressure to the magnetic pressure. This gives:

$$\frac{dr_s}{dt} = -\left[\frac{\mu_0}{\rho_0}(\gamma + 1)\right]^{\frac{1}{2}} \frac{I}{4\pi r_p} \tag{5}$$

where γ is the specific heat ratio. The piston position is then allowed to separate from the shock position by an adiabatic rule[8], resulting in:

$$\frac{dr_p}{dt} = \frac{\frac{2}{\gamma+1}\frac{r_s}{r_p}\frac{dr_s}{dt} \quad \frac{r_p}{\gamma I}\left(1 - \frac{r_s^2}{r_p^2}\right)\frac{dI}{dt} - \frac{1}{\gamma+1}\left(1 - \frac{r_s^2}{r_p^2}\right)\frac{dz_f}{dt}}{(\gamma-1)/\gamma + (1/\gamma)(r_s/r_p)^2} \tag{6}$$

It is noted here that the length of the imploding column, z_f, is allowed to increase in a self-consistent manner by coupling the axial shock front of the imploding column to the plasma pressure. Thus: $\frac{dz_f}{dt} = \frac{dr_s}{dt}$. The circuit equation may then be written as:

$$\left[L_0 + \frac{\mu}{2\pi}(\ell n \frac{b}{a}) z_0 + \frac{\mu}{2\pi}(\ell n \frac{b}{r_p}) z_f\right]\frac{dI}{dt} + I\frac{\mu}{2\pi}(\ell n \frac{b}{r_p})\frac{dz_f}{dt}$$

$$- I\frac{\mu}{2\pi}\frac{z_f}{r_p}\frac{dr_p}{dt} = V_0 - \frac{\int I\,dt}{C} \tag{7}$$

The following normalization procedure is adopted.

$\kappa_s = r_s/a, \qquad \kappa_p = r_p/a, \qquad \zeta_f = z_f/a, \qquad i = I/I_0, \qquad \tau = t/t_c,$

The normalized equations are then:

shock motion: $$\frac{d\kappa_s}{d\tau} = \alpha\alpha_1 i/\kappa_p \tag{8}$$

piston motion: $$\frac{d\kappa_p}{d\tau} = \tag{9}$$

$$\frac{(\frac{2}{\gamma+1})\frac{\kappa_s}{K_p}\frac{d\kappa_s}{d\tau} - \frac{1}{\gamma}\frac{\kappa_p}{i}(1-\frac{\kappa_s^2}{\kappa_p^2})\frac{di}{d\tau} - (\frac{1}{\gamma+1})\frac{\kappa_p}{\zeta_f}(1-\frac{\kappa_s^2}{\kappa_p^2})\frac{d\zeta_f}{d\tau}}{(\gamma-1)/\gamma + (1/\gamma)(\kappa_s/\kappa_p)^2}$$

circuit:

$$[1+\beta-\frac{\beta_1}{F}(\ell_n\frac{\kappa_p}{c})\zeta_f]\frac{di}{d\tau} - \frac{\beta_1}{F}(\ell_n\frac{k_p}{c})i\frac{d\zeta_f}{d\tau} - \frac{\beta_1}{F}\frac{i\zeta_f}{k_p}\frac{dk_p}{d\tau} = 1 - \int i d\tau \tag{10}$$

axial shock: $$\frac{d\zeta_f}{d\tau} = \frac{d\kappa_s}{d\tau} \tag{11}$$

where $c = b/a$.

The additional parameters are:

$$\alpha_1 = [(\gamma+1)(c^2-1)]^{\frac{1}{2}} F/2\ell nc$$

$$\beta_1 = \beta/\ell n\, c, \qquad \text{and } F = z_0/a$$

The radial compression phase starts when the axial phase reaches $\zeta = 1$; at which time,

$$\tau = \tau_0, \quad \kappa_s = 1, \quad \kappa_p = 1 \qquad \zeta_f = 0.$$

The compression ends when $\kappa_s = 0$.

Integration

To start the numerical integration from $\tau = 0$ for the axial phase, an estimated value for $\frac{d^2\zeta}{d\tau^2}$ at $\tau = 0$ has to be made. This was done by a trial-and-error method checking for maximum numerical stability and rapid convergence of solution. A value of -0.02, typically, was found to be suitable. The transition from the axial to radial phase was problem-free. The actual integration for $\zeta, i, \kappa_s, \kappa_p, \zeta_f$ was done by a linear approximation method; though of course a Runge-Kutta method would be an easy improvement.

This procedure for the complete module I was implemented on a Sinclair Spectrum 48K microcomputer in the BASIC language. The program also runs well on other microcomputers such as the Apple. Some results for an ideal gas with a fixed γ of 5/3 are shown in Figs. 2 and 3. The final radius ratio of 0.16 compares with a value of 0.14 based on an independent energy balance model[7]. Computation with a variable γ to take into account real gas compressibility is in progress. This will take the form of three separate modules.

Modules for inclusion of real gas effects

The three modules to be developed will compute the partition functions and excitation energies with the input being atomic energy levels from standard tables supplemented by iso-electronic estimates and the outputs in the form of polynomials or in a form suitable for interpolation.

Thus the partition functions may be conveniently stored as a set of coefficients. The same procedure would be adopted to store the excitation energies.

For the next module, the partition functions are used to compute the ionization fractions from the Saha equations, again these being output in polynomial form.

The next module will use the ionization fractions and the excitation energies to compute values of γ, resulting finally in a polynomial or several polynomials describing γ as a function of temperature. These polynomial may then be used in module I to provide a suitable value of γ at each step of the trajectory integration; the temperature at each point of the trajectory being known from the shock speed.

Conclusion

Computations for the trajectories of compressed gas columns, with real gas effects, are of sufficient complexity to warrant full-scale codes in various computer centres. We have demonstrated that major parts of such codes may also be adequately run using a low-cost microcomputer. Indeed, because of the full access and control that an operator has over a microcomputer it was found that a continuous approach could be adopted with immediate and unlimited turn-round. This has resulted in a greatly improved model from the physics point of view. Using a modular computation approach the control over the physics of the problem is greatly enhanced and we expect to be able to implement a major code completely, and with advantage, on a microcomputer.

REFERENCES

1. K.H. Ng and K.Y. Chua, International Conference on Teaching Aids in Physics Education, Bangi 1982.
2. Zainul Abidin Md. Shariff, International Conference on Teaching Aids in Physics Education, Bangi 1982.
3. C.C' Foong, G. Singh and C.M. Tang, Bull. Phys. M'sia 3, 144 (1982).
4. C.M. Tang, K.S. Lee and H.S. Ng. Bull. Phys. M'sia 3, 149 (1982).
5. S. Lee and Y.H. Chen, Proc. Twelfth Int. Conf. on Phenomenon in IOnized Gases, Eindhoven, Paper 353 (1975).
6. Y.C. Yong and S. Lee, Proc. of Symposium on Physics, Kuala Lumpur, 149 (1977).
7. S. Lee, Bul. Fizik Malaysia 2, 240 (1981) also "Energy balance and the radius of electromagnetically pinched plasma columns" accepted by Plasma Physics.
8. D.E. Potter, Nucl. Fusion 18, 813 (1978).

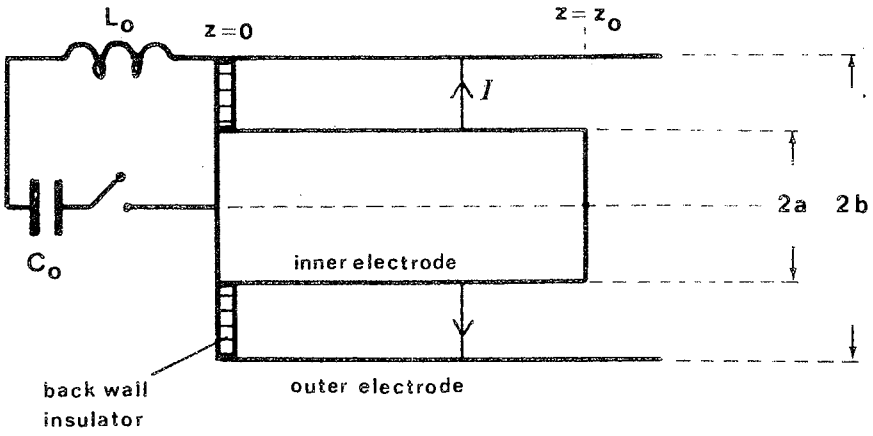

Fig. 1a Phase1: axial acceleration phase

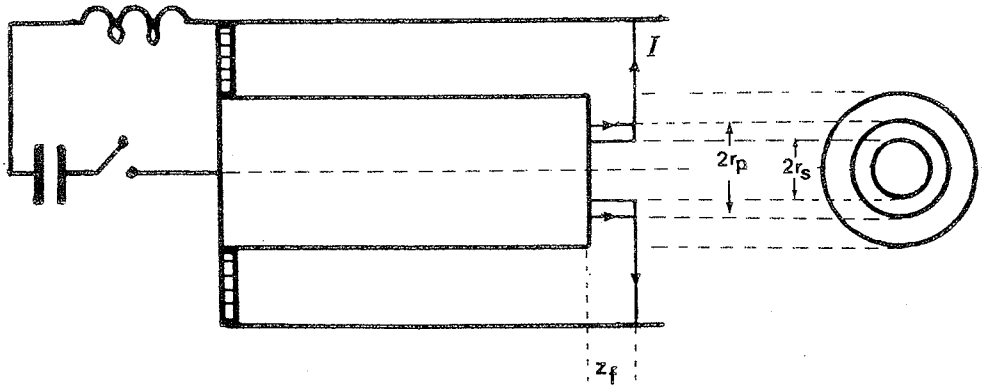

Fig. 1b Phase 2: radial compression phase

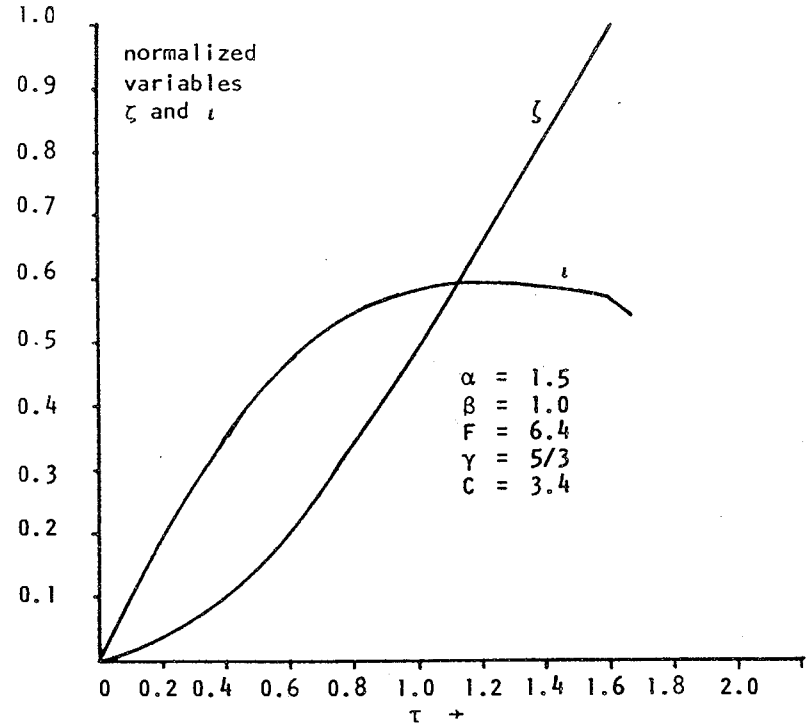

Fig. 2. Solutions of ζ and ι as functions of τ-axial phase

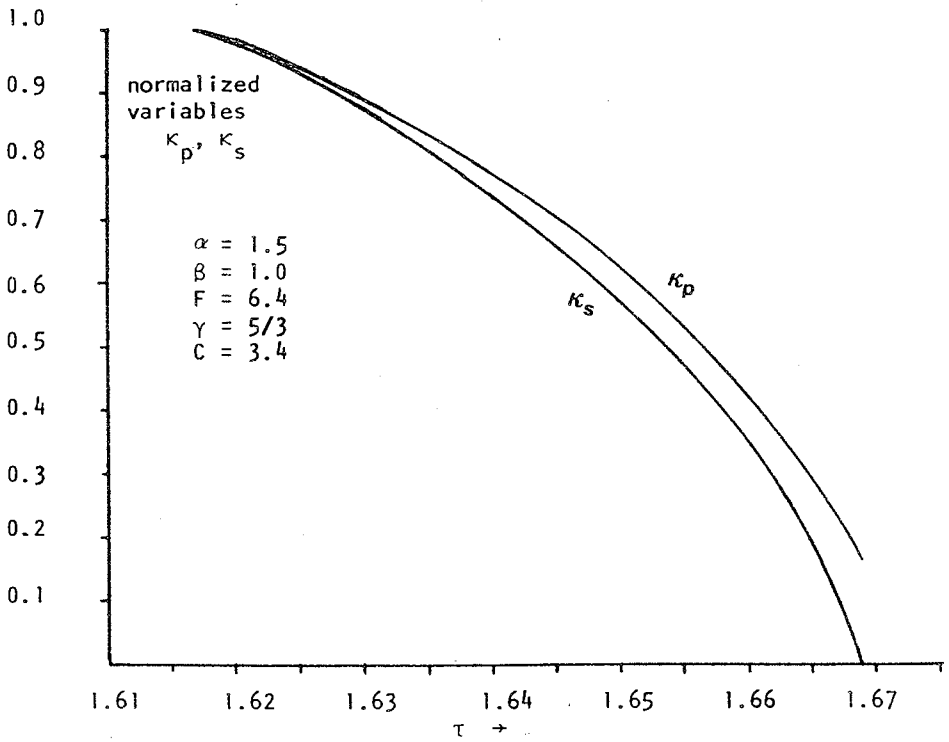

Fig. 3. Solutions of κ_p and κ_s as functions of τ - radial phase

Plasma Physics, Vol. 25, No. 5, pp. 571 to 576, 1983
Printed in Great Britain.

0032-1028/83$03.00 + .00

Energy Balance and the Radius of Electromagnetically Pinched Plasma Columns*

(*Received* 30 *July* 1982; *and in revised form* 15 *October* 1982)

Abstract—A general model is adopted with the magnetic piston perfectly coupled to the imploding plasma. The work done by the piston in moving from initial radius r_0 to equilibrium radius r_p is equated to the enthalpy of the plasma column at r_p. This, together with pressure balance, suffices to produce an expression for the pinch ratio dependent only on γ, the specific heat ratio of the pinched plasma. For a constant current, constant length pinch with $\gamma = 5/3$ a pinch ratio of 0.29 is predicted. For the pinch phase of a $\gamma = 5/3$ plasma focus treated as a constant current pinch having a length which increases with decreasing radius, a pinch ratio of 0.14 is predicted. These compare well with experimentally observed values.

1. INTRODUCTION

ELECTROMAGNETICALLY pinched columns of plasma find numerous applications, for example, as spectroscopic, X-ray and neutron sources, and for fusion studies. In the design of devices for these applications the radius of the plasma column is often an important parameter. For a dynamically compressed pinch it is convenient to separate the discussion of the dynamic compression phase with its predominant electromagnetic mechanism from the subsequent quasi-static phase when the pinch column is governed by Joule heating competing with energy losses through radiation and end-electrode effects (HAINES, 1981).

The classical treatment for the dynamic phase is a snow-plough model which leads to a zero radius column. A modified snow-plough model incorporating a retarding kinetic pressure term has been used to derive a finite radius for the plasma focus pinch column (LEE and CHEN, 1975). POTTER (1978) has used a slug model with a slug of plasma imploding inwards between a shock front and a driving magnetic piston. The plasma pressure, assumed uniform, is governed by the shock speed and matched to the magnetic piston pressure. The adiabatic law is used to relate the shock and piston positions. The piston comes to rest as the shock front implodes on axis. With a constant driving current the pinch ratio of the equilibrium column is derived to be:

$$\frac{r_p}{r_0} = \left(\frac{\gamma}{\gamma+1}\right)^{\left(\frac{\gamma}{\gamma-1}\right)}$$

where r_0 is the wall radius and γ the specific heat ratio.

These and other models proposed in the literature all employ specific assumptions to obtain the radius and it has not been realised that the radius of the electromagnetically compressed pinch is in fact determined once energy and pressure balance are applied. Such an energy method is simple and general and may be used, with little modification, for all electromagnetic pinch devices including the classical linear pinch, the hollow pinch and the plasma focus.

2. THEORY

The following general model is used. To form an axisymmetrically pinched cylindrical plasma column it is necessary that the current, I, starts flowing axisymmetrically at a position defined by r_0 (see Fig. 1a). The current must be suitably large so that interacting with its azimuthal self magnetic field, B, it implodes inwards, sweeping up ahead of it all the mass it encounters. No specific distribution of the mass need be assumed although for the sweeping-up action to be complete the plasma must have a sufficiently high electrical conductivity. In practice this requirement is generally met since implosion Mach numbers typically exceed 100 in these devices creating a plasma with high temperature and high electrical conductivity. In such an implosion a compressed column of plasma bounded by the current sheath must eventually be formed. As the compression proceeds further the energy per unit volume must eventually become sufficiently high to slow down the magnetic piston enabling the temperature and density to move towards uniform values as the piston comes to stop at position r_p, with the plasma also stationary.

* This work was partly done whilst the author was on sabbatical leave at the Blackett Laboratory, Imperial College of Science and Technology, London SW7 2BZ, U.K.

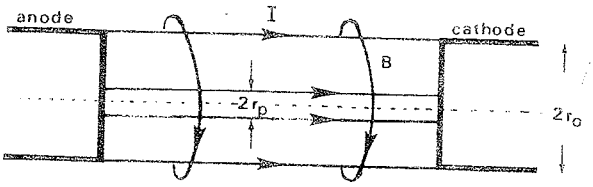

(a)

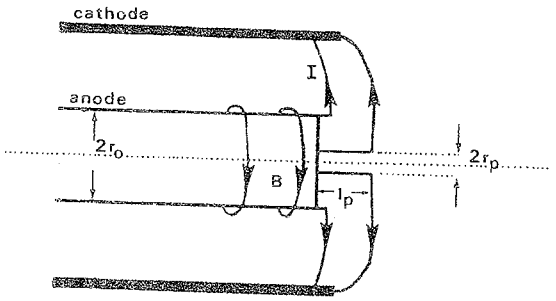

(b)

FIG. 1.—Comparison of linear Z-pinch and plasma focus pinch. (a) Linear Z-pinch; (b) Plasma focus pinch.

We consider the energy balance between the initial state and the final state with the piston at r_0 and r_p respectively. Such a consideration is applicable whether the compression is wholly adiabatic or partly influenced by shock waves and reflected shock waves. It is applicable even if the current sheath rebounds and oscillates. Experimentally it has been observed that under some conditions the plasma column undergoes oscillations in radius before settling down to a quasi-static column. In such a case it would be reasonable to assign the position r_p to the radius of the quasi-static column.

The magnetic piston, or current sheath, exerts a magnetic pressure $P_m = B^2/2\mu$, where the azimuthal induction $B = \mu I/2\pi r$. I is the current flowing through the plasma-magnetic field boundary at instantaneous radius r.

3. CONSTANT CURRENT, CONSTANT LENGTH PINCH

For this case the work done by the magnetic piston in driving from r_0 to r_p is:

$$\int_{r_p}^{r_0} P_m 2\pi r l \mathrm{d}r = \int_{r_p}^{r_0} \frac{\mu l I^2}{4\pi r} \mathrm{d}r \tag{1}$$

where l is the constant length of the pinch column.

Expressing this as W, the work done per unit mass of the plasma column in the final state at r_p gives:

$$W = \frac{\mu I^2}{4\pi^2 \rho r_p^2} \ln\left(\frac{r_0}{r_p}\right) \tag{2}$$

where ρ is the pinch density in the final state at r_p.

The equation of state is $P = \rho(R_0/M)T_z$ so that the plasma enthalpy per unit mass $h = (P/\rho)[\gamma/(\gamma - 1)]$ in the final state may be written as:

$$h = \frac{R_0}{M} T_z \left(\frac{\gamma}{\gamma - 1}\right) \tag{3}$$

studies (LEE, 1981) an empirical relationship between instantaneous length l and radius r may be written as:

$$l = \left(\frac{l_p}{r_0 - r_p}\right)(r_0 - r) \tag{9}$$

where r_0, the radius of the inner electrode may also be considered to be the initial radius of the focus pinch.

The work done by the whole current sheath in moving from r_0 to r_p is as given in equation (1) but for this case l is a function of r as given in equation (9).

The work done per unit mass of the pinched plasma is:

$$W = \frac{\mu I^2}{4\pi^2 \rho r_p^2}\left(\frac{r_0}{r_0 - r_p}\right)\left[\ln\frac{r_0}{r_p} - \left(1 - \frac{r_p}{r_0}\right)\right]. \tag{10}$$

Equating W with h given in (3) gives the pinch temperature as:

$$T = \frac{\mu I^2}{4\pi^2 \rho r_p^2}\left(\frac{r_0}{r_0 - r_p}\right)\left[\ln\frac{r_0}{r_p} - \left(1 - \frac{r_p}{r_0}\right)\right]\frac{M}{R_0 z}\left(\frac{\gamma - 1}{\gamma}\right). \tag{11}$$

Combining (11) with (7) gives:

$$\ln\left(\frac{r_0}{r_p}\right) = \left(1 - \frac{r_p}{r_0}\right)\left[1 + \frac{\gamma}{2(\gamma - 1)}\right]. \tag{12}$$

For the case $\gamma = 5/3$:

$$\ln\left(\frac{r_0}{r_p}\right) = 2.25\left(1 - \frac{r_p}{r_0}\right). \tag{13}$$

this gives a focus pinch ratio of 0.14.

6. EXPERIMENTAL OBSERVATIONS

For the constant current pinch the pinch ratio predicted by the above theory has already been discussed in Section 3 with published results of the Imperial College Mark II Z-pinch.

For the typical plasma focus it is often difficult to identify a stable pinch phase when the plasma column is sufficiently uniform in radius and the structure is sufficiently steady to be considered as being in quasi-static equilibrium.

The steady pinch phase usually constitutes only a very transient phase leading to a violent pinch disassembly phase during which most of the fusion neutrons are produced. However, shadowgrams taken of the Frascati 1MJ Plasma Focus (BILBAO *et al.*, 1980) operated at 25 kV 4 torr deuterium have shown a uniform column stable for 50 ns before the violent pinch break-up. Their results indicate a pinch ratio of 0.1.

With the Universiti Malaya Dense Plasma Focus, UMDPF, facility (CHOW *et al.*, 1972) experiments have been performed with a pinch current sufficiently low to avoid the violent pinch disassembly phase (LEE and TAN, 1975). The device was operated at 0.2 torr deuterium and at the peak of a sinusoidal current which was effectively constant over the time-scale of the pinch. Streak photographs were taken with a slit positioned 3 mm off the end of the anode in a direction perpendicular to the axis of the anode. These show a stable and uniform pinch column lasting for up to 500 ns. A typical streak photograph is shown in Fig. 2 with $r_0 = 2$ cm and pinch current I constant at 80 kA. The pinch ratio is measured as 0.13 which compares with a value of 0.14 from equation (13).

It may be further remarked that the long lifetime of the stable column seems to indicate a stability enhancement factor (CHOI *et al.*, 1978) in excess of 10. this could indicate finite Larmor radius (fLr) stabilization (HAINES, 1981), as with a line density of 10^{19} m^{-1} the UMDPF pinch had a Larmor radius to pinch radius ratio of 0.26.

Finally, experiments with argon have been performed at Imperial College (BALDOCK *et al.*, 1982) and in the UMDPF pinch. In these experiments the argon pinch ratios were observed to be considerably smaller than the corresponding pinch ratios in hydrogen or deuterium. This is in qualitative agreement with equations (8) and (12) since for freely ionizing argon γ is less than 5/3, resulting in smaller pinch ratios when compared with a $\gamma = 5/3$ gas.

where T, z and γ are respectively the temperature, the departure coefficient and the effective specific heat ratio of the plasma in the final state and R_0 and M are respectively the universal gas constant and the molecular weight of the ambient gas.

For energy balance we now assume that W is converted into h without loss. Thus:

$$\frac{R_0}{M} Tz\left(\frac{\gamma}{\gamma - 1}\right) = \frac{\mu I^2}{4\pi^2 \rho r_p^2} \ln\left(\frac{r_0}{r_p}\right). \tag{4}$$

This gives a pinch temperature of

$$T = \frac{\mu I^2}{4\pi^2 \rho r_p^2} \ln\left(\frac{r_0}{r_p}\right) \frac{M}{R_0 z}\left(\frac{\gamma - 1}{\gamma}\right). \tag{5}$$

We may also obtain independently another equation for the pinch temperature by equating the magnetic pressure P_m at r_p to the plasma pressure exerted by the plasma column in the final state. Thus:

$$\frac{\mu^2 I^2}{4\pi^2 r_p^2 (2\mu)} = \rho \frac{R_0}{M} Tz \tag{6}$$

and

$$T = \frac{\mu I^2}{8\pi^2 \rho r_p^2} \frac{M}{R_0 z}. \tag{7}$$

From equations (5) and (7) we obtain the pinch ratio as:

$$\frac{r_p}{r_0} = \exp\left[\frac{-\gamma}{2(\gamma - 1)}\right]. \tag{8}$$

From this equation in the limit $\gamma = 1$, corresponding to an infinite number of degrees of freedom for the pinched gas, the pinch ratio is zero as expected. For $\gamma = 5/3$ corresponding to an ideal gas, or, in practice, a fully ionized gas with 3 degrees of freedom, the pinch ratio according to (8) is 0.29, compared to a value of 0.31 from Potter's slug model. Experimentally a pinch ratio of about 1/3 has been observed in the Imperial College Mark II Z-pinch operated essentially as a constant current, constant length $\gamma = 5/3$ pinch (HAINES, 1981; CHOI *et al.*, 1978).

The difference in the pinch ratio computed here and Potter's pinch ratio is due to the non-uniform temperature vs radius profile implicit in his slug model. The enthalpy equation (3) applied to Potter's column would contain an integral of the temperature across the column. Such an integral could be considered, where necessary, to result in a correction factor to the enthalpy equation, but would not be discussed further here.

Since the above derivation depends only on energy and pressure balance it is readily adaptable to the discussion of pinches such as the classical pinch with sinusoidal current and the pinch phase of the plasma focus, which may be regarded as a pinch of non-constant length.

4. PINCH DRIVEN BY SINUSOIDAL CURRENT

For this case the pinch current may rise from a few kA at r_0 to tens of kA or greater at r_p. In this case in equation (1) the constant current I has to be replaced by $I \sin \omega t$, where the time t and the radius r need to be related by an equation so that (1) may be integrated. The integration results in the same expression for W as in (2) except that I has to be replaced by a factor fI, where f is a factor less than unity. The resultant pinch ratio is considerably reduced. This agrees with experimental observations in classical pinches where $\gamma = 5/3$ pinch ratios are observed to be considerably less than 0.3.

5. PINCH PHASE OF THE PLASMA FOCUS

In a plasma focus (see Fig. 1b) as the current sheath sweeps around the anode into the start of the radial pinch phase its length may be considered as zero. As the pinching progresses the length of the column increases with decreasing radius until a maximum value of l_p is attained at radius r_p. From shadowgraphic

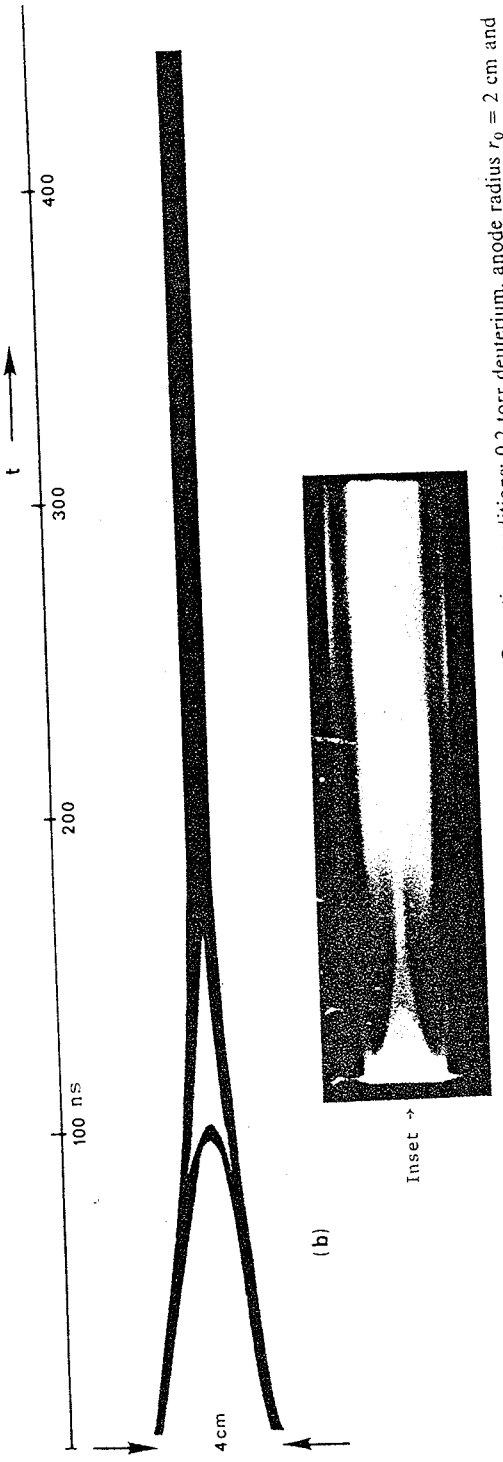

FIG. 2.—UMDPF operated in a "No-focus" mode to show a stable pinch phase. Operating conditions: 0.2 torr deuterium, anode radius $r_0 = 2$ cm and constant pinch current $I = 80$ kA. Total length of the streak in the inset photograph is 1 μs. The line drawing is a reconstruction from the inset to show the shock wave preceding the magnetic piston.

7. CONCLUSION

It is shown that by equating the plasma enthalpy in the stationary pinch column to the work done by the magnetic piston an expression for the pinch ratio of a constant current, constant length pinch is obtained, dependent only on the specific heat ratio, γ, of the pinched plasma. For $\gamma = 5/3$ the theory predicts a pinch ratio of 0.29. This compares with published experimental results of the Imperial College Mark II Z-pinch with a hydrogen pinch ratio of about 1/3.

The theory is applied to the pinch phase of the plasma focus, treated as a constant current pinch but with a column length which increases with decreasing radius. A pinch ratio of 0.14 is obtained for a $\gamma = 5/3$ gas. The UMDPF facility has been operated with a low constant pinch current to produce a stable pinch in a plasma focus configuration without the characteristic violent pinch disassembly phase. A stable deuterium column has been observed on streak photographs. The pinch ratio was measured to be 0.13.

Thus it appears that the radius of an electromagnetically pinched column may be adequately estimated simply from energy and pressure balance. Such a simple procedure should be particularly useful for designers of devices utilizing electromagnetically pinched plasma columns.

Acknowledgement— The author is grateful to Professor M. G. HAINES for valuable discussions in connection with this paper.

S. LEE

Plasma Physics Laboratory, Physics Department, University of Malaya, Kuala Lumpur 22–11, Malaysia

REFERENCES

BALDOCK P. F. M., DANGOR A. E., FAVRE DOMINGUEZ M. B., GRIMSLEY D., HARES J. D., KAHAN E. and LEE S. (1982) High Density High Temperature Plasma Production in Fast Z-pinches, Ninth Ann. Conf. in Plasma Physics, Oxford.

BILBAO L., BRUZZONE H., NIKULIN V. Y. and RAGER J. P. (1980) Plasma Dynamics During Neutron Production in the Frascati 1 MJ Plasma Focus Device, CNEN Report 80.11.

CHOI P., DANGOR A. E., FOLKIERSKI A., KAHAN E., POTTER D. E., SLADE P. D. and WEBB S. J. (1978) *Plasma Physics and Nuclear Fusion Research*, Vol. II. 69, IAEA Vienna.

CHOW S. P., LEE, S. and TAN, B. C. (1972) *J. Plasma Phys.* **8**, 21.

HAINES M. G. (1981) *Phil. Trans. R. Soc. Lond.* **A300**, 649.

LEE S. and CHEN Y. H. (1975) *Proc. 12th Int. Conf. on Phenomena in Ionized Gases*, Eindhoven, Vol. I, Paper 353.

LEE S. (1981) *Bull. Inst. Phys. Malaysia* **2**, 240.

LEE S. and TAN T. H. (1975) *Proc. 7th Europ. Conf. on Cont. Fusion and Plasma Phys.*, Lausanne, Vol. I, Paper 65.

POTTER D. E. (1978) *Nucl. Fusion* **18**, 813.

Observation of radial equilibrium and transition to a helix of a gas-embedded Z pinch

A. E. Dangor, M. B. Favre Dominguez, S. Lee,* and E. Kahan
The Blackett Laboratory, Imperial College of Science and Technology, London SW7 2BZ, United Kingdom
(Received 4 October 1982)

A laser-initiated, gas-embedded Z pinch is operated with a preheat current which adjusts the plasma parameters by Joule heating and expansion so that when the main current is injected, the plasma core is heated under conditions of pressure balance. This results in a pinch which has a constant radius during the time of current rise. The pinch is stable during this time and thereafter undergoes a rapid transformation into a radially expanding helical structure. The growth time and wavelength of the instability is in good agreement with the theoretical predictions of the $m = 1$ magnetohydrodynamic instability.

It is well known[1–3] that in a Joule-heated pinch it is necessary to have a particular rate of current rise $\dot{I}$ to maintain the pinch in radial equilibrium. In the laser-initiated, gas-embedded Z-pinch experiment reported by Jones *et al.*[4] the pinch, powered by a source with an $\dot{I}$ of 10^{12} A s^{-1}, was found to expand radially over the whole duration of the current. Using a source with an $\dot{I}$ of 5×10^{12} A s^{-1}, we have observed a similar expansion. Here we report on a laser-initiated gas-embedded pinch in which a preheat current is used to raise the temperature whilst lowering the density by expansion, so that when the main current is injected, the pinch is heated under conditions of pressure balance. The pinch maintains a constant radius during the time of current rise. No instabilities are observed during this time. At the end of the current rise, the pinch becomes transformed into a helical structure similar to that reported by Smärs.[5] The structure expands radially but does not break up catastrophically.

A schematic diagram of the apparatus is shown in Fig. 1. The 200-kV, 0.125-μF Marx bank pulse charges a 3-Ω, 50-ns coaxial water line. This is connected via a water gap, shunted by a 250-Ω resistor, to a matched 10-ns transfer line and then to the Z-pinch assembly. The pinch electrode separation is 5 cm. A pulsed ruby laser beam (1 J, full width at half maximum, 30 ns) is focused axially through a hole in the earth electrode onto the live negative electrode. The pinch chamber can be evacuated and pressurized up to 2 atm. Hydrogen is used in the experiments reported here.

The shunt resistor across the water gap enables operation of the pinch with a preheat current. Its value is chosen so that, during the pulse charging from the Marx bank, the transfer line is charged to a

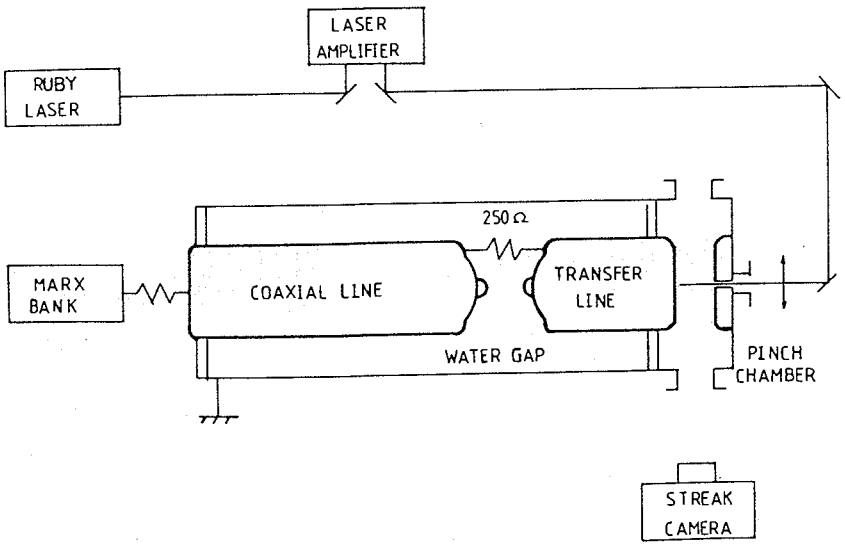

FIG. 1. Schematic diagram of the apparatus.

voltage of one-tenth that of the coaxial line. Thus, when the laser is fired, a predischarge, powered by the transfer line acting as a capacitor, is initiated between the electrodes. The predischarge has a ringing period of 80 ns and a maximum current of 6 kA. The water gap is adjusted to overvolt during the predischarge such that the main current, produced by discharge of the coaxial line, begins near the end of the first half-cycle of the predischarge. A main current of up to 50 kA with a maximum $\dot{I}$ or 5×10^{12} A s^{-1} can be generated.

The condition necessary to maintain the pinch in radial equilibrium, derived in Refs. 1–3, can be obtained more directly from the energy and pressure balance equations if we assume that, during the time under consideration, radiation and conduction losses have not yet become significant. Thus the energy balance after integration over the pinch cross section can be written as

$$\frac{d}{dt}\left(\tfrac{3}{2}\times 2NkT\right)=\frac{\eta}{\pi a^2}I^2 \ , \tag{1}$$

which equates the rate of increase of the plasma energy to the Joule heating. Here k is the Boltzmann constant, N is the electron or ion line density ($Z=1$), T is the temperature taken to be the same for electrons and ions, I is the current which is assumed to flow uniformly over the cross section of the pinch, a is the radius, and η is the Spitzer transverse resistivity. For pressure balance, we use the Bennett relation

$$\mu_0 I^2 = 16\pi NkT \ . \tag{2}$$

Differentiating (2) and combining with Eq. (1), we obtain

$$\dot{I}=5.5\times10^{-6}\ln\Lambda\frac{N^{1/2}}{a^2T} \ , \tag{3}$$

where T is in eV. This equation specifies the value of $\dot{I}$ required to ensure that the magnetic pressure increases at the same rate as the increase in the kinetic pressure due to Joule heating. The condition for radial equilibrium derived by Manheimer[2] reduces to an identical expression if radiation and conduction losses are ignored. Assuming initial plasma conditions of $T=1$ eV, $N=3\times10^{18}$ m^{-1}, $a=10^{-4}$ m corresponding to operation at 1 atm, Eq. (3) gives $\dot{I}=3.4\times10^{14}$ A s^{-1}, which is much larger than the available $\dot{I}$. With a preheat current we may expect both a and T to be increased and thus the required $\dot{I}$ reduced.

Figure 2 shows typical streak photographs taken transversely of the pinch with and without preheat. Without preheat the pinch is seen to expand continuously; with preheat, the pinch has a constant-radius phase. The luminosity before the constant-radius phase corresponds to the preheat discharge. Similar results are obtained over the whole pressure range (0.2 to 2 atm) investigated. The constant-radius phase has duration of 40–50 ns at the low pressure and 5 ns at the high pressure. Schlieren observations of the discharge give a column radius which is identical to that obtained from the streak photographs. These observations are limited to the discharge at 1-atm hydrogen with preheat, and without preheat to the whole pressure range.

Assuming that during this time the pinch is governed by the equilibrium Eqs. (1) and (2), we may rewrite the equations to

$$T=36.1\left[\ln\Lambda\frac{I}{\dot{I}a^2}\right]^{2/3} \ , \quad N=1.6\times10^{11}I^2/T \ ,$$

from which T and N may be inferred taking I and $\dot{I}$ from the current waveforms and a from the streak

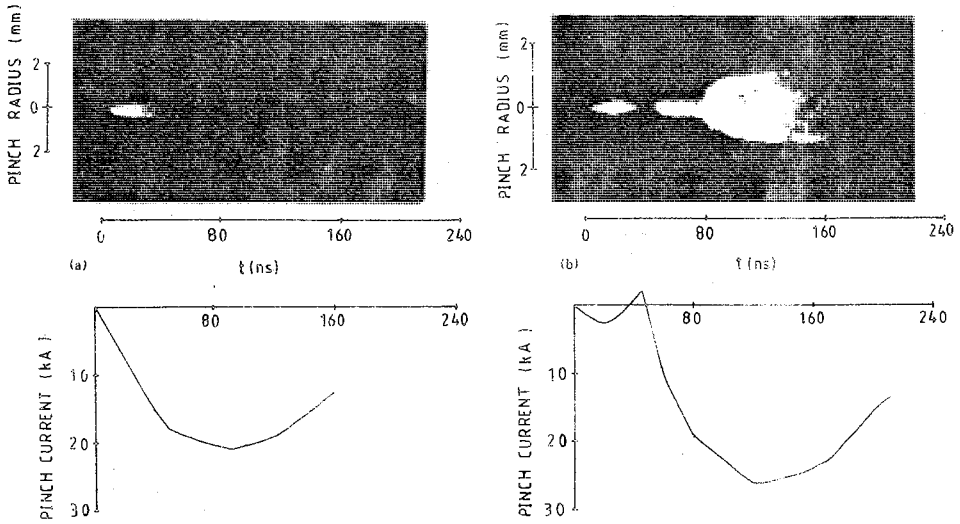

FIG. 2. Streak photographs and current wave forms at 0.33 atm in hydrogen (a) without preheat and (b) with preheat.

TABLE I. Plasma parameters calculated at the end of the constant-radius phase.

P (atm)	a (mm)	T (eV)	N (10^{18} m^{-1})	n (10^{18} cm^{-3})
0.20	0.38	52.3	1.0	2.1
0.33	0.45	34.6	1.8	2.8
1.00	0.40	19.4	3.2	6.4
1.70	0.45	16.2	3.8	6.1

photographs. Some values calculated at the end of the constant-radius phase are given in Table I. The inferred plasma parameters indicate a short electron-ion equilibration time and a current penetration depth of the order of the column radius in agreement with the assumptions made in writing Eq. (1). The table shows that the temperature decreases with pressure, which is as expected. The calculated density, however, is less than the initial density by a factor ranging from 3 at 0.2 atm to 9 at 1.7 atm. The lower density is probably due to the main pinch being formed in the rarefied core of the expanded decaying preheat discharge. This is supported by the streak photographs which show that there is an expansion of the preheat discharge. At the beginning of the main current the photographs do not show any implosion; instead, the column expands from a narrow filamentary discharge to its equilibrium radius in a time <5 ns.

The expansion seen in the streak photographs in Fig. 2 at the end of the constant-radius phase is, in fact, associated with the transformation of the pinch into a helix which then expands radially. This can be seen in Fig. 3 which shows a typical sequence of framing photographs. The top sequence shows the preheated column followed by the narrower pinch with constant radius and then the transition to a helical structure. The lower sequence shows the radial expansion of the helical structure with a better time resolution. At higher pressures the structure is less well defined. The rapid transition to a helix and the subsequent radial expansion constitute a large rate of change of inductance $\dot{L}$ and hence a large "dynamic resistance" in the circuit. Estimates of the value of $\dot{L}$ indicate that it may easily exceed the line impedance. This possibly accounts for the different current waveforms observed at different gas pressures.

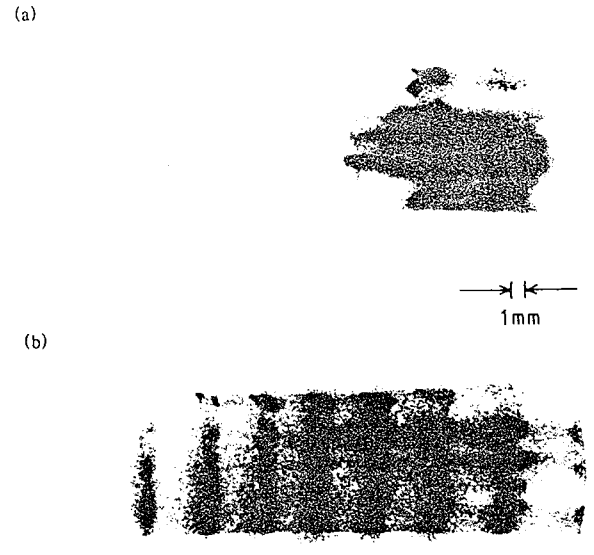

FIG. 3. Framing camera photographs at 0.33 atm in hydrogen. Time between frames is (a) 13.3 ns in the upper sequence and (b) 3.3 ns in the lower sequence.

The observed characteristics of the helical instability appear to be in good agreement with the calculations of Felber and Rostocker[6] for the magnetohydrodynamic $m=1$ instability. At 0.33 atm the ratio of the pitch of the helix to the column radius is observed to be 4.6. The theoretical prediction for the fastest growing modes is $\lambda/a=4$, where λ is the wavelength and a is the radius. The growth time obtained by calculating $r/\dot{r}$ from the streak photographs immediately after the constant current phase increases with pressure being 10 ns at 0.2 atm and 15 ns at 1.7 atm. The theoretical values are 3.5 ns at the low pressure and 7.4 ns at the high pressure. The discontinuity in the expansion seen in the streak photographs is presumably due to the onset of nonlinearity and occurs at $r/a \sim 3.36 \pm 0.01$ (averaged over all shots over the whole pressure range), where r is the major radius of the helix. Nonlinear behavior is predicted when the perturbation amplitude becomes equal to $4a$.

It is of interest to note that stabilization due to finite Larmor radius is predicted for the $m=0$ mode in the Z pinch[7] and for all modes in the θ pinch.[8,9] In our experiment the ratio of the ion Larmor radius to the pinch radius is >0.1, but $\omega\tau<1$ for the ions. Stabilization due to the surrounding gas predicted by Manheimer *et al.*[10] is presumably not occurring due to the low density of the surrounding gas caused by the preheat discharge.

*Permanent address: Department of Physics, Universiti Malaya, Kuala Lumpur, Malaysia.

[1]M. G. Haines, Proc. Phys. Soc. London 76, 250 (1960).
[2]W. M. Manheimer, Phys. Fluids 17, 1767 (1974).
[3]H. W. Bloomberg, M. Lampe, and D. G. Colombant, J. Appl. Phys. 51, 5277 (1980).
[4]L. A. Jones, K. H. Finken, A. E. Dangor, E. Källne, S. Singer, I. R. Lindemuth, J. H. Brownell, and T. A. Oliphant, Appl. Phys. Lett. 38, 522 (1981).
[5]E. A. Smärs, Ark. Fys. 29, 97 (1964).
[6]F. S. Felber and N. Rostocker, Phys. Fluids 24, 1049 (1981).
[7]D. E. Potter, Phys. Fluids 14, 1911 (1971).
[8]E. Bowers and M. G. Haines, Phys. Fluids 14, 165 (1971).
[9]J. P. Freidberg, Phys. Fluids 15, 1102 (1972).
[10]W. M. Manheimer, M. Lampe, and J. P. Boris, Phys. Fluids 16, 1126 (1973).

Application of energy balance to compute plasma pinch ratios

S. Lee
Plasma Research Laboratory, Physics Department, University of Malaya, Kuala Lumpur, Malaysia

(Received 24 January 1983; accepted for publication 15 February 1983)

From energy balance the pinch ratio r_p/r_0 (where r_p = equilibrium pinch radius and r_0 = original radius) may be directly computed for the case of a constant current electromagnetic pinch. For the case of a varying current, to solve the energy integral requires the current as a function of the pinch radius. To achieve this an approximate pinch trajectory is first estimated using a snow-plow model. This trajectory by itself gives a zero pinch ratio but it enables the energy integral to be performed. The theoretically predicted values of r_p/r_0 for several cases are found to be in satisfactory agreement with experimental values. This procedure would be useful for designers of pinch devices.

PACS numbers: 52.55.Ez

The plasma pinch has been established as a classical device with several practical applications. However, its theoretical treatment is far from complete. The standard snow-plow model leads to a plasma column of zero radius whilst the Bennett treatment deals with the column as a purely static situation without relationship with the collapse phase. The snow-plow model has been modified to include a kinetic retarding pressure term.[1] Such a model is capable of giving equilibrium pinch radius for the plasma focus in agreement with experimental results. However, the form of the retarding pressure term has not been written in a self-consistent manner and the trajectory is subject to the adjustment of parameters, somewhat arbitrarily.

For a self-consistent estimate of pinch radius ratio r_p/r_0 (where r_p = equilibrium pinch radius, r_0 = original radius) a simple energy balance theory has been suggested.[2] In this communication this theory is reviewed and its application to the computation of radius ratios is demonstrated for the cases of (1) a constant current, constant length pinch, (2) a constant current, varying length pinch, and (3) a constant length, varying current pinch. The results are compared with experimentally measured values.

We consider the following general model for the pinch. On initiation the current I flows axisymmetrically in a thin sheath of radius r_0, as shown in Fig. 1(a). The current acting as a magnetic piston with field B_θ then implodes inwards compressing the plasma sheath which collapses into a column when the front-running shock wave has imploded onto the axis. The magnetic piston continues moving inwards until the temperature of the column becomes high enough to eventually stop the piston motion leading to a quasistatic column at pinch radius r_p.

The magnetic piston exerts a magnetic pressure $P_m = B_\theta^2/2\mu$ where $B_\theta = \mu I/2\pi r$. The work done by the piston in moving from position r_0 to r_p is

$$W = \frac{1}{\rho \pi r_p^2 l_p} \int_{r_p}^{r_0} \frac{\mu^2 I^2}{4\pi^2 r^2 (2\mu)} 2\pi r l dr, \tag{1}$$

per unit mass of the final plasma column. Here, in general I and pinch length l are functions of r (or time t) and ρ, r_p, and l_p are the density, radius, and length of the quasiequilibrium pinch.

We write the enthalpy per unit mass of the pinched plasma as

$$h = \frac{P}{\rho} \frac{\gamma}{\gamma - 1} = \frac{R_0}{M} T\zeta \frac{\gamma}{\gamma - 1}, \tag{2}$$

where $P = (R_0/M)T\zeta\rho$ is the plasma pressure and T, ζ, and γ are the temperature, the departure coefficient, and the specific heat ratio of the pinched plasma, respectively. Also, R_0 is the universal gas constant and M the molecular weight.

Assume that the work done by the magnetic piston is completely converted into the enthalpy of the pinched plasma. Thus, we equate Eq. (1) to Eq. (2) and obtain

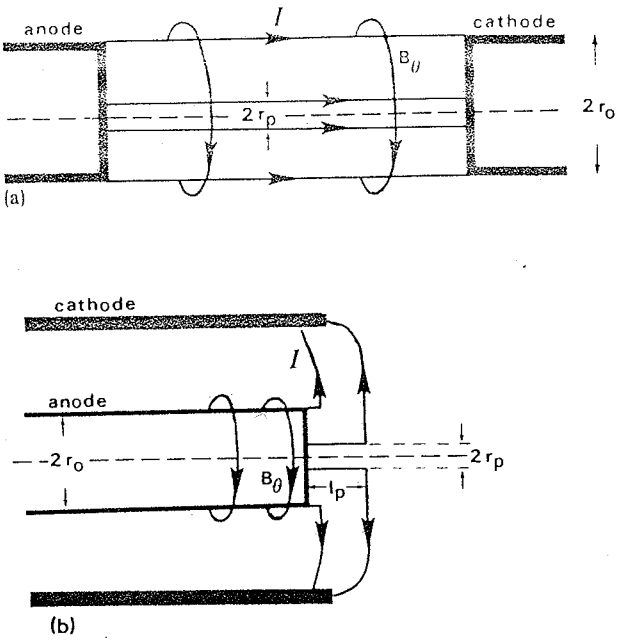

FIG. 1. Comparison of linear Z pinch and plasma focus pinch: (a) linear Z pinch; (b) plasma focus pinch.

 0021-8979/83/063603-03$02.40

$$T = \frac{\mu}{4\pi^2 \rho r_p^2 l_p} \frac{M}{R_0} \frac{\gamma - 1}{\gamma} \frac{1}{\zeta} \int_{r_p}^{r_0} \frac{I^2 l dr}{r}. \tag{3}$$

But in its state of quasiequilibrium we may obtain independently another equation for the pinch temperature from pressure balance, $P_m = P$. Thus,

$$T = \frac{\mu I_p^2}{8\pi^2 \rho r_p^2} \frac{M}{R_0} \frac{1}{\zeta}, \tag{4}$$

where I_p is the current flowing at the time the quasiequilibrium pinch is first established. Combining the independently derived Eqs. (3) and (4) we have

$$I_p^2 = \frac{2(\gamma - 1)}{\gamma l_p} \int_{r_p}^{r_0} I^2 l \frac{dr}{r}. \tag{5}$$

In general the integral in Eq. (5) which we may call the energy integral may be solved only if I and l are known functions of r.

We shall discuss several specific cases.

Case 1: For this case I = constant, l = constant, and Eq. (5) gives the pinch ratio as

$$\frac{r_p}{r_0} = \exp\left\{\frac{-\gamma}{2(\gamma - 1)}\right\}. \tag{6}$$

For $\gamma = 5/3$, Eq. (6) predicts $r_p/r_0 = 0.29$. This case has already been dealt with earlier.[2]

Case 2: This case, of particular interest to a plasma focus, is depicted in Fig. 1(b). As discussed earlier[2] a working empirical relationship between l and r for the plasma focus may be written as

$$l = \frac{l_p}{(r_0 - r_p)}(r_0 - r).$$

For $\gamma = 5/3$, Eq. (5) then gives a value of $r_p/r_0 = 0.14$.

Case 3a current of form $I = I_0 \omega t$: To see the effect of a changing current on the pinch ratio we consider the case $I = I_0 \omega t$. This is the case of a pinch which reaches r_p very early in a sinusoidal capacitor discharge. The effect of this variation in current may be evaluated from Eq. (5) if we have I^2 as a function of r so that the integration in Eq. (5) may be performed. To do this we may use the snow-plow equation:

$$\frac{d}{d\tau}\left\{(1 - \kappa^2)\frac{d\kappa}{d\tau}\right\} = -\tau^2/\kappa, \tag{7}$$

where $\kappa = r/r_0$, $\tau = t/t_p$, $t_p = (4\pi^2 \rho_0 r_0^4/\mu I_0^2 \omega^2)^{1/2}$. This snow-plow model produces a well-known trajectory[3] which yields by itself a nonphysical radius ratio of $r_p/r_0 = 0$ at $\tau = 1.47$. However, this approximate trajectory may be used to give us a relationship between I^2 and κ in the form

$$I^2 = f(\kappa) = 2.180 - 0.797\kappa - 1.835\,\kappa^2 + 1.081\,\kappa^3 - 0.955\,\kappa^4 + 0.326\,\kappa^5. \tag{8}$$

Equation (5) may then be written as

$$f(\kappa_p) = 2\left(\frac{\gamma - 1}{\gamma}\right)\int_{\kappa_p}^{1} \frac{f(\kappa)}{\kappa} d\kappa \tag{9}$$

For $\gamma = 5/3$, the solution of this equation gives a pinch ratio of $r_p/r_0 = 0.17$. We note that in this procedure we have used an approximate trajectory having a nonphysical final pinch ratio of $r_p/r_0 = 0$ to compute a nonzero pinch ratio based on energy balance.

Case 3b $I = I_0 \sin \omega t$: In the same manner we may consider a current of the form $I = I_0 \sin \omega t$ driving the pinch. The snow-plow equation of motion would be

$$\frac{d}{d\tau}\left\{(1 - \kappa^2)\frac{d\kappa}{d\tau}\right\} = -\alpha^2 \sin^2 \tau/\kappa,$$

where $\kappa = r/r_0, \tau = t/t_c, \alpha = t_c/t_p, t_c = (L_0 C_0)^{1/2} = \{4\pi^2 \rho_0 r_0^4/\mu I_0^2\}^{1/2}$.

Solving the trajectory described by this equation of motion, we fit a polynomial of $\sin^2 \tau$ against κ to enable the energy integral to be performed. For $\gamma = 5/3$ and $\alpha = 1$, the pinch ratio was found to be $r_p/r_0 = 0.21$.

Comparison—Case 1: Published results of the Imperial College Mark II Z pinch[4] show that it is a constant length pinch driven by a constant 60-kA current lasting 100 ns. With hydrogen at 0.07 Torr as the test gas, the resulting plasma has $\gamma = 5/3$ and a pinch ratio from streak photographs of $\sim 1/3$ was reported[4] together with a computation predicting a pinch ratio of 0.31. This result has been confirmed in an upgraded device[6] operated with a higher current of 150 kA. Our energy balance theory predicts a pinch ratio of 0.29.

Comparison—Case 2: Published results of the University of Malaya Dense Plasma Focus (UMDPFI) indicates that for a variable length pinch imploding at approximately constant current in deuterium with $\gamma = 5/3$ a pinch ratio of 0.1 was observed from early streak photographs.[2] Recent las

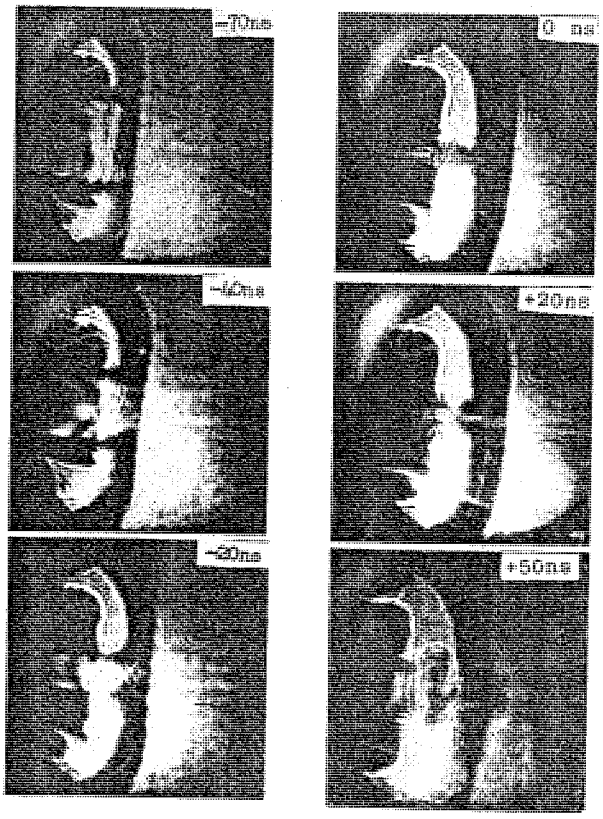

FIG. 2. Side on laser shadowgraph of a 20-kV 60 μF, 4-Torr deuterium plasma focus, showing a pinch ratio $r_p/r_0 \sim 0.13$.

'ABLE I. Pinch ratios r_p/r_0 for $\gamma = 5.3$.

		Energy balance theory	Experimental observations
:ase 1	constant l, constant I	0.29	$\sim 1/3^a$
:ase 2	variable l, constant I	0.14	0.13^b
:ase 3a	constant l, $I = I_0\omega t$	0.17	...
:ase 3b	constant l, $I = I_0 \sin \omega t$	0.21	0.23^c

Imperial College.[4,6]
UMDPFI.[2,7]
Bodin *et al.*[8]

;hadowgraphs[7] of which a sequence is reproduced in Fig. 2 ıave confirmed this radius for the UMDPFI. The energy ɔalance theory predicts a pinch ratio of 0.14.

Comparison—Case 3: Many pinch studies made in the :arly 1960's are of the type in which the current may be ıpproximated as sinusoidal. For example, Bodin *et al.*[8] had :rajectories in hydrogen which indicate that for an operating :ondition close to $\alpha = 1$, a pinch ratio of 0.23 was observed. This compares with a theoretical value of 0.21 from the ener- gy balance theory for a sinusoidal drive current. It should be ıoted that in Bodin's pinch the current waveform was dis- :orted by the pinch motion so that at the expected peak cur- rent time of 1.1 μs the current was depressed below its ex- pected peak value. If this effect were included in the energy ɔalance computation, for example, by coupling the current to the plasma motion through a circuit equation, a pinch ratio greater than 0.21 may be expected from the energy balance.

The results of the above computation based on energy balance are summarized in Table I, with some comparison experimental results.

It would appear that a procedure based on energy balance may be applied to obtain practical estimates on radius ratios for different classes of electromagnetically compressed plasma pinches. In this paper the case of $\gamma = 5/3$ only has been elaborated upon. Equation (6) however predicts lower radius ratios for plasmas having values of γ less than 5/3. This agrees with experimental results in argon[2,6] and nitrogen.[8]

The assistance ot K. K. Jee, W. O. Wong, W. V. Kow, and C. S. Keng in part of the computation is acknowledged.

[1]S. Lee and Y. H. Chen, Proceedings of the Twelfth International Conference on Phenomena in Ionized Gases, Eindhoven *I*, Paper 353, 1975.
[2]S. Lee, Bul. Fizik Malaysia 2, 240 (1981).
[3]S. Glasstone and R. H. Lovberg, *Controlled Thermonuclear Reactions* (Van Nostrand, New York, 1960), p. 232.
[4]M. G. Haines, Philos. Trans. R. Soc. London Ser. A **300**, 649 (1981).
[5]D. E. Potter, Nucl. Fusion **18**, 813 (1978).
[6]P. F. M. Baldock, A. E. Dangor, M. B. Favre Dominguez, D. Grimsley, J. D. Hares, E. Kahan, and S. Lee, Ninth Annual Conference on Plasma Physics Oxford, 1982.
[7]S. Lee and Y. H. Chin, Bul. Fizik Malaysia **2**, 105 (1981).
[8]H. A. B. Bodin, A. A. Newton, and N. J. Peacock, Nucl. Fusion **1**, 54 (1960).